REGULATION OF PERLECAN AND 2OST EXPRESSION IN PROSTATE CANCER PROGRESSION BY STRESS- ACTIVATED TRANSCRIPTION FACTORS

A Dissertation

by

BRENT WADE FERGUSON

Submitted to the Office of Graduate Studies of
Texas A&M University
in partial fulfillment of the requirements for the degree of

DOCTOR OF PHILOSOPHY

December 2010

Major Subject: Biochemistry

Regulation of PERLECAN and 2OST Expression in Prostate Cancer Progression by Stress-activated Transcription Factors

REGULATION OF PERLECAN AND 2OST EXPRESSION IN PROSTATE CANCER PROGRESSION BY STRESS-ACTIVATED TRANSCRIPTION FACTORS

A Dissertation

by

BRENT WADE FERGUSON

Submitted to the Office of Graduate Studies of
Texas A&M University
in partial fulfillment of the requirements for the degree of

DOCTOR OF PHILOSOPHY

Approved by:

Chair of Committee,	Sumana Datta
Committee Members,	Stephen Safe
	Donald Pettigrew
	Brian Perkins
Head of Department,	Gregory Reinhart

December 2010

Major Subject: Biochemistry

ABSTRACT

Regulation of PERLECAN and 2OST Expression in Prostate Cancer Progression by Stress-activated Transcription Factors. (December 2010)

Brent Wade Ferguson, B.S., West Texas A&M University

Chair of Advisory Committee: Dr. Sumana Datta

Heparan sulfate proteoglycans modulate many of the growth factor pathways that drive prostate cancer progression. Prior to being secreted into the extracellular matrix, the covalently attached HS chains are modified by sulfation which has been shown to increase the affinity of binding growth factors. The specific HSPG that I focus on in this dissertation is Perlecan (Pln).

Previously, our group along with collaborators found that 54% of prostate cancer tumors had upregulated levels of Pln protein that correlated with increasing Gleason score [93]. The LNCaP-DU145-LN4 cell line series is introduced as a model for this subset of tumors because Pln levels increase 50-fold as the cells become more metastatic. It was found that three stress-induced transcription factors, HIF1α, NFkB, and ATF2, all stimulate Pln expression. ChIP analysis reveals that HIF1α and NFkB directly bind the Pln promoter while ATF2 does not. The ROS-generating NADPH Oxidase and the ROS-inducible p38 MAPK were also found to induce Pln expression.

To address the subset of prostate cancer tumors that reach metastasis without upregulation of Pln, I focused on the 2-o-sulfotransferase enzyme and its effect on

proliferation and invasion in the LNCaP-C4-2B cell model which does not show upregulation of Perlecan expression. 2OST RNAi resulted in a significant decrease in proliferation in each line of the series. 2OST RNAi in highly metastatic C4-2B cells caused a significant decrease in cell invasion. Cells with decreased levels of 2OST had increased accumulation of actin and E-cadherin suggesting the possible formation of adherens junctions. I also found that expression of 2OST increases four-fold as cells become more metastatic. I found HIF1α and ATF2 act in a direct manner while NFkB acts indirectly to stimulate 2OST expression.

In summary, I have analyzed the effect of cellular stress on the expression of the Pln and 2OST genes and investigated the phenotype of 2OST knockdown in metastatic prostate cancer cells. These studies lead me to propose that the tumor stress response is necessary for prostate cancer progression due to the role of stress in the upregulation of extracellular HS that is required for growth factor signaling and metastatic behaviors.

DEDICATION

This dissertation is dedicated to my God, family and friends. First and foremost I thank God for blessing me richly with wonderful family, friends and colleagues. Psalms 27:5 states: "For in the day of trouble he will keep me safe in his dwelling; he will hide me in the shelter of his tabernacle and set me high upon a rock." Graduate school has not always been easy but God has always taken care of me by putting wonderful people around me. I also thank my loving and caring wife Scarlett. She is everything to me and the reason I wake up every morning. She has been EXTREMELY patient with me during this process partly because she knows what I am going through. She is my best friend, my lover, and my eternal companion. I love her very much. I also dedicate this dissertation to my parents and my brother Nathan. They have guided, supported and loved me for all these years. I would not be here without them. I love them very much. John Wooden once said "Success is peace of mind which is a direct result of self-satisfaction in knowing that you did your best to become the best you are capable of becoming." All of these people have been instrumental in helping me become what I am. Knowing them makes me successful.

ACKNOWLEDGEMENTS

I would like to thank my advisor, Dr. Suma Datta for her continual guidance, patience and willingness to allow me to address scientific questions independently. I could not have asked for a better boss. I also want to thank my advisory committee for their guidance and involvement in overseeing my progress as a graduate student. I would like to thank my lab mate, Jonathan Lindner for helpful discussions regarding research as well as some that did not pertain to research. I would like to acknowledge Ms. Mo Mahdavi for performing some of the qRT-PCR experiments that I present in Chapter IV of this dissertation.

ABBREVIATIONS

Pln	Perlecan
2OST	Heparan Sulfate 2-O-Sulfotransferase
HS	Heparan Sulfate
HSPG	Heparan Sulfate Proteoglycan
SHH	Sonic Hedgehog
FGF	Fibroblast Growth Factor
VEGF	Vascular Endothelial Growth Factor
TGFβ	Transforming Growth Factor β
HIF1α	Hypoxia-Inducible Factor 1 α
NFkB	Nuclear Factor Kappa B
ATF2	Activating Transcription Factor 2

TABLE OF CONTENTS

Page

ABSTRACT iii

DEDICATION v

ACKNOWLEDGEMENTS vi

ABBREVIATIONS vii

TABLE OF CONTENTS viii

LIST OF FIGURES x

CHAPTER

I INTRODUCTION 1

Growth Factors and Prostate Cancer Progression 4
Regulation of Growth Factor Signaling by Heparan Sulfate Proteoglycans 20
Cellular Stress and Cancer 29
Cell Line Models of Prostate Cancer Progression 38

II STRESS-ACTIVATED TRANSCRIPTION FACTORS STIMULATE PERLECAN EXPRESSION IN A MODEL OF PROSTATE CANCER PROGRESSION 42

Materials and Methods 45
Results 49
Discussion 63

III HEPARAN SULFATE 2-O-SULFOTRANSFERASE REGULATES PROLIFERATION AND INVASION OF PROSTATE CANCER CELLS 70

Materials and Methods 72
Results 75
Discussion 86

CHAPTER Page

IV HEPARAN SULFATE 2-O-SULFOTRANSFERASE REGULATES GROWTH FACTOR SIGNALING AND ITS EXPRESSION IS STIMULATED BY STRESS-ACTIVATED TRANSCRIPTION FACTORS IN PROSTATE CANCER CELLS…….. 88

Materials and Methods …..……..…….. 93
Results 97
Discussion 112

V SUMMARY…….116

REFERENCES..... 124

VITA 140

LIST OF FIGURES

FIGURE		Page
1-1	Prostate cancer progression	4
1-2	SHH signaling pathway	6
1-3	FGF signaling pathway	10
1-4	VEGF signaling pathway	13
1-5	TGFβ signaling pathway	16
1-6	Wnt signaling pathway	19
1-7	Perlecan-Growth Factor Interactions	22
1-8	Heparan Sulfate Biosynthesis/Modification	27
1-9	Hypoxia and HIF1α	31
1-10	Reactive Oxygen Species, NFkB, and ATF2	37
2-1	Perlecan is upregulated and modulates growth factor signaling in cell line model of prostate cancer progression	52
2-2	HIF1α activates Pln expression in model of prostate cancer progression	56
2-3	Inhibition of NADPH Oxidase (NOX) or NFkB results in decreased Pln mRNA	60
2-4	Inhibition of p38 MAPK or ATF2 results in decreased Pln mRNA	64
2-5	Model for regulation of Pln transcription by stress-activated transcription factors	69
3-1	Inhibition by 2OST RNAi decreases prostate cancer cell proliferation	77
3-2	2OST expression correlates with metastatic potential	80
3-3	Inhibition by 2OST RNAi increases actin foci in C4-2B cells	84

FIGURE Page

4-1 2OST modulates growth factor signaling in cell line model of prostate cancer progression 100

4-2 HIF1α activates 2OST expression in model of prostate cancer progression 104

4-3 Inhibition of p38 MAPK or ATF2 results in decrease in 2OST mRNA.... 108

4-4 Inhibition by NFkB RNAi results in decreased 2OST mRNA 111

4-5 Model for upregulation of 2OST transcription by stress-activated transcription factors 115

5-1 Overall model for stress regulation of extracellular HS 120

CHAPTER I

INTRODUCTION

According to the American Cancer Society, prostate cancer is the second leading cause of cancer death in American men, behind only lung cancer in its severity. It is predicted that approximately 192,280 new cases of the disease will be diagnosed in the next year and 27,360 men will die because of it (1). One in five American men will be diagnosed with prostate cancer at some point in their lifetime. These statistics make it vitally important for the scientific community to learn as much as possible about the mechanisms of onset and progression as well as diagnosis and treatment of this disease. At present, patients who present with different stages of prostate cancer have dramatically different outcomes. Patients whose prostate cancer is detected in its early stages have an excellent prognosis. When the tumor is still localized to the prostate, patients have a 5-year survival rate that approaches 100 percent (1). However, the majority of cases that are diagnosed are in an advanced stage in which the tumor has invaded or metastasized to other parts of the body. The prognosis for patients in this category is still very poor.

This dissertation follows the style of *Cancer Research*.

Currently the only effective therapy for advanced disease is androgen deprivation (2). This therapy results in decreased symptoms and tumor volume in approximately 80% of patients. However most of these patients relapse within 2 years and develop hormone-refractory disease in which the tumor is no longer responsive to androgen signaling (3). In summary, the majority of diagnosed cases are advanced, metastatic disease and currently not curable.

There are currently four different methods for detecting prostate cancer in patients. Transrectal ultrasound and the Digital Rectal Exam (DRE) are used to either "see" (via ultrasound imaging) or feel a tumor on the prostate respectively. The Prostate Specific Antigen (PSA) test is a blood test that quantifies the amount of a substance made exclusively in the prostate that has been shown to increase in patients that have prostate cancer (1). This test is still thought to be the gold standard for non-invasive prostate cancer screening despite many problems with false-positives as well as false-negatives. If any of these diagnostic tests turn out to be positive for prostate cancer a biopsy will be done to both confirm the presence of a tumor as well as determine how advanced the tumor is. The cells from the prostatic tumor are visualized under a microscope and assigned a Gleason Score. This score is a number between 2 to 10 with a low number indicating that the cells look most similar to normal prostate cells and a high number indicating that the tumor is most likely to metastasize if it has not already (1). The biopsy is the most invasive but also the most definitive way to analyze the progression of prostate cancer.

In order to better understand advanced, metastatic disease it is imperative to learn the molecular mechanisms by which a prostate tumor progresses from normal prostate epithelium to a localized tumor, eventually becoming invasive and metastatic (Fig. 1-1, (4)). Attempting to define a certain molecular "roadmap" that describes how a cell within the adult male prostate develops into a tumor and progresses has been impossible due to the extreme genetic and cellular heterogeneity of the disease. The type of cell in which prostate tumors originate is still a mystery because cells within a tumor have phenotypic and morphological characteristics of both luminal epithelial and basal cells ((5) (6)). Much of the heterogeneity of prostate cancer cells can be attributed to the genetic makeup of the individual patient. Extensive research has gone into determining the key regions of chromosomes that have been altered in prostate cancer resulting in either overexpression of oncogenes or decreased expression of tumor-suppressor genes such as *p53* (7).

These intracellular events have been the focus of cancer research for many years. In this dissertation I will describe a more recent trend in cancer biology that focuses on the role of the tumor

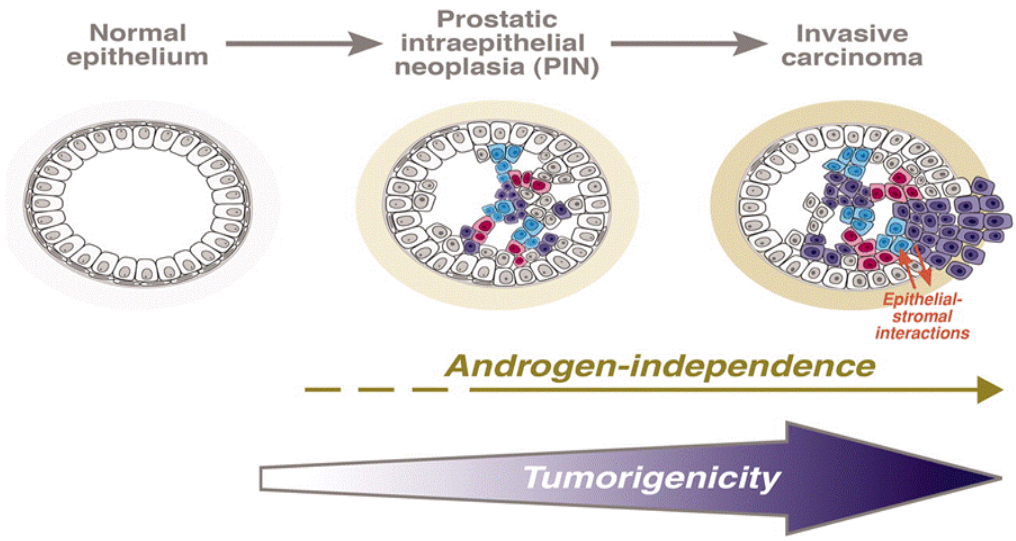

Figure 1-1: Prostate Cancer Progression (Gao et al, 2006)

microenvironment and how cells within the prostate and prostate tumor communicate with one another via growth factor signaling pathways.

Growth Factors and Prostate Cancer Progression

Humans and other multicellular organisms have highly coordinated mechanisms to control cellular interactions. Growth factor signaling networks have been shown to mediate interactions involved in normal embryonic development, tissue homeostasis, wound healing and many others. These factors can act as either positive or negative modulators of cell proliferation, patterning, and differentiation. Genetic mutations in signaling components have been linked to developmental abnormalities as well as chronic diseases such as cancer. It is thought that cancerous cells arise in a tissue due to the unregulated activation/deactivation of growth factor pathways in a subset of cells

thereby causing quiescent cells to exit the G0 phase of the cell cycle and proceed to G1 for cell proliferation (8). The hormone testosterone, and its more active form dihydrotestosterone, (collectively called androgens) continue to be the paramount signaling pathway that is studied in prostate cancer. This pathway is not the focus of my research and will not be covered here but has been reviewed (9). The five growth factor signaling pathways that I will focus on have also been intimately linked to prostate cancer progression: Sonic Hedgehog (SHH), Fibroblast Growth Factor (FGF), Vascular Endothelial Growth Factor (VEGF), Transforming Growth Factor β (TGFβ), and Wnt signaling. Each of these pathways is crucial for normal human development and regulates such processes as cell proliferation, differentiation, motility, and survival. Upon cancer initiation these pathways can be hijacked in the adult prostate to promote progression of a tumor.

Sonic Hedgehog and Prostate Cancer

The Hedgehog (Hh) growth factor and much of its signaling system was initially discovered in genetic screens by Nusslein-Volhard and Wieschaus in the fruit fly *Drosophila melanogaster* (10). This pathway was found to play an essential role in embryonic patterning and development. Since its discovery it has been shown to be highly conserved in other multicellular organisms and to regulate cell proliferation and differentiation in development.

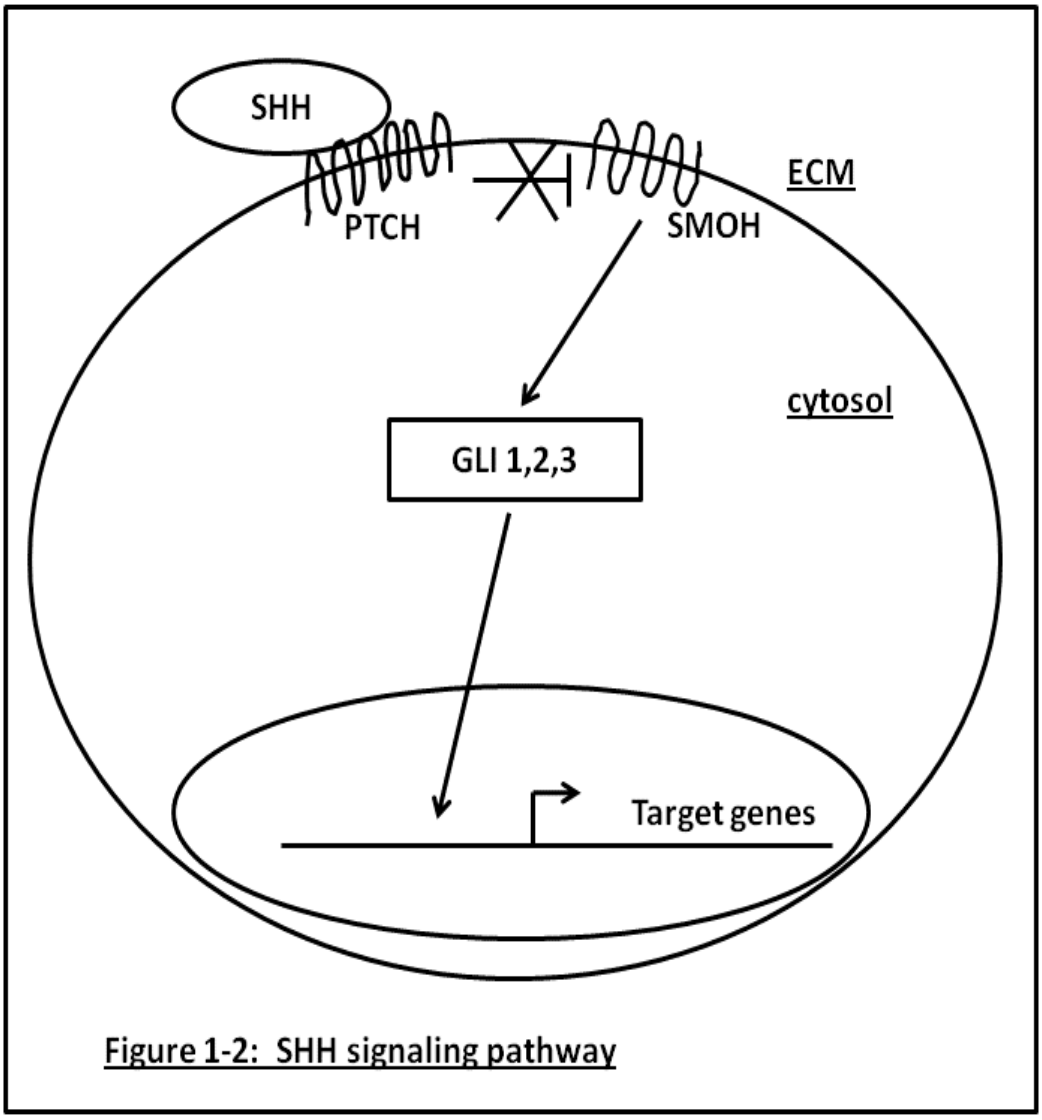

Figure 1-2: SHH signaling pathway

In mammals there are three known Hh ligands: Sonic Hedgehog (SHH), Indian Hedgehog, and Desert Hedgehog. These growth factors are secreted from the cell into the extracellular matrix where they can act in either an autocrine or paracrine fashion to activate signaling (Fig 1-2). They exert their function on the receiving cell by binding to a 12-pass transmembrane protein called Patched (PTCH) (11). This binding event results in relief of the inhibitory effect of PTCH on a serpentine protein called

Smoothened (SMOH) and allows signal transduction to occur. The pathway ultimately activates the Gli family of transcription factors (Gli1, Gli2, and Gli3) that either activate or repress transcription of target genes. GLI1 and PTCH are two examples of target genes and their expression is frequently used to determine the level of active Hh signaling. For the purposes of this dissertation I will be focusing on the SHH growth factor due to the abundance of evidence that points to its role in prostate cancer progression.

The major role of the SHH pathway is in the embryo to control patterning and development but it can be reactivated in adult tissues in response to injury or genetic mutation of a pathway component. In this case normally quiescent cells start to divide. If the pathway is activated for an extended period time it could then facilitate tumor initiation and progression (12). This pathway is used in the development of a number of different organs and is reactivated in many types of cancer including pancreatic, esophageal, stomach, skin, and lung (reviewed (13)). Prostate cancer is no exception. SHH signaling plays a vital role in prostate fetal development as well as carcinoma in adult males.

Most of what has been learned about SHH in prostate development has been from experiments done in rodent models. The precursor to the mature prostate is the urogenital sinus, a hollow cylinder of pseudostratified urothelium surrounded by mesenchymal cells (14). When an increase in testicular androgen occurs, the epithelial cells of urogenital sinus begin to invade the surrounding mesenchyme producing prostatic buds. These buds continue to grow and form prostatic ducts ((14), (15)).

Expression of SHH can be seen throughout this ductal patterning process in the epithelium of the urogenital sinus and at the leading edge of the invading ducts. Complementary expression of PTCH and GLI1 can be seen in the adjacent mesenchymal cells showing active SHH signaling during the process ((16), (17), (18)). A causal relationship between SHH signaling and progression of ductal morphogenesis has also been shown in mouse models (19).

Just as SHH is important in the development of the fetal prostate it is also critical for the development of carcinoma of the prostate. Familial genetic mapping studies have shown that regions of chromosomes associated with prostate cancer susceptibility contain genes coding for critical SHH pathway components such as SMOH, GLI1, and GLI3 ((20), (21), (22)). There is also significant data showing that this developmental pathway is indeed reactivated in prostate cancer, initially at lower levels, then more strongly as the disease progresses. The SHH growth factor has been shown by many groups (including the Datta Lab) to be upregulated in prostate tumors compared to normal tissues. This upregulation continues in more aggressive tumors and in their metastatic lesions ((23), (20), (24)). Evidence of active signaling by localization of PTCH and GLI1 or use of a Hh reporter suggest that SHH can act either in a paracrine or autocrine manner to promote tumor progression.

FGF signaling and Prostate Cancer

There are currently 18 known mammalian FGF ligands that signal through four highly conserved receptor tyrosine kinases (FGFR-1, -2, -3, -4) to control a variety of biological processes (25). These processes include cellular proliferation, angiogenesis,

differentiation, migration, and survival. This signaling pathway has been shown to control such developmental events as mesodermal patterning in the early embryo as well as the formation of many organ systems ((26), (27)). Much like SHH, FGF can also function in adults as it regulates both angiogenesis and wound repair. Due to its role in these developmental events, FGF signaling can also be subverted by cancer cells to promote their progression.

FGFs are secreted glycoproteins that travel through the extracellular matrix (ECM) and have a high affinity for heparan-sulfate (HS) and heparan-sulfate proteoglycans (HSPGs) (discussed more fully below). Due to this high affinity the growth factors are sequestered in the ECM as they bind to HSPGs (28). This binding interaction is thought to protect against degradation and create a sort of extracellular growth factor repository (29). The FGFs are then released from the HSPGs by enzymes such as heparinases or proteases to allow the ligand to migrate and bind to cell-surface HSPGs. These HSPGs stabilize the interaction between the FGF ligand and the FGF receptor forming a ternary complex (30). The specificity of the FGF-FGFR interaction is controlled by tissue-specific expression of both ligands and receptor paralogues (31). Upon ligand binding, FGFRs will dimerize, this activates the intracellular tyrosine kinase domains of the receptors which then transphosphorylate each other (Fig.1-3). The phosphorylated tyrosines of the receptor act as docking sites for adaptor proteins that facilitate the activation of a number of different signal transduction pathways. These pathways include the phospholipase Cγ, Phosphoinositide-3 Kinase, Mitogen-Activated Protein Kinase (MAPK), or Signal Transducer and Activator of Transcription

(STAT) pathways (Fig. 1-3). These pathways activate many target proteins including transcription factors in the nucleus that control target gene expression. Each of these pathways is upregulated in prostate cancer and are important for its progression (32).

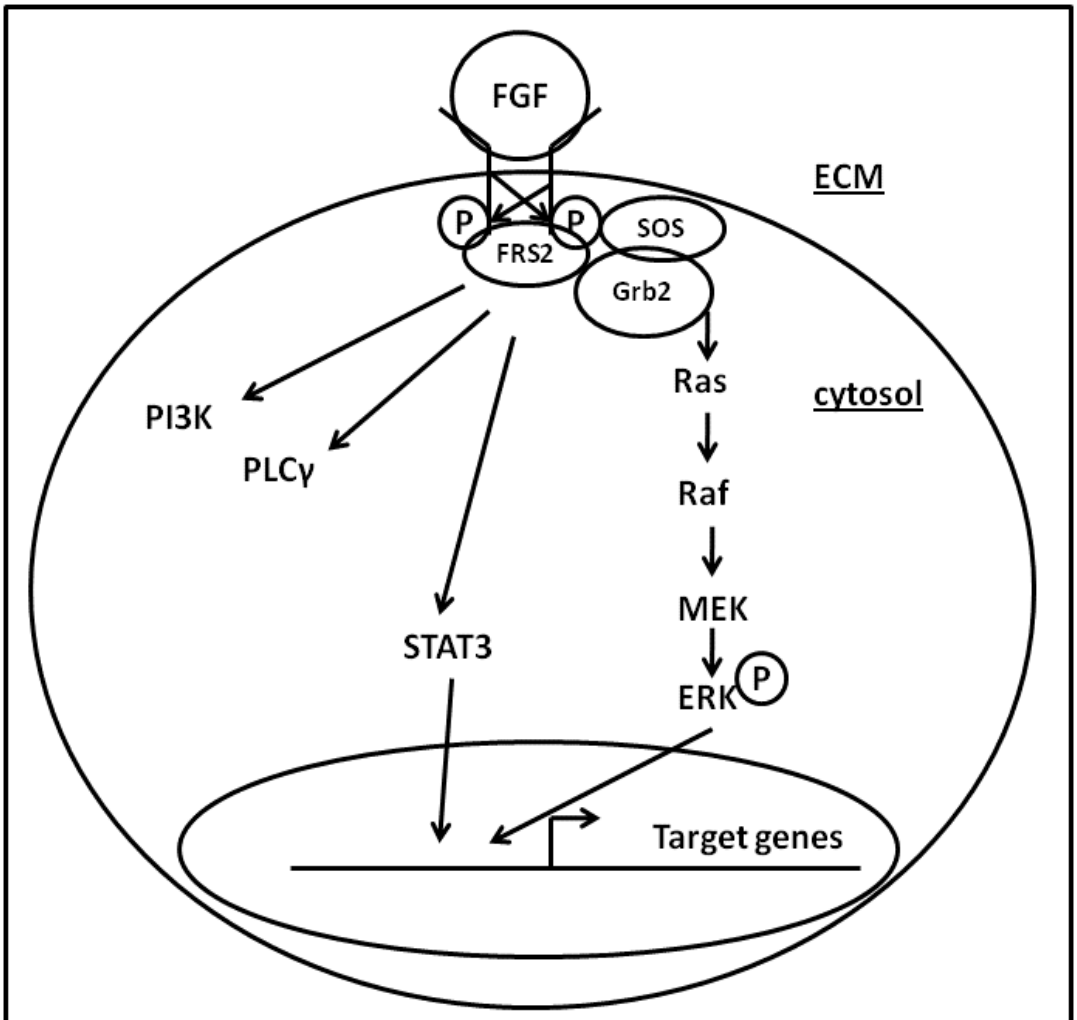

Figure 1-3: FGF signaling pathway

In the normal human prostate, which is composed of ductal epithelial cells surrounded by stromal cells, the major source of FGF ligand expression is the stromal cells. FGF ligands are secreted and act in a paracrine manner on FGFRs on the outer membrane of the ductal epithelial cells. FGF-2, -7, and -9 are the ligands that are available in biologically significant quantities to exert their effect.

In prostate cancer the major FGF isoforms that are expressed are FGF-1, -2, and -8 ((33), (34), (35)). Each of these isoforms is expressed at much higher levels in localized tumors compared to normal tissue and increases further as the disease progresses to a metastatic state. Immunohistochemical analysis of tumor tissue reveals that each can act in either an autocrine or paracrine manner as their expression is confined to stromal cells in early stage disease and expands to multiple cell types in later stages. Due in part to analysis of relatively small sample sizes the expression of any one isoform has not been shown to be an independent prognostic factor (32).

Multiple mechanisms exist to describe how FGF signaling is increased in prostate cancer. These mechanisms include: increased expression of FGFs and FGFRs, increased mobilization from the ECM, and loss of negative regulation of the pathway. This increase in signaling has been shown to upregulate proliferation (36), cell survival (37), motility (38), angiogenesis (39), and metastasis (40).

Each of these processes is vital for the progression of prostate cancer. Overall, the disruption of FGF signaling in prostate cancer has become an attractive therapeutic target.

VEGF Signaling and Prostate Cancer

Angiogenesis is the sprouting of new blood vessels from pre-existing ones and is crucial for both fetal development as well as tissue repair. This process has also been exploited in cancer progression. Tumor cells must overcome many roadblocks in their growth and progression including hypoxia (low oxygen concentration) and nutrient deprivation (29). A tumor cannot progress beyond 2 – 5 mm in diameter without obtaining its own blood supply ((41), (42), (43)). In other words, tumor growth rapidly surpasses the ability of the surrounding blood vessels to deliver adequate amounts of oxygen and nutrients. The hypoxic stress response induced by a lack of oxygen initiates the activation of oncogenes that promote neovascularization. The major inducer of angiogenesis in tumor cells is Vascular Endothelial Growth Factor (VEGF). This mitogenic growth factor binds to two types of tyrosine kinase receptors, VEGFRI and VEGFRII, located on the membranes of endothelial cells that makeup nearby blood vessels (44). Upon ligand binding at least two different cell survival/angiogenesis pathways are activated, PI3K/Akt and Ras-mediated MAPK signaling. (Fig. 1-4)

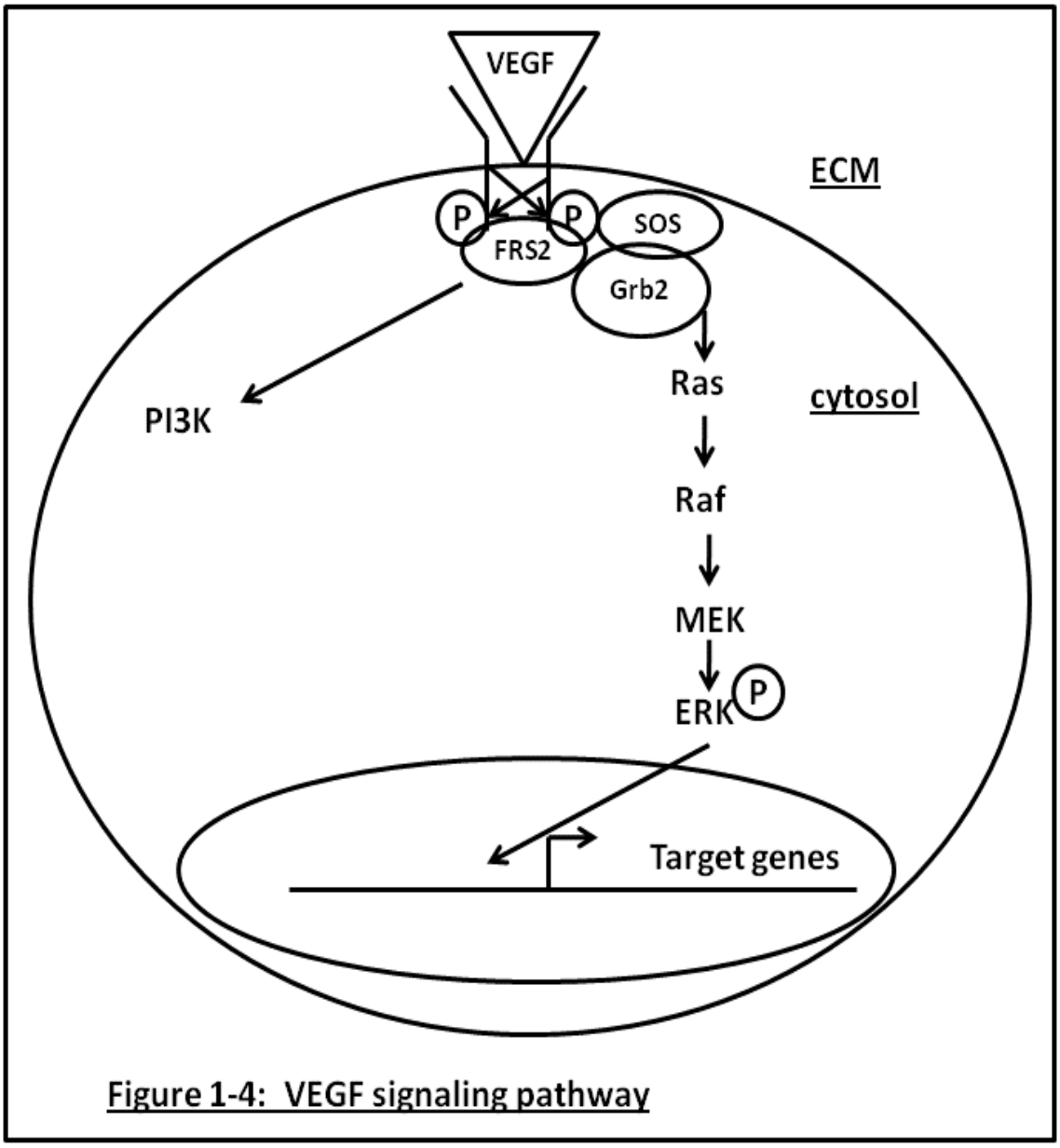

Figure 1-4: VEGF signaling pathway

VEGF is highly expressed in prostate cancer ((45), (46)) and increases with increasing Gleason grade (47). VEGF expression can be induced by many different signals. Since oxygen availability is such a dire need for the progression of tumors the transcription factor Hypoxia Inducible Factor-1α (HIF1α) plays a major role in VEGF

expression (43) (discussed more fully below). Cytokines such as IL-8 and TNFα, generally associated with wound healing, also play a role in stimulating VEGF expression to induce angiogenesis (48). The Signal Transducer/Activator of Transcription-3 (STAT3) transcription factor also binds directly to the VEGF promoter in prostate cancer cells to induce expression.

Overall, VEGF signaling plays a role in proliferation, angiogenesis, and survival of prostate cancer cells. The ability to understand how this pathway is regulated both intra- and intercellularly is a critical step in stopping tumor growth and progression.

TGFβ and Prostate Cancer

The prostate, like many other tissues, has a delicate balance between apoptosis, cell proliferation, and differentiation (2). This balance is maintained by many factors in the normal prostate. Growth and functional maintenance is achieved primarily by androgens as well as the growth factors discussed previously. Inhibition of cell proliferation is primarily achieved by the action of Transforming Growth Factor β (TGFβ) (49). This factor is extremely important for maintaining normal organ size since prostate cells are continually stimulated to grow by the presence of androgen.

TGFβ counteracts this by inducing differentiation, activating apoptosis, and inhibiting cell proliferation ((50), (51)). The efficacy of anti-androgen treatment is based upon the resultant activation of the TGFβ pathway and activation of apoptosis thus decreasing tumor volume (52).

TGFβ is a superfamily of more than 30 multifunctional growth factors that regulate a wide array of cellular processes. The biological effect on the target cell is dependent upon what type of cell the target is, its growth conditions, the presence of other growth factors, and its stage of differentiation (2). For example, TGFβ specifically is known to stimulate cell growth in fibroblasts but inhibits the same in epithelial and endothelial cells in normal prostate (53).

TGFβ is secreted from the stromal cells and acts in a paracrine manner to exert its effect on nearby epithelia. The growth factor will traverse the extracellular matrix until it binds to its primary receptor TGFβRII on the target cell. Upon binding TGFβRII will heterodimerize with TGFβRI to initiate the intracellular signal cascade (54). (Fig.1-5) Heterodimerization activates the serine/threonine kinase activity of the receptors which then recruits and phosphorylates SMAD proteins (SMAD2 and 3).

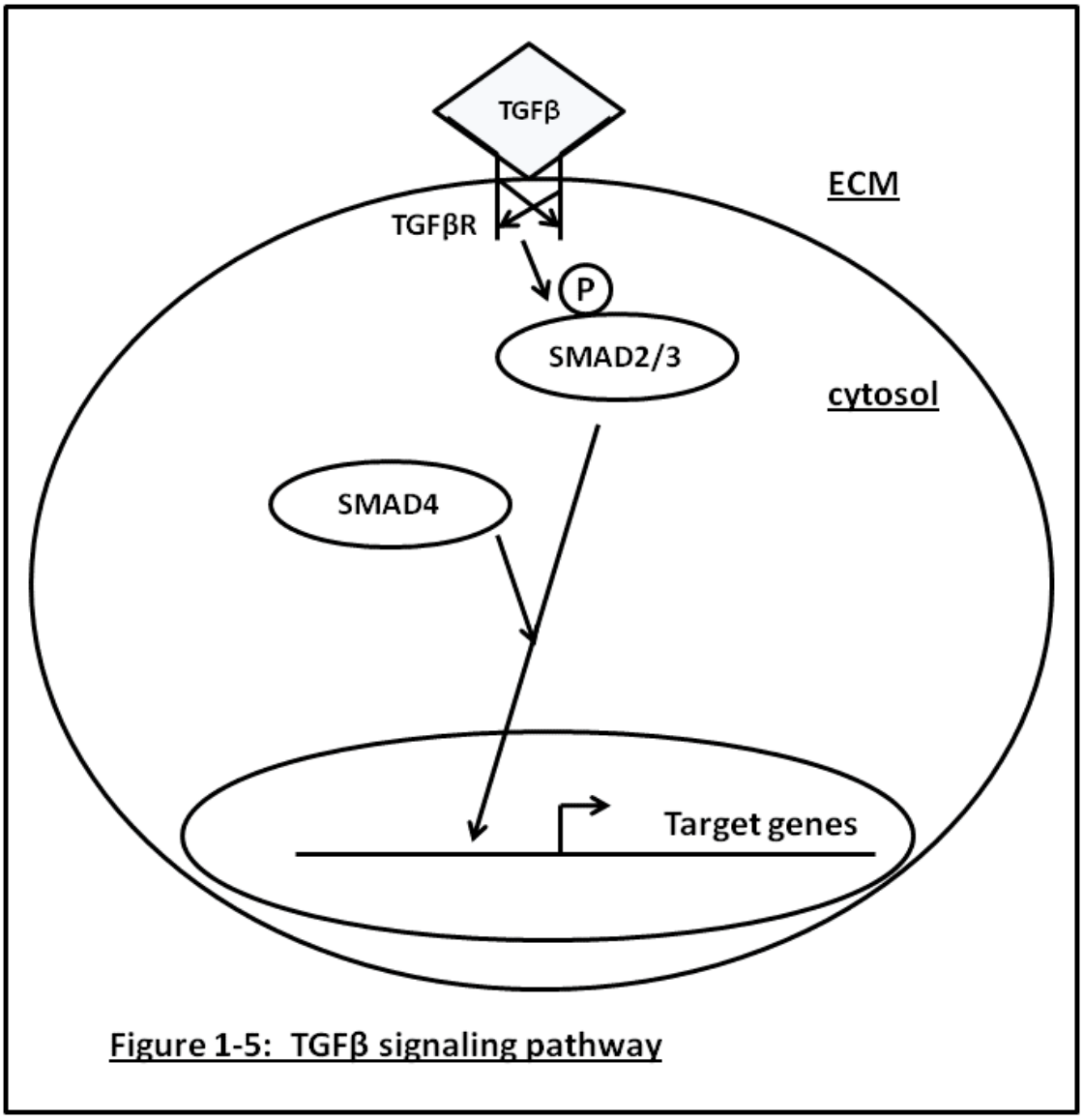

Figure 1-5: TGFβ signaling pathway

The phosphorylated SMADs translocate to the nucleus and activate a series of transcription factors that induce genes involved in cell growth, apoptosis, induction of ECM proteins, regulation of cell adhesion, and modulation of protease expression ((53), (2)). Experimentally, the phosphorylation of either SMAD2 or SMAD3 can be assayed to monitor active TGFβ signaling.

The TGFβ pathway is interesting in that it has growth inhibitory effects in the early stages of prostate cancer (much like in normal prostate) but then switches to a more oncogenic effect in later stages of the disease by a still unknown mechanism (2). The major isoform of TGFβ in the adult prostate is TGFβ1. The expression of this isoform increases in low-grade tumors compared to normal tissue and continues to increase with increasing tumor grade and metastatic potential ((55), (56)). At first glance this increase in a growth factor known to inhibit cell growth would seem to contradict the goal of tumor cells to rapidly proliferate and evade apoptosis. However, tumor cells acquire a selective resistance to the growth-inhibitory/apoptotic effects of TGFβ while still retaining the other responses such as expression of ECM proteins, cell-adhesion proteins, and proteases ((57), (58)). There have been several mechanisms proposed for this phenomenon. Proposed mechanisms include alterations in TGFβ receptor or SMAD expression, modulation of binding partners, or loss of downstream mediators of growth inhibition and apoptosis (2). Increased levels of proteins known to disrupt the ability of TGFβ to induce apoptosis such as Bcl-2 and Prostate Specific Antigen may also provide a possible mechanism ((59), (60)).

Overall, the TGFβ signaling pathway is intimately linked to the progression of prostate cancer. The disruption of the pathway's oncogenic effects, as well as the reintroduction of its ability to induce apoptosis, is avenues for therapeutic targeting.

Wnt Signaling and Prostate Cancer

The Wnt signaling pathway has been implicated in embryonic development and regulation of processes such as proliferation, cell-fate specification, cell polarity, and

migration (61). This highly conserved pathway is activated by the Wnt ligand of which there are currently 19 known genes (62). Wnt ligand is a glycoprotein that is secreted from a signal sending cell into the extracellular matrix and remains tightly associated with components in the matrix until it is liberated to reach its receptor on a signal receiving cell (63). Wnt ligands can be classified into two groups. The first group activates the canonical Wnt pathway (examples Wnt-1, -2, -3, and -3a). In this pathway, in the absence of Wnt ligand, the central cytoplasmic signal transducer β-catenin is sequestered and destroyed by the "destruction complex" (64). This multiprotein complex consists of Glycogen Synthase Kinase 3β (GSK3β), Adenomatous Polyposis Coli (APC) and a scaffolding protein called Axin. GSK3β will phosphorylate β-catenin thereby marking it for ubiquitin-mediated degradation (65). Upon binding of the Wnt ligand to its seven-transmembrane receptor Frizzled and coreceptor LRP5 (or LRP6) (66), Frizzled activates the cytoplasmic protein Dishevelled (Dvl). Dvl will then dephosphorylate Axin, causing it to disassociate from the destruction complex thus decreasing GSK3β kinase activity. The result is a stabilized pool of β-catenin in the cytoplasm. Stabilized β-catenin can act in two different ways. The first is to participate in a complex with E-cadherin at the plasma membrane to facilitate inter-cellular adhesion (67). The second mode of action is for β-catenin to accumulate in the cytoplasm and then translocate into the nucleus. Once in the nucleus it will associate with members of the T-cell factor (TCF) and lymphoid enhancer factor (LEF) family of transcription factors and activate transcription of target genes (68). (Fig.1-6)

The other category of Wnt ligands consists of those that activate one of many non-canonical pathways. These pathways are similar to the canonical pathway in that they require a Frizzled receptor but do not require a LRP coreceptor and are independent of β-catenin (69). One example of non-canonical

Wnt signaling is an increase in the influx of cytosolic calcium that leads to the activation of Protein Kinase C and Calmodulin kinase II (70).

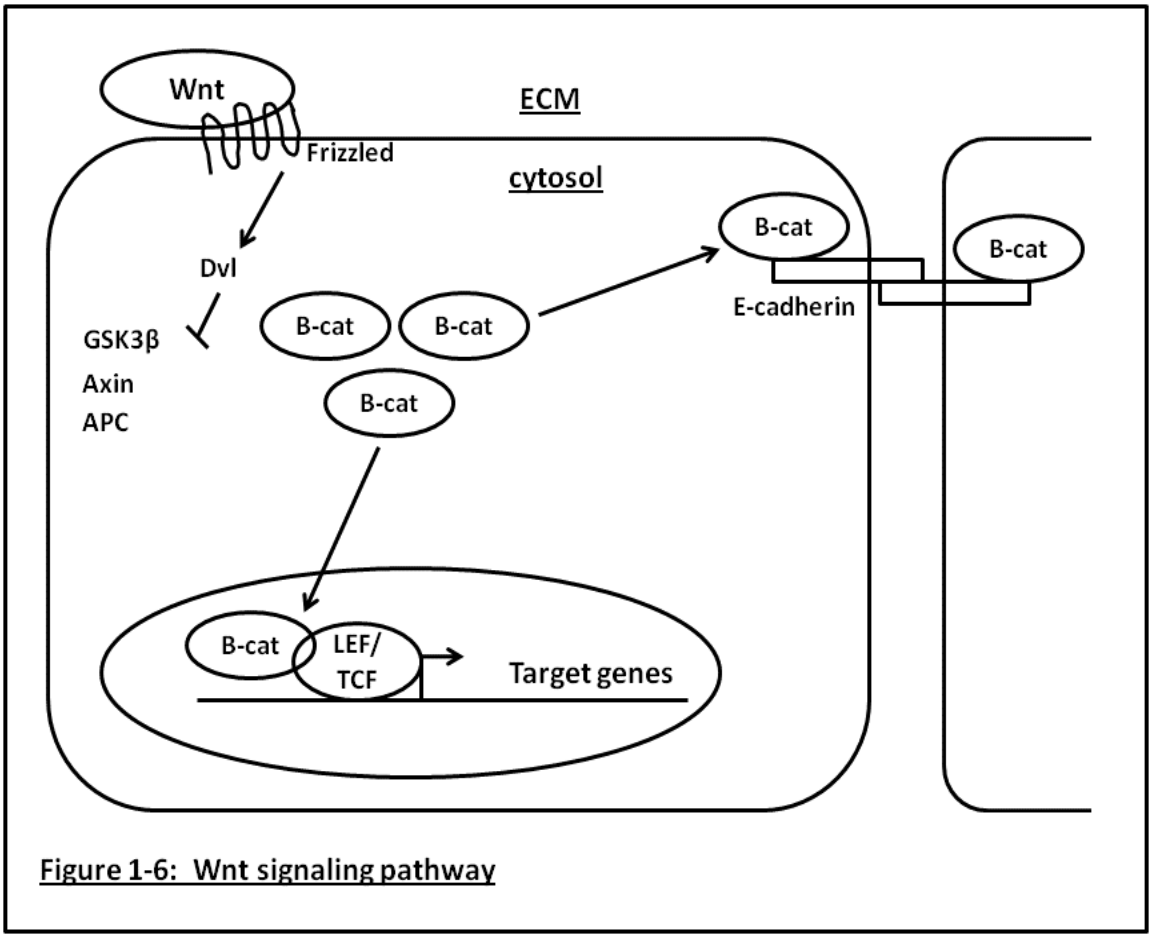

Figure 1-6: Wnt signaling pathway

Wnt signaling is thought to be involved in three different functions that have relevance in cancer progression: maintenance of stem cell-like phenotypes, promotion of epithelial to mesenchymal transitions (EMT) and inhibition of apoptosis (67). Increased Wnt signaling has been demonstrated in prostate cancer by increased expression of Wnt ligands ((71), (72), (73)) as well as decreased expression of Wnt inhibitory protein (WIF1) (74). However, there is much debate surrounding the presence of nuclear-localized β-catenin in tumor cells. Data suggest that accumulation of β-catenin in the nucleus only occurs in a small percentage of prostate cancer (67). However, increased accumulation in the cytoplasm and the nucleus in patients with more aggressive tumors has led scientists to infer that Wnt signaling is upregulated and important for the progression of the disease to advanced metastatic cancer (75). This pathway has also been shown to play a key role in metastasis of prostate cancer cells to bone (76). Overall, it is very important to determine how this pathway is regulated and how to abolish it in prostate cancer.

Regulation of Growth Factor Signaling by Heparan-Sulfate Proteoglycans

Research regarding the regulation of growth factor signaling in prostate cancer and cancer in general has focused on understanding how the signal is modulated inside the cell from the plasma membrane to the nucleus. However, recently more and more groups are looking outside the cell in the extracellular matrix for points of regulation. Each of these growth factors is secreted into the ECM from the signal sending cell and travels through it until they reach their receptors on the signal receiving cell. The growth factors come in contact with many ECM molecules. This review will focus on a

class of molecules that is found in most mammalian tissues (77) called heparan-sulfate proteoglycans (HSPGs).

HSPGs are cell-surface molecules that consist of a protein core with covalently attached glycosaminoglycan (GAG) chains. These molecules have been assigned a wide range of functions spanning from regulation of cell adhesion, migration, proliferation, differentiation (78) all the way to plasma membrane carriers for viruses (79). HSPGs can either be located on the cell surface or secreted into the ECM. This localization is determined by the protein component. The attached GAG chains are primarily responsible for mediating interactions with extracellular ligands such as growth factors or adhesion molecules (78). Three major groups of HSPGs have been described: syndecans, glypicans, and perlecan. The focus of my research and this dissertation deals primarily with perlecan.

Perlecan and Prostate Cancer

Perlecan (Pln) is a ubiquitous proteoglycan known to control many growth factor signaling pathways through either protein-protein or protein-heparan-sulfate interactions. This gives Pln a role in cellular proliferation, differentiation, and migration. Pln was originally isolated from mouse Engelbreth-Holm-Swarm tumors by Hassell and colleagues in 1980. This group also showed that it was expressed at the cell surface of human colon carcinoma cells (80). Since this discovery it has been found that Pln is highly conserved in organisms ranging from nematodes to mammals. It is found in the pericellular space of most cells and nearly all basement membranes that separate the

epithelial and stromal compartments of mesenchymal organs. This localization is ideal for Pln to mediate either paracrine or autocrine growth factor signaling (81).

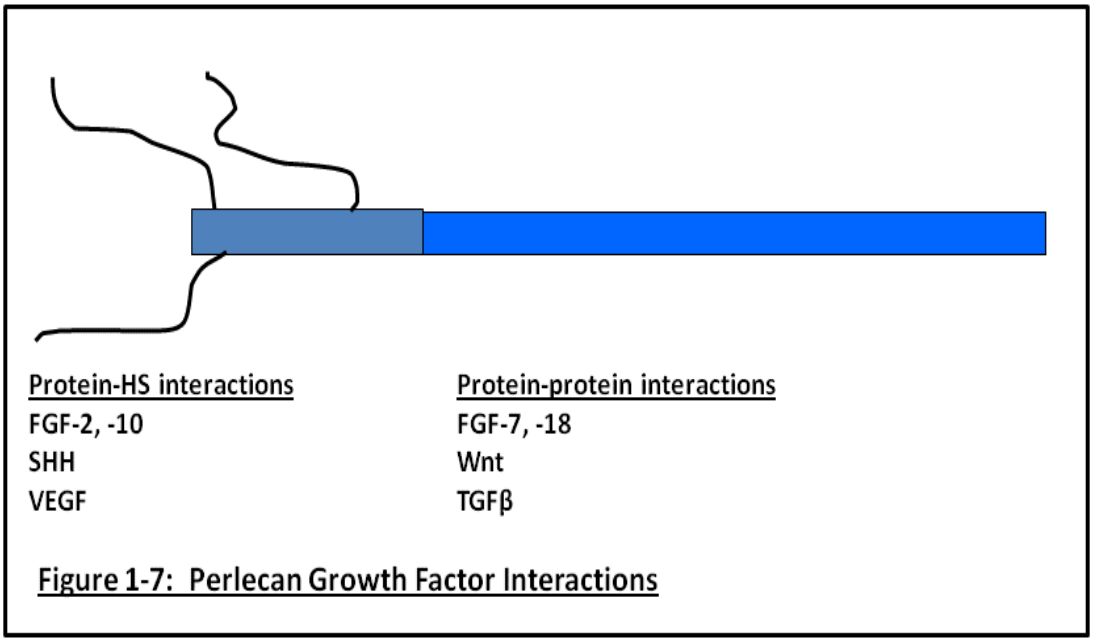

Figure 1-7: Perlecan Growth Factor Interactions

Pln is very large at both the gene and protein level. It has an mRNA that is >15 kilobases which is used to produce a protein of 4,391 amino acids of which 21 are cut off with signal peptidase (82). This protein core of >400 kilodaltons is folded into 5 distinct globular domains that are linked by short linear pieces giving it a "beads on a string" appearance. This structural observation is where the name "perlecan" is derived. The 5 domains of the protein core are homologous to proteins involved in lipid metabolism and cell adhesion (81). Pln continues to increase in molecular weight during protein maturation as heparan-sulfate (HS) chains are added to three distinct HS attachment sites on Domain I of the protein core and possibly more on Domain V. (Fig.

1-7) After these HS chains are modified by sulfation the secreted form of Pln is estimated to be >700-800 kilodaltons (83). The expression and modification of Pln allows it to regulate growth factor signaling in many different contexts from development to diseases such as cancer.

Insights into the role of Pln in development and disease have come from observations of Pln-knockout mice. Two articles in 1999 described the mice as having various complex phenotypes that extended into many different organ systems ((84), (85)). These mice were embryonic lethal and had shortened long bones as well as a dwarf-like phenotype. These observations eventually led to the discoveries that mutations in the Pln gene were associated with such diseases as Schwartz-Jampel syndrome as well as Silverman-Handmaker type dyssegmental dysplasia. Loss-of-function of Pln orthologs in other organisms has also been described. UNC-52 in *Caenorhabditis elegans* was shown to be important for gonadal cell migration as well as the mediation of FGF, TGFβ, and Wnt signaling ((81), (86)). Also, work from the Datta Lab has demonstrated the role of Trol, the Drosophila Pln homologue, in stimulating the proliferation of neural stem cells called neuroblasts in the embryonic brain of Drosophila. Trol modulates FGF and Hh signaling in the developing brain (87), is present on and controls the number of circulating plasmatocytes suggesting a role in the mediation of VEGF signaling and modulates Decapentaplegic (a TGFβ family member) and Wingless (a Wnt growth factor) signaling in second instar brains and eye discs (88). Later studies in mouse have demonstrated that Pln plays an essential role in neurogenesis by regulating the amount of available SHH at the floor plate (89).

The fact that Pln regulates many of the growth factor pathways that play essential roles in both development and cancer has led researchers to study its role in various types of cancer. Cohen et al discovered that Pln mRNA and protein increased 15-fold in invasive tissue compared to normal in metastatic melanoma patient samples. This group also utilized the MeWo and the more metastatic 70W melanoma cell lines and discovered a corresponding increase in Pln as metastatic potential increased (90). This study suggested that Pln was involved in the progression to an invasive and possibly a metastatic phenotype. Another study by Sharma et al demonstrated the importance of Pln in the proliferation and responsiveness to FGF signaling of colon carcinoma cells by way of gene-targeted knock-down (91). In a beautiful set of experiments in mice, Zhou et al reported on the importance of the HS chains on the N-terminus of Pln. In $Hspg2^{\Delta 3/\Delta 3}$ mice the HS-attachment sites are mutated thus leaving an intact protein core without HS. These mice demonstrated significant delays in wound healing, decreased FGF2-induced tumor formation, and defective angiogenesis (92).

Pln has also been associated with prostate cancer. The Pln gene is located in region 1p36 of human chromosome 1. A genetic association between prostate cancer and the brain cancer glioblastoma multiforme has been mapped to this region (Carcinoma Prostate Brain, CaPB locus). Due to this association the Datta lab and their collaborators analyzed the expression and role of Pln in the progression of prostate cancer. They demonstrated that Pln expression correlates significantly with increased metastatic potential of prostate cancer cells based upon tumor Gleason score in 600 patient samples. It was also shown that Pln increased the activity of the SHH pathway

which in turn regulates cell proliferation (93). Another study by Savore et al analyzed the effect of Pln in the androgen-independent, bone targeted prostate cancer cell line C4-2B. In these cells Pln expression was stably knocked down via ribozyme directed toward the Pln message. The Pln knock-down clones showed decreased proliferation as well as decreased responsiveness to FGF2 and VEGF-A. In vivo effects were analyzed by inoculating athymic mice with either control or knock-down clones. The Pln-deficient clones resulted in smaller tumor volume, decreased vascularization and had no increase in serum PSA levels (94).

The observations from these studies and others indicate that Pln has the potential to be a therapeutic target as well as a marker of advanced prostate cancer. For this to become a reality we need to learn more about how Pln expression and activity is regulated.

Synthesizing Perlecan

Pln is a secreted proteoglycan so it follows the protein secretion pathway. The Pln gene is transcribed in the nucleus to produce Pln mRNA. The message is translocated to the rough endoplasmic reticulum to be translated by the ribosomes. Since the mRNA contains a signal sequence the resulting protein is co-translationally funneled into the lumen of the ER. From this point the Pln protein will be transported to the Golgi apparatus via transport vesicles. Once in the Golgi apparatus, the Pln protein core will have HS chains polymerized onto HS attachment sites. These sites consist of the Ser-Gly sequence usually with flanking acidic residues.

HS chain polymerization begins with the transfer of Xylose from UDP-Xylose by the enzyme Xylosyltransferase to the serine residue in the attachment site. From there two consecutive Galactose residues and then a Glucuronic acid (GlcA) residue is added to form what is called the linker tetrasaccharide. This linker region is common to the synthesis of chondroitin sulfate, dermatan sulfate, and HS. However, the subsequent addition of α4-N-Acetylglucosamine (GlcNAc) commits the intermediate to HS chain synthesis. Polymer formation then proceeds with alternating addition of GlcAβ4 and GlcNAcα4 residues by the EXT1 and EXT2 copolymerases that are products of the *ext* tumor suppressor genes.

At the same time the HS chain is polymerized it can be modified at different positions on the GlcA/GlcNAc disaccharide by HS modification enzymes (HSMEs). (Fig.1-8) These modification enzymes act in a stepwise manner such that the action of one enzyme provides the correct substrate for the next enzyme in the series (95). The first modification is generally the removal of the N-acetyl group and subsequent N-sulfation of GlcNAc residues by the enzyme GlcNAc N-deacetylase N-sulfotransferase of which four tissue-specific isoforms exist. The next modification is usually the epimerization of the C5 position of GlcA residues into Iduronic acid (IdoA) by the enzyme C5-GlcA epimerase (GLCE). GLCE has only one known isoform and provides the substrate needed for the transfer of sulfate to the C2 position of either GlcA or IdoA by the enzyme 2-O-sulfotransferase (2OST). The single 2OST enzyme has a five-fold greater affinity for IdoA residues than GlcA. Further sulfation reactions can occur at the C6 or C3 positions of glucosamine residues by way of the 6-O-sulfotransferase (6OST)

or 3-O-sulfotransferase (3OST) enzymes respectively. Each of the 6OST and 3OST enzymes exists as multiple tissue-specific isoforms. The redundancy of multiple isoforms of the same gene allows for maintenance of function in the event of a loss-of-function mutation in one isoform.

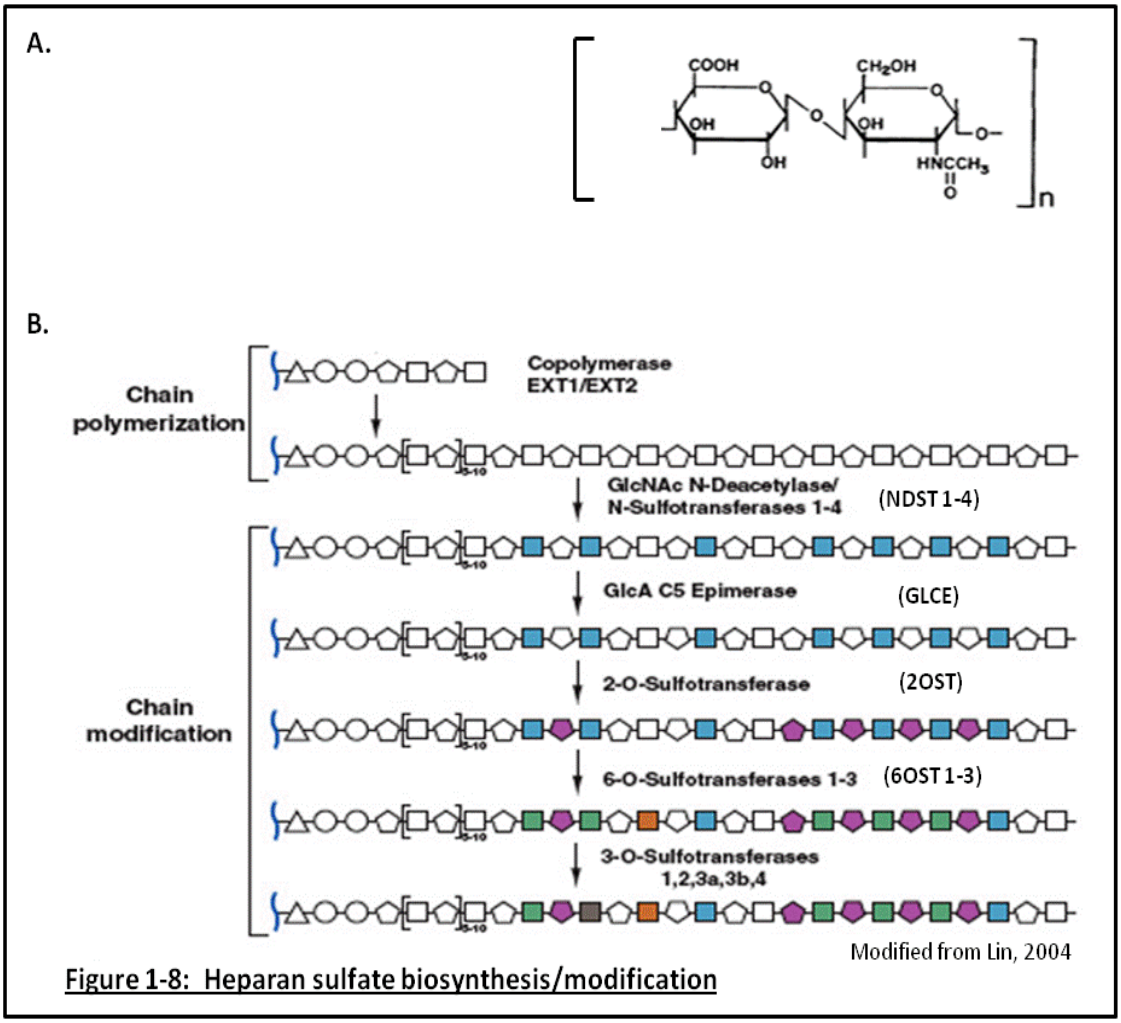

Figure 1-8: Heparan sulfate biosynthesis/modification

Twenty four unique GlcA-GlcNAc disaccharides can be produced by the variable action of these HSMEs. The number of possible modification patterns grows

exponentially when analyzing an entire HS chain that may reach 100 disaccharides in length. The HS chain generally contains short segments of highly modified sugars interspersed between unmodified regions of variable length (95). This variability in modification stems from the substrate specificity of each of the HSMEs as well as their tissue-specific and condition-specific expression levels. HS modification patterns, especially sulfation patterns, regulate how well an HSPG will be able to bind a growth factor. Thus Pln secreted from cells of different tissues or under different cellular conditions will have different capabilities of regulating growth factor signaling. I described above the importance of Pln's ability to regulate growth factor signaling in various cancers including prostate cancer. Due to the importance of sulfation to this ability I have focused on the role the enzyme 2OST plays in regulating the HS fine structure of Pln and subsequently its biological effects in prostate cancer cells.

2OST

As mentioned previously the 2OST enzyme catalyzes the transfer of sulfate from 3'-phosphoadenosine-5'-phosphosulfate (PAPS) to the C2 position of either GlcA or IdoA residues of maturing HS chains (96). HS with IdoA residues modified in this way have been found in virtually all HS preparations analyzed to date. The enzyme was originally cloned, purified and functionally verified in Chinese Hamster Ovary (CHO) cells by Kobayashi et al in 1997 (97). Since this breakthrough 2OST has been shown to be highly conserved from nematodes to vertebrates. Mutations of this gene in various organisms have shown a wide array of phenotypes that point to the essential function that 2OST plays in development. Hs2st-null mice were generated via a gene trap

strategy and resulted in renal agenesis, eye and skeletal defects, as well as neonatal lethality (98). A mutation in the hst-2 gene in *C. elegans* resulted in severe cell migration defects (99). Recently it was found that 2OST is essential for the FGF signaling required for chick limb bud outgrowth and development (100). The dHs2st homolog in *Drosophila* from the *Segregation disorder* locus has been functionally verified (101) and enzymatically characterized (102). dHs2st was also shown to affect FGF signaling in *Drosophila* tracheal formation (103). The expression dynamics of the 2-OST gene in zebrafish have also been elucidated (104). The focus of my research is to determine the effect knockdown of 2OST expression has on growth factor signaling in prostate cancer cells as well as to determine how changes in cellular stress conditions affect its expression.

Cellular Stress and Cancer

Many articles spanning scientific journals and mainstream media have addressed the effect of patient psychological stress on cancer onset and progression. However, the stress stimuli that cells within a tumor sense and respond to may be the much more important form of stress on which to focus. Cells respond to stress stimuli in various ways. They can either activate signaling pathways that promote their survival and recovery from the insult or activate cell pathways designed to eliminate the damaged cell. The first instinct is for self-preservation and recovery but if the insult is too great for the cell to respond to at that moment they choose the cell death pathway (105). Cellular or physiological stress can be present in many forms. My focus will be on

hypoxia (decreased availability of oxygen) and Reactive Oxygen Species (ROS) and their effect on tumor progression.

Hypoxia and Cancer

Solid tumors make up approximately 90% of all cancers and result in significant mortality due to cell invasion and metastasis to distant vital organs such as the brain and lungs (106). These tumors progress via rapid cellular proliferation and changes in the tumor microenvironment. A tumor can only grow to a certain diameter before it must obtain new vasculature via angiogenesis. The process of angiogenesis is designed to provide the oxygen and nutrients that tumor cells need to continue to progress. However, tumor cells generally grow at a rate that angiogenesis cannot keep up with. Also, tumor cells can still be deficient in both oxygen and nutrients after angiogenesis due to problems in vessel formation in the tumor that cause leakage and a reduced amount of oxygen in the blood due to cancer treatment-induced anemia (107). The oxygen diffusion limit through tissue has been measured at 150 microns (108). Due to this hypoxia, tumors generally contain a central core of necrotic cells when examined histologically. The lack of vasculature also has another drawback in the treatment of the disease in that chemotherapy drugs do not have an adequate delivery system into the tumor (109).

The hypoxic stress response of tumor cells can allow them to overcome the oxygen deficiency by inducing pathways that activate proteins involved in cell survival or metastasis that allows them to escape from the stressful environment. The key

transcription factor involved in mediating the hypoxic stress response is hypoxia inducible factor 1 (HIF1).

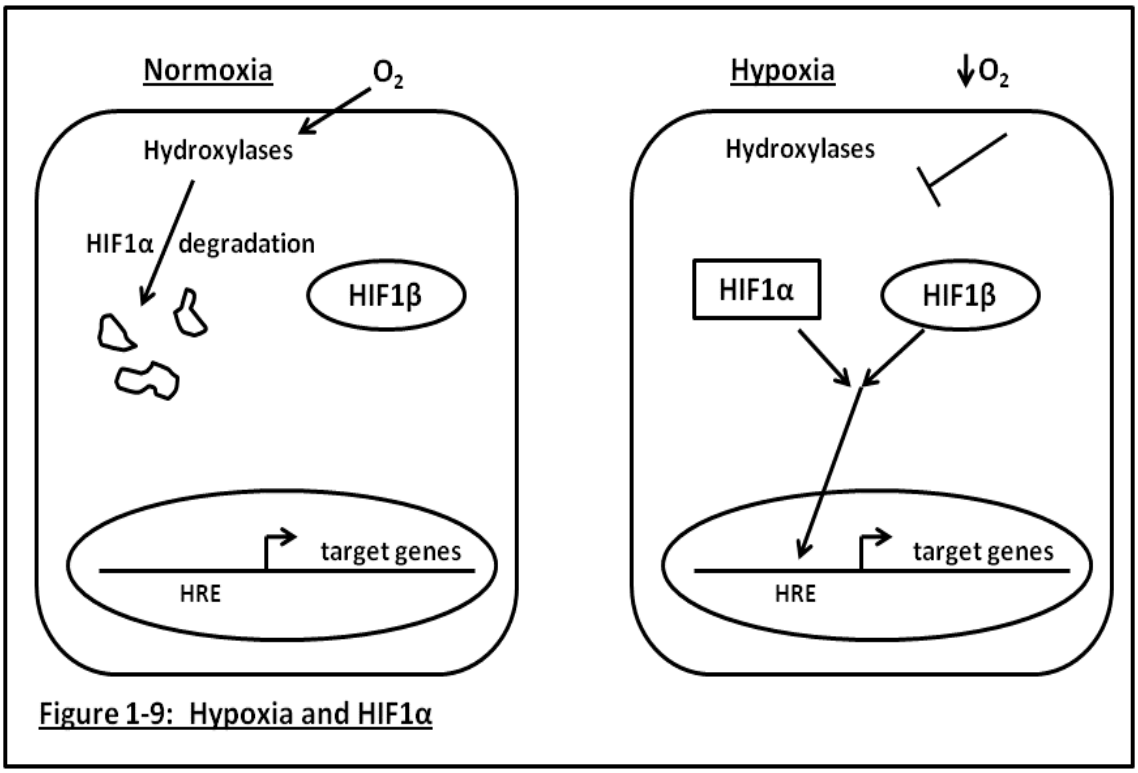

Figure 1-9: Hypoxia and HIF1α

HIF1 is a α/β heterodimeric complex of transcription factors (HIF1α and HIF1β) that induces a wide array of genes in response to oxygen deficiency. It was first identified by Semenza and colleagues as a regulator of erythropoietin expression (110). It binds to hypoxia responsive elements (HREs) in the promoters of these genes. It is estimated that 1-2% of the entire human genome contains HREs which leads to the upregulation or downregulation of gene transcription by HIF1 (111). Under normoxic conditions HIF1β is constitutively expressed but HIF1α is continually degraded by

oxygen-dependent prolyl hydroxylases that destabilize the protein and target it for the von Hippel-Lindau E3 ubiquitin ligase and ultimately proteosomal degradation (112). (Fig.1-9) Under hypoxic conditions, the hydroxylases are inhibited and HIF1α is stabilized which allows it to translocate into the nucleus, pair with HIF1β and regulate transcription of target genes. The genes that are upregulated in cancer are those involved in angiogenesis, cell survival/death, metabolism, pH regulation, cell adhesion, ECM remodeling, migration, and metastasis ((113), (114), (115)).

Hypoxia has been associated with virtually all solid tumors and prostate cancer is no exception. When analyzing prostate tumors with a polarographic needle oxygen electrode it was found that on average prostate cancer tissue had a partial pressure of oxygen of 2.4 mmHg while normal muscle tissue was 30 mmHg (116). Hypoxia has been shown to correlate with increased tumor invasiveness and metastasis (117). Hypoxia is also suggested to provide resistance to radiotherapy in vivo (118). Overall the effects of hypoxia and HIF1α have indicated a therapeutic target for solid tumors that must be addressed.

Oxidative Stress and Prostate Cancer

Oxidative stress is defined as a cellular situation in which the balance between free radicals, reactive oxygen species (ROS) and the endogenous antioxidant defense system is disturbed and shifted toward being pro-oxidant. This type of stress has been associated with processes such as DNA damage, proliferation, cell adhesion and survival. Generally the levels of ROS are increased during oxidative stress. There are two subgroups of ROS. The first subgroup is made up of oxygen containing free

radicals such as superoxide (O_2^-) and the second subgroup consists of non-radical ROS such as hydrogen peroxide (H_2O_2). It is estimated that 1-3% of pulmonary oxygen intake by humans is converted into ROS (119). These reactive species can be acquired via the environment from pollutants, tobacco smoke, and radiation as well as from inside the cell due to the activity of the electron transport chain in the mitochondria and the enzyme NADPH oxidase in the cytosol ((120), (121)).

The cellular defense against these damaging species are ROS scavengers such as superoxide dismutases (ie MnSOD and CuZnSOD) which convert superoxide radicals into peroxide which is in turn converted into water via peroxidases. Loss of this defense system has been linked to many types of cancers. CuZnSOD knockout mice have an increased rate of liver cancer in late life (122). MnSOD knockout mice die soon after birth due to the deleterious effects of a large increase in ROS (123). Heterozygotes of MnSOD mice are able to live to adulthood but have increased rates of many cancers (124). Mice deficient in peroxidase activity have an increased rate of intestinal cancers (125).

One of the most studied results of ROS accumulation is the radiation-induced direct damage of DNA brought about by the formation of 8-hydroxy-2'-deoxyguanosine by the hydroxyl radical OH^- (126). However, oxidative stress is also an important regulatory mechanism for other processes involved in cancer progression. Many of these processes depend on the cell type and the level of ROS accumulation (127). For example, in "normal cells" high levels of ROS generally promote apoptosis due to the amount of damage to proteins, DNA and membranes. However in some malignant cells

ROS has the opposite effect. Overexpression of NADPH oxidase (NOX), a major contributor of cellular ROS, is anti-apoptotic in pancreatic cancer cell lines (128). This is thought to be the result of oxidative inactivation of caspases involved in apoptosis (127). ROS also promotes cellular proliferation. NIH-3T3 cells transfected with the ras oncogene displayed increased superoxide production due to increased NOX activity and promoted abnormal proliferation (129). As if ROS had not done enough to promote carcinogenesis and tumor progression, it also promotes metastasis by the expression and activation of matrix metalloproteases that degrade the ECM (130). The accumulation of ROS correlates with the metastatic potential of cancer cells when compared to normal or benign cells (131). The effect of ROS has also been seen in prostate cancer cells. These cells have increased levels of mutations in their mitochondrial DNA that increase the levels of ROS (132). Also overexpression of NOX1 in prostate cancer cell lines leads to the overproduction of superoxide radicals that increase cellular proliferation and angiogenesis (133).

As discussed the accumulation of ROS in cancer cells has many effects that promote the progression of tumors. One of the principal effects of ROS accumulation is the regulation of gene expression via activation of stress-activated protein kinases (SAPKs). Four examples of ROS-induced SAPKs are Src, Abl, c-Jun N-terminal kinase (JNK) and p38 MAPK. These kinases are used to activate transcription factors that induce expression of genes involved in cancer progression. I will focus on two ROS-inducible transcription factors: nuclear factor kappa B (NFkB) and activating transcription factor 2 (ATF2). (Fig.1-10)

The NFkB transcription factor has been associated with the processes of inflammation and cancer for many years. It is a member of the Rel family of transcription factors, is ubiquitously expressed and forms both homodimers and heterodimers with other members of the family to control gene expression (Verma, 1995). NFkB was originally identified in B cells as the transcriptional activator of the kappa immunoglobulin light chain gene (134). Since this discovery it has been shown to activate many types of genes usually involved in cellular defense (135). Under normal conditions where no stress is being perceived by the cell NFkB is sequestered in the cytoplasm by the protein Inhibitor of NFkB (IkB). Upon stimulation by cellular stress, protein kinases phosphorylate IkB Kinase (IKK) which in turn phosphorylates IkB leading to IkB ubiquitination and degradation by the proteosome. This allows NFkB to translocate into nucleus, dimerize with its partner and activate transcription. NFkB-induced gene expression affects many different cellular processes. It is anti-apoptotic in that mice with a deficiency of the p65 subunit of NFkB are embryonic lethal due to massive apoptosis in the liver (136). NFkB activates many anti-apoptotic proteins such as bcl-2, TRAF1 and TRAF2. It has also been shown to activate genes involved in cell growth, proliferation, angiogenesis, and metastasis.

NFkB is activated by several SAPKs. These kinases are responsible for phosphorylating downstream kinases that ultimately activate IKK which relieves the repression of IkB on NFkB allowing NFkB to enter the nucleus. Src and Abl kinases are also activated by oxidative stress. These kinases phosphorylate either Protein Kinase D (PKD) or Protein Kinase C γ (PKCγ) which in turn phosphorylate IKK on certain tyrosine residues (137). Oxidative stress has also been shown to activate JNK ultimately resulting in the activation of NFkB though the exact mechanism is yet unknown (135). Constitutively activated NFkB is present in many types of cancer such as lymphomas, leukemias, and many solid tumors including prostate cancer (138). It is constitutively activated in a number of prostate cancer cell lines as well as xenografts ((139), (140)). In these cell lines, NFkB activation was inversely correlated with Androgen Receptor (AR) signaling. The highly metastatic lines that have lost their AR signaling had the highest amount of nuclear NFkB. Blockade of NFkB activity in highly metastatic prostate cancer cells resulted in slow growing tumors and decreased metastatic ability when inoculated into nude mice (141).

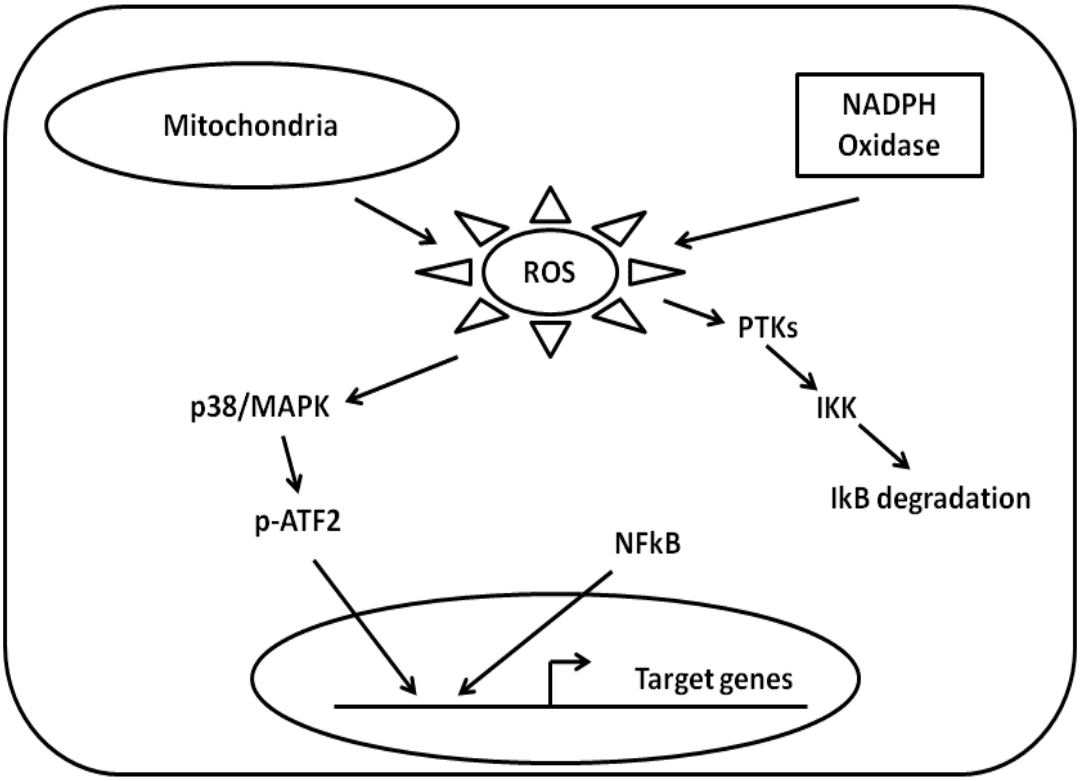

Figure 1-10: Reactive Oxygen Species, NFkB and ATF2

The ROS-inducible p38 mitogen activated protein kinase (MAPK) regulates gene expression by the direct phosphorylation of a variety of transcription factors. Activation of the ATF2 transcription factor has been directly linked to p38 MAPK because inhibition of p38 results in decreased phosphorylation of ATF2 and subsequent decrease in proliferation (142). (Fig.1-10) Transcription activation via the p38/ATF2 pathway has been seen in cell cycle genes such as cyclin D1, genes involved in invasion such as MMP2 and urokinase plasminogen activator, cytokines such as IL-8, cell adhesion molecules such as E-selectin and anti-apoptotic genes such as bcl-2 (143).

ATF2 is a member of the ATF/CREB family of bZIP transcription factors. All of the members of this family share the ability to respond to environmental signals such as oxidative stress (143). These transcription factors can homodimerize or heterodimerize with other members of the family to regulate gene expression by directly binding promoters. ATF2 knockout mice demonstrate the requirement for the transcription factor in skeletal and central nervous system development as well as maximal induction of genes with cAMP Response Elements (CRE) in their promoters (144).

The consensus binding site for ATF2 is TGACGT(C/A)(G/A) (145). ATF2 overexpression in multiple human and mouse cancer lines results in increased cell proliferation. ATF2 localization has been extensively analyzed in prostate cancer patients. Immunohistochemical analysis reveals that levels of nuclear localized, phosphorylated ATF2 is increased in benign tumors as compared to normal tissue and is even higher in advanced tumors. These results along with gene expression data suggest that ATF2 promotes both cell survival and proliferation (146). ATF2 has also been implicated in the progression of breast cancer, leukemias, melanoma, and lung cancer (143).

Cell Line Models of Prostate Cancer Progression

Immunohistochemical analysis of protein levels in prostate cancer patients has revealed many correlations between stage of disease and the increasing or decreasing amount of a protein. However, in order to gain a mechanistic understanding of the key events that promote prostate cancer progression one must look to models that reflect the system under study. Over the years several different cell models have been developed to

address these types of questions in prostate cancer. This has not been an easy task in that only rats, dogs and humans have been shown to spontaneously develop prostate cancer (147). Several different in vivo models of prostate cancer have been used with the Dunning rat model and subsequent sublines being the most studied. These cell lines have yielded substantial evidence as to the effects of androgen ablation therapy as well as epithelial-stromal interactions in prostate cancer (147). Canine models of the disease are used mainly to study metastasis to bone and knockout and transgenic mouse cell lines can also be used to study a multitude of cancer processes. Nonetheless, prostate cancer is primarily a human disease and thus models of human origin are usually more revealing on the actual nature of the disease. I have taken advantage of two different human cell line models of prostate cancer progression to address the questions of my research. Both of these models begin with the trademark benign cell line in prostate cancer research LNCaP.

The LNCaP prostate cancer cell line was originally derived from a supraclavicular lymph node metastasis of a primary prostatic carcinoma (148). It was shown to be weakly tumorigenic when inoculated into nude male mice. This line displays characteristics of early stages of prostate cancer in that it is sensitive to androgen signaling. However, it has also been shown to be sensitive to anti-androgens due to expression of a mutated androgen receptor (149). LNCaP also mimics early stage disease in that these cells secrete low levels of prostate specific antigen (PSA) (148). The first prostate cancer progression cell line model that I will describe was originally developed in the laboratory of Leland Chung ((150), (151)). This series of lines was

established via serial transplantation of cancer cells into nude mice. The C4 subline was developed by subcutaneous co-inoculation of LNCaP cells with non-tumorigenic MS fibroblasts from bone into intact male nude mice. The resulting tumors were allowed to grow for eight weeks, the mice were castrated, and then tumors were extracted and expanded into cell culture four weeks after castration. The resulting C4 cells show higher levels of PSA expression than LNCaP, produce approximately 10 times more colonies in soft agar, and are androgen-sensitive. The next subline in the series is C4-2 which was developed by co-inoculation of C4 cells with MS fibroblasts into a castrated male host where they were allowed to form tumors for 12 weeks, whereupon the cells were expanded into cell culture. The resulting C4-2 cells are highly tumorigenic on their own, androgen-insensitive, and metastasize to both the lymph node and bone. The final subline of the series is C4-2B which was developed by inoculation of C4 cells either subcutaneously or orthotopically into a castrated male host and selected for their ability to rapidly metastasize to the bone. This subline mimics the most advanced stage of prostate cancer. C4-2B cells are androgen-insensitive, secrete the highest levels of PSA and exhibit the highest rate of metastasis and invasion.

The other cell line model of prostate cancer progression that I will describe consists of three independent cell lines beginning with the aforementioned weakly tumorigenic LNCaP line and progressing with two lines of increasing metastatic potential, DU145 and LN4. The DU145 cell line was originally derived from a metastasis of a primary prostatic adenocarcinoma in a human patient (152). These cells grow slowly but produce large colonies in soft agar, are androgen-insensitive, and are

moderately metastatic. The most metastatic cell line of the series is PC3M-LN4 (LN4). This cell line was derived from the androgen-insensitive PC3 cell line that was originally derived from a bone metastatic lesion. PC3 cells were inoculated into nude mice and a resulting liver metastasis was expanded into the PC3M cell line. These cells were used for four rounds of serial orthotopic implantation and the resulting lymph node metastasis of the fourth round was expanded into the highly metastatic LN4 cell line. This line is rapidly growing, androgen-insensitive, and metastasizes to both regional and distant sites such as the abdomen and bone (153).

The purpose of this study was to evaluate two different models in which increased extracellular HS may drive prostate cancer progression. First I wanted to determine whether upregulation of an HS modification enzyme could contribute to metastatic behaviors as upregulation of the HSPG protein core Pln has already been shown to do. Secondly, I wanted to investigate whether increased expression of the Pln protein core and the 2OST enzyme is due to a common general mechanism, specifically stress responses that increase in prostate cancer cell lines with increasing metastatic potential.

From previous work in our lab and those of our collaborators, we identified two subsets of prostate tumors. It was observed that 54% of tumors in this study had increased levels of Pln that correlated with increasing Gleason Grade while the remaining 46% either maintained or had decreased levels of Pln but still progressed to advanced disease. I set out to determine possible molecular mechanisms for both of these subsets.

CHAPTER II

STRESS-ACTIVATED TRANSCRIPTION FACTORS STIMULATE PERLECAN EXPRESSION IN A MODEL OF PROSTATE CANCER PROGRESSION

Prostate cancer is the second leading cause of cancer mortality in American men, behind only lung cancer in its severity (1). Determining the molecular mechanisms that regulate the progression of prostate cancer is of utmost importance. Perlecan (Pln) is a heparan sulfate proteoglycan that is secreted into the extracellular matrix and regulates many growth factor signaling pathways that are essential to prostate cancer progression (154). The Datta lab and their collaborators recently found that the PLN gene is located in a region of chromosome one with a statistically significant genetic association between prostate cancer and the brain tumor glioblastoma multiforme termed carcinoma prostate brain or CAPB locus (93). Immunohistochemistry of Pln protein secreted into the lumen of prostate cancer revealed that Pln is present in 54% of malignant prostate cancer glands but not normal glands and is significantly upregulated in invasive tumors when compared to benign tissue or high grade prostatic intraepithelial neoplasia. Pln expression correlated with tumors of higher Gleason score and those with increased prostate cell proliferation. Analysis of Pln mRNA in normal and tumor tissues correlated well with the data derived from tissue microarrays. This increase in Pln protein and message levels in malignant versus normal tissue led me to seek to determine the mechanisms by which Pln expression is upregulated in prostate cancer progression.

The rapid proliferation of malignant cells to form a solid tumor generally results in a situation of cellular stress. Cells within a tumor can respond to this stressful situation in various ways. They can choose to eliminate themselves through programmed cell death if the stress insult is too severe or decide to activate genes that are involved in cell survival and the ability to recover from the insult. Therefore, cellular stress is a mechanism of selection for cells within a tumor that will progress to more advanced disease. One source of cellular stress is decreased availability of oxygen, or hypoxia. A solid tumor generally cannot grow larger than 2-5 mm in diameter before obtaining its own blood supply (43). However, tumor cells usually grow at a rate that exceeds the requirement for new blood vessels. The resulting hypoxia stabilizes the transcription factor hypoxia-inducible factor 1 α (HIF1α) which heterodimerizes with HIF1β in the nucleus and activates transcription of target genes (112). The genes activated by the HIF heterodimer in cancer are those involved in angiogenesis, cell survival, metabolism, cell adhesion, migration, metastasis and many other cellular processes ((113), (114, 155)). Prostate tumors are hypoxic (118) and this correlates with their tumor invasiveness and metastasis (117). HIF1α is overexpressed in prostate tumors (156) as well as in rat and human prostate cancer cell lines (157), making hypoxia and the HIF transcription factor potential candidates for generating upregulation of Pln expression. Another source of cellular stress is reactive oxygen species (ROS). ROS are generated by many different mechanisms. The major source of ROS is the mitochondria where increased electron transport chain activity or mutations in mitochondrial DNA cause ROS to accumulate in the cytosol of prostate cancer cells and

activate signaling pathways (132, 158). Another extra-mitochondrial source of ROS is the cytosolic enzyme NADPH oxidase (NOX). Accumulation of ROS activates a number of stress-activated protein kinases that are used to activate transcription factors to induce expression of genes involved in cancer progression. Nuclear factor kappa B (NFkB) is a ROS-inducible transcription factor that is constitutively activated in many cancers including prostate cancer (138). The ROS-inducible p38 MAPK regulates gene expression by direct phosphorylation of a variety of transcription factors. Activation of ATF2 has been directly linked to p38 MAPK because inhibition of p38 results in decreased phosphorylation of ATF2 and a subsequent decrease in proliferation (142). Transcription activation via the p38/ATF2 pathway has been seen in cell cycle genes such as cyclin D1, genes involved in invasion such as MMP2 and urokinase plasminogen activator, cytokines such as IL-8, cell adhesion molecules such as E-selectin and anti-apoptotic genes such as bcl-2 (143). Phosphorylated ATF2 is strongly overexpressed in prostate tumors compared to normal tissue (146). ATF2 is pro-proliferative and plays a role in prostate cancer progression (143). These characteristics make ROS signaling through the p38/ATF2/NFkB pathway another attractive candidate for stimulating increased expression of Pln.

In the present study the role of stress-activated transcription factors in the overexpression of the PLN gene in prostate cancer progression was investigated using a cell line model of prostate cancer progression that overexpresses Pln as observed in a subset of prostate cancer patients. My results also show that Pln modulates SHH, FGF, Wnt, and TGFβ signaling in this model. I observed that the proximal Pln promoter

contains consensus binding sites for the transcription factors HIF1α, NFkB and ATF2. SiRNA-mediated knockdown of each transcription factor resulted in significantly reduced levels of Pln mRNA. Overexpression of a stabilized HIF1α resulted in increased levels of Pln in more metastatic cell lines. Inhibition of ROS mediated signaling pathways also resulted in decreased levels of Pln with the more metastatic lines being the most sensitive. Chromatin immunoprecipitation analysis revealed that HIF1α directly binds the Pln promoter, NFkB binds in the most metastatic cell line, and the effect of ATF2 is indirect in all cell lines and no physical interactions with the Pln promoter were detected.

Materials and Methods

Cell Lines and Culture Conditions

LNCaP, DU145, and PC3M-LN4 (LN4) cell lines were obtained from ATCC and cultured in RPMI 1640 medium supplemented with 10% fetal bovine serum and 5% Pen-Strep. Cells were maintained at 37^{o}C and 5% CO_2.

Reagents and Antibodies

SB202190 (Cat. # S7067) and diphenyliodonium chloride (DPI) (Cat. # 43088) were purchased from Sigma Aldrich. Primary antibodies purchased from Santa Cruz Biotechnology (SCBT) are as follows: mouse anti-β-catenin (sc-7963, 1:500), mouse anti-phospho-ERK (sc-81492, 1:1000), rabbit anti-phospho-SMAD2/3 (sc-11769, 1:1000), mouse anti-phospho-ATF2 (sc-52941, 1:500). Purified mouse anti-β-actin antibody (A5316, 1:1000) was purchased from Sigma Aldrich. Anti-mouse HRP and anti-rabbit HRP secondary antibodies (1:10,000) were purchased from Jackson Labs.

Antibodies for chromatin immunoprecipitation were used at a final concentration of 0.3 mg/mL and as follows: mouse anti-HIF1α (Novus Biologicals #NB100), rabbit anti-ATF2 (SCBT sc-6233), and rabbit anti-NFkB p65 (SCBT sc-109).

Transient Transfections

Transient transfections of siRNA were performed using Lipofectamine 2000 reagent (Invitrogen #11668027) according to manufacturer's protocol. Briefly cells were cultured in 6-well plates and allowed to attach for 24 hours. siRNA was applied and cells were harvested for either protein or RNA after 24 hours. Scrambled siRNA was used as the negative control. Transient transfection of stabilized HIF1α (stHIF1α) (a kind gift from Dr. Eric Huang) was also performed using Lipofectamine 2000 reagent according to manufacturer's protocol.

RNA Isolation and Real-Time PCR

Cells were grown to 80-90% confluence, scraped, centrifuged and washed with PBS. RNA isolation was performed with Qiagen RNEasy Mini-kit (#74104) according to manufacturer's protocol. 2 μg of RNA was used in each DNAse I reaction using DNAse I Amplification Grade from Invitrogen (#18068). Reverse transcription was performed with oligo dT and random hexamer primers using SuperScript III reverse transcriptase from Invitrogen (#18080044). Real-time PCR was performed using Taqman Gene Expression Assays with Taqman Universal PCR Master Mix from Applied Biosystems (#4324018). Each sample was run in triplicate at three different concentrations and normalized to levels of 18S rRNA. Reactions were performed using

a BioRad C1000 Thermal Cycler machine. Data for each sample is presented as the mean fold change compared to control and error is presented as standard deviation.

Western Blotting

Isolation of total protein was done using the Mammalian Cell Lysis Kit from Sigma Aldrich (#MCL-1KT) according to manufacturer's protocol. Phosphatase inhibitors were used for each sample (Sigma Aldrich #P0044). Samples were prepared and run on 15% SDS-PAGE and transferred onto nitrocellulose. Western blots were developed with Pierce ECL Western Blotting Substrate (#32106). Images and densitometry were obtained on a BioRad ChemiDoc XRS machine using Quantity One software. Densitometry values represent the mean of two independent experiments.

Chromatin Immunoprecipitation

LNCaP, DU145, and LN4 cells were cross-linked by adding formaldehyde directly to cell culture medium to a final concentration of 1%. Cross-linking was allowed to proceed for 10 minutes at room temperature then stopped with addition of glycine to a final concentration of 0.125 M. Cells were washed twice with ice-cold PBS and swollen with PBS for 10 minutes at 37^{o}C. Cells were scraped, washed once with PBS then pelleted by centrifugation. Pellets were resuspended in Cell Lysis Buffer (5 mM PIPES pH 8.0, 85 mM KCl, 0.5% Triton X-100, protease inhibitor cocktail) for 10 minutes on ice. Cellular extract was pelleted by centrifugation then nuclei were resuspended in Nuclei Lysis Buffer (50 mM Tris-Cl pH 8.0, 10 mM EDTA, 1% SDS, protease inhibitor cocktail) for 10 minutes on ice.

Total chromatin was then sonicated for twelve 20 second pulses at setting 2. After centrifugation chromatin was pre-cleared with Protein A/G Plus Beads then divided into aliquots. Antibody was added to each aliquot for a final concentration of 0.3 mg/mL and incubated on a rotating platform overnight at 4^{o}C. Antibody-protein complexes were immunoprecipitated with Protein A/G Plus Beads. Samples were washed extensively and eluted in Elution Buffer (50 mM $NaHCO_3$, 1% SDS). Bound DNA fragments were isolated and analyzed by PCR. ChIP primers were used to amplify a short portion of the Pln promoter. Primers used to amplify the region from -1199 to -964 (H1 and A2) were: 5'-aggcactgtgattagtgggtgaga-3' and 5'-cggcctcagcctcctgaata-3'. Primers used to amplify the region from -697 to -470 (H2) were: 5'-ccctggtggaggtgagagtt-3' and 5'-ggatctccttcccacgctca-3'. Primers used to amplify the region from -1786 to -1557 (A1 and N2) were: 5'-atgagaggccccaatgtgct-3' and 5'-gaaaacctttgagtaatgatagaggagga-3'. Primers used to amplify the region from -2500 to -1970 (N1) were: 5'-cggacagggagtttccaagtg-3' and 5'-gctccaggcacagcactga-3'.

Promoter Analysis

Prediction of transcription factor binding sites in the PERLECAN promoter was done with the ALGGEN-PROMO prediction program.

Results

Perlecan Expression Increases Significantly with Increasing Metastatic Potential and Modulates Growth Factor Signaling in a Cell Line Model of Prostate Cancer Progression

Expression of the PLN gene is upregulated in 54% of prostate cancers (93). I sought to identify an in vitro cell model of disease progression that demonstrated the increasing levels of Pln that correlated clinically with increasing metastatic potential. The cell line LNCaP was chosen as the least tumorigenic line of the model. The LNCaP prostate cancer cell line was originally derived from a supraclavicular lymph node metastasis of a primary prostatic carcinoma (148). It has shown to be weakly tumorigenic when inoculated into nude mice, is non-metastatic and androgen-sensitive. DU145 was chosen as the next cell line of the model. DU145 was originally derived from a brain metastasis, is tumorigenic in mice, moderately metastatic, and androgen-insensitive (152). LN4 was the chosen as the final cell line of the series. LN4 is a subline of the PC3 cell line which was originally derived from a bone metastasis as is androgen-insensitive (153). The LN4 subline was developed from PC3 based on its rapid metastasis to the lymph node and bone in mice.

To determine if Pln expression is upregulated with increasing metastatic potential of this cell line series, I evaluated Pln mRNA levels in each cell line via quantitative real-time PCR. Each of the cell lines were grown at standard conditions and mRNA was isolated at 80% confluence. Pln levels in DU145 and LN4 were normalized to those in the least metastatic cell line LNCaP which was set to 1. Pln expression increased 20-fold in DU145 and 50-fold in LN4 (Fig. 2-1A). These results demonstrate that I have identified a cell line model of prostate cancer progression that mimics the upregulation of Pln expression observed clinically and correlates with increasing metastatic potential. To determine if Pln modulates growth factor signaling in my cell line model, I evaluated commonly used assays to determine levels of SHH, FGF, Wnt, and TGFβ signaling in cells transfected with Pln RNAi. To verify that Pln levels were down-regulated by Pln RNAi in each cell line I used qRT-PCR to compare cells transfected with the RNAi (grey bars) to cells transfected with scrambled negative control RNAi (black bars). Pln RNAi decreased levels of Pln approximately 70% in each of the cell lines (Fig. 2-1B). To determine the effect of Pln RNAi on SHH signaling, I performed qRT-PCR and evaluated levels of the response genes *PTCH* (black bars) and *GLI1* (grey bars).

SHH signaling was decreased approximately 20% in LNCaP and 80-90% in DU145 and LN4 (Fig. 2-1C). To determine the effect of Pln RNAi on FGF signaling, I performed quantitative western blots analyzing levels of phospo-ERK. Densitometry shows that phospho-ERK levels were decreased 70% in LNCaP and DU145 and approximately 50% in LN4 when using levels of actin as a normalization control (Fig. 2-1D). I then assayed levels of β-catenin as a readout of the effect of Pln RNAi on Wnt signaling. Levels of β-catenin were increased 4.9, 2.2, and 3.6 fold in LNCaP, DU145, and LN4 respectively (Fig. 2-1E). Finally, I assayed the effect of Pln knockdown on TGFβ signaling by performing quantitative western blots for phospho-SMAD 2/3 while once again using actin as a normalization control. Levels of phospho-SMAD were decreased approximately 85% in all three cell lines transfected with Pln RNAi (Fig 2-1F). Overall, I have demonstrated that Pln modulates essential growth factor signaling pathways in this model of prostate cancer progression.

Figure 2-1: Perlecan is upregulated and modulates growth factor signaling in cell line model of prostate cancer progression. A.) Relative Pln mRNA levels as assayed by Real-time PCR. LNCaP, DU145, and LN4 cells were seeded in 6-well culture plates and allowed to grow for 24 hours. RNA was isolated as described in Materials & Methods. Real-time PCR was performed in triplicate at three different concentrations. Levels of Pln were normalized to levels of 18S rRNA for each sample. Pln levels for DU145 and LN4 are normalized to LNCaP at 1. Error bars indicate standard deviation. B.) Inhibition by Pln RNAi in LNCaP, DU145, and LN4 verified by Real-time PCR. Black bars represent cells treated with scrambled negative control RNAi and gray bars represent cells treated with Pln RNAi. Pln RNAi samples were normalized to control at 1. Error bars indicate standard deviation. C.) Decreased SHH signaling in cells treated with Pln RNAi. Real-time PCR analysis of SHH pathway response genes PTCH and GLI1. Error bars indicate standard deviation. Asterisk indicates $p < 0.05$. D.) Decreased FGF signaling in cells treated with Pln RNAi. Western blotting for phospho-ERK and β-actin performed as described in Materials & Methods. Levels of p-ERK are normalized to β-actin. Densitometry figures are shown below each sample and are representative of two independent experiments. E.) Increased Wnt signaling in cells treated with Pln RNAi. Levels of β-catenin normalized to β-actin. F.) Decreased TGFβ signaling in cells treated with Pln RNAi. Levels of p-SMAD 2/3 normalized to β-actin.

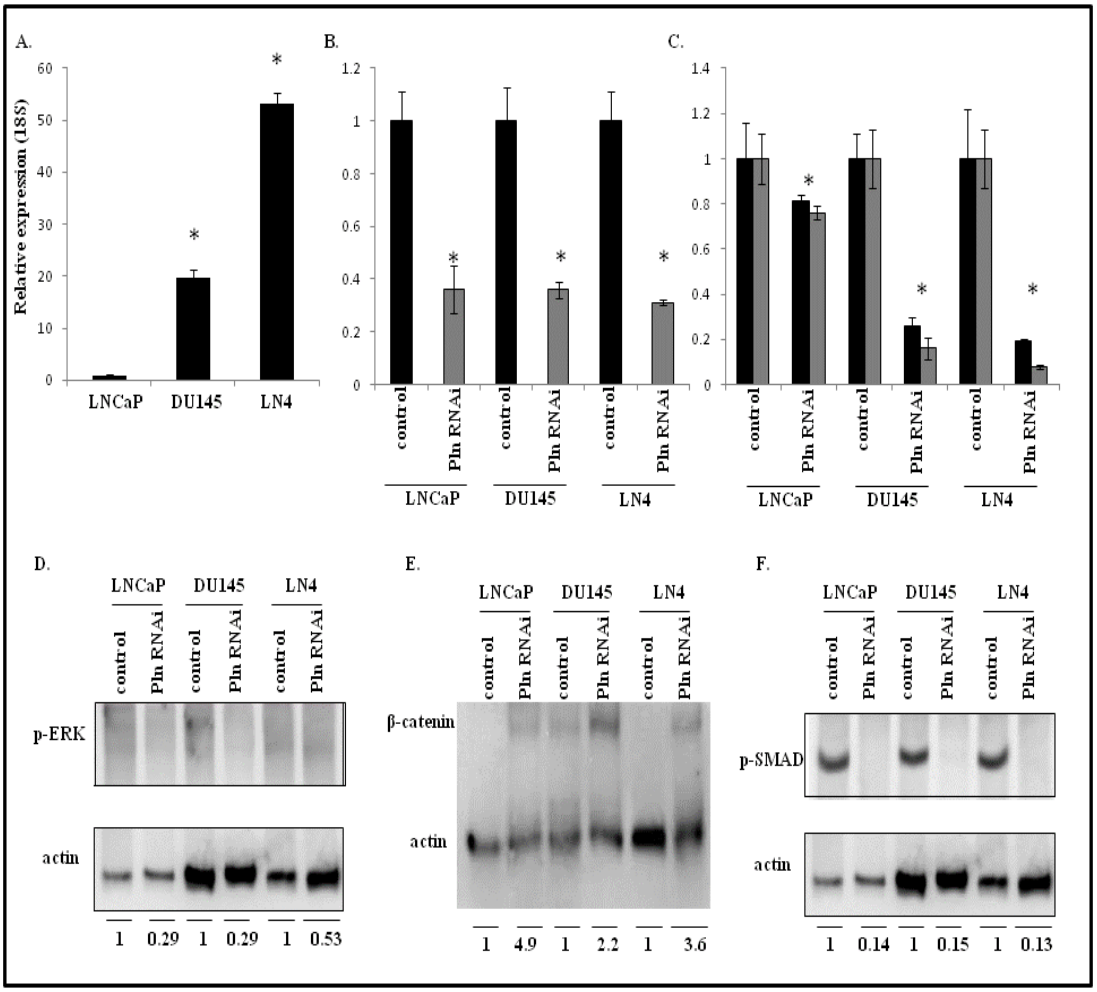

HIF1α Activates Transcription of Perlecan

Hypoxia has been shown to correlate with increased tumor invasiveness and metastatic potential (117). The presence of low amounts of oxygen is sensed by the cell and results in the stabilization of the HIF1α transcription factor that is then able to activate transcription of genes involved in the hypoxic tumor cell response by binding to Hypoxia Response Elements (HREs) in the promoter of the genes (155). To determine if

HIF1α stimulates transcription of Pln, I first analyzed the sequence of the PLN promoter to see if it contained HREs that bind HIF1α. Two regions of the PLN promoter (H1 and H2) contained putative HREs (Fig. 2-2A, H1 and H2). To determine if overexpression of HIF1α affected levels of Pln mRNA, I transfected each cell line of the model with a vector expressing a stabilized form of HIF1α (stab. HIF1α, grey bars) and compared that to a vector only control (black bars). qRT-PCR analysis of each sample resulted in a slight decrease in Pln levels in LNCaP cells while Pln was increased 2-fold in DU145 and LN4 cells (Fig. 2-2B). Western blot analysis showed that HIF1α accumulated in cells transfected with the stabilized HIF1α transgene (data not shown). To determine if RNAi-mediated knockdown of HIF1α expression affected levels of Pln mRNA, I analyzed levels of both HIF1α (grey bars) and Pln mRNA (white bars) in samples transfected with HIF1α RNAi compared to control RNAi samples (black bars) (Fig. 2-2C). HIF1α levels were decreased 90% in LNCaP and DU145 and 40% in LN4 while Pln mRNA was decreased 50%, 75%, and 50% in LNCaP, DU145, and LN4 respectively. These results demonstrate that HIF1α stimulates Pln expression in prostate cancer cells.

To determine if the effect of HIF1α on Pln transcription is direct or indirect, I performed chromatin immunoprecipition (ChIP) assays in each cell line of the series. HIF1α directly binds the VEGF promoter (43) and primers for this promoter flanking HREs were used as a positive control (PC). PCR analysis of chromatin pulled down with HIF1α IP demonstrated that HIF1α does indeed bind this promoter in the three cell lines of the model (Fig. 2-2D, top panels). PCR analysis using primers flanking the H1 and H2 regions of the PLN promoter showed that HIF1α binds directly to both sites in the LN4 cell line while only the H2 site is bound in LNCaP and DU145 (Fig. 2-2D). These results demonstrate that HIF1α is necessary for optimal Pln expression and the transcription factor binds directly to the PLN promoter to increase transcription.

Perlecan Transcription Is Activated by NADPH Oxidase Signaling and NFkB

Recently Kumar et al analyzed levels of ROS in LNCaP, DU145, and PC3 prostate cancer cells (159). They found that oxidative stress is inherent to these cells and that PC3 had the highest levels of ROS. The group also found that the extra-mitochondrial ROS generator NADPH Oxidase (NOX) is critical for the malignant phenotype of these cells.

Figure 2-2: HIF1α activates Pln expression in model of prostate cancer progression. A.) Schematic of PLN promoter with regions of HREs (H1 and H2). B.) LNCaP, DU145 and LN4 cells were transfected with vector expressing stHIF1α. Real-time PCR for Pln levels normalized to 18S levels in each sample. Black bars represent control vector alone transfected samples and gray bars represent stHIF1α transfected samples. Error bars indicate standard deviation. C.) Inhibition of HIF1α by RNAi results in decreased levels of Pln mRNA. Real-time PCR analysis of HIF1α and Pln normalized to levels of 18S. Black bars represent samples treated with scrambled RNAi treated samples, gray bars represent HIF1α levels in HIF1α RNAi treated cells, white bars represent Pln levels in HIF1α RNAi treated cells. Error bars indicate standard deviation. Asterisk indicates $p < 0.05$. D.) HIF1α binds directly to the PLN promoter at predicted HREs. Chromatin Immunoprecipitation analysis of LNCaP, DU145 and LN4 total chromatin, HIF1α IP, no antibody (NoAB) and Mock samples. Samples were analyzed by PCR with primers flanking each HRE site. Positive control primers were used from the VEGF promoter (43).

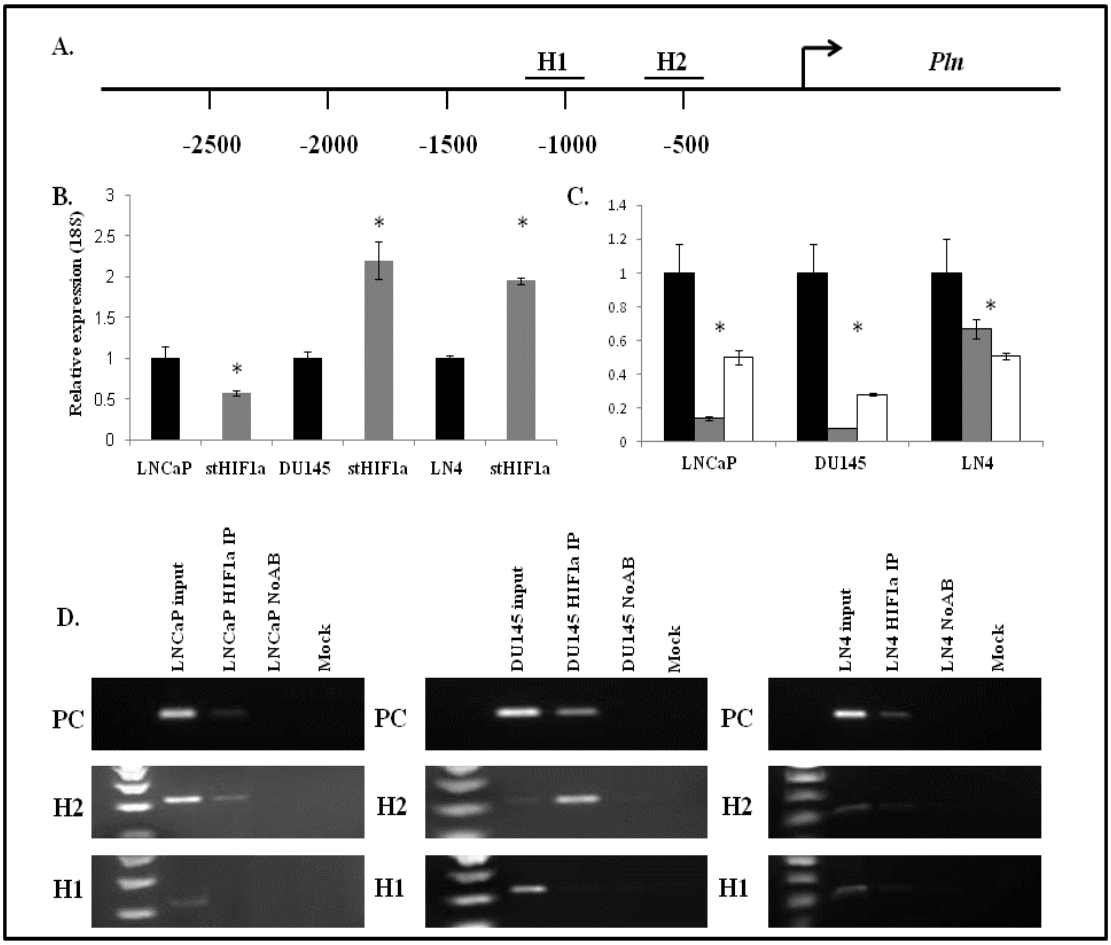
A.
H1
H2
Pln
-2500
-2000
-1500
-1000
-500
B.
Relative expression (18S)
LNCaP
stHIF1a
DU145
stHIF1a
LN4
stHIF1a
C.
LNCaP
DU145
LN4
D.
LNCaP input
LNCaP HIF1a IP
LNCaP NoAB
Mock
DU145 input
DU145 HIF1a IP
DU145 NoAB
Mock
LN4 input
LN4 HIF1a IP
LN4 NoAB
Mock
PC
H2
H1

To determine if ROS generation by NOX affects Pln expression in the LNCaP-DU145-LN4 cell line series, I evaluated Pln mRNA levels in cells treated with varying concentrations of the specific NOX inhibitor diphenyliodonium (DPI) by qRT-PCR (Fig. 2-3B). DPI treatment in LNCaP resulted in a slight increase in Pln expression at 20 μM but an 80% decrease at 40 μM. Pln levels in DU145 decreased in a dose-dependent manner at 20 and 40 μM. DPI treatment in LN4 resulted in a 75% decrease in Pln mRNA at 20 μM and a 60% decrease at 40 μM. These results indicate that NOX activity stimulates Pln transcription in prostate cancer cells. One possible way that NOX-induced accumulation of ROS could activate Pln expression is through the ROS-inducible transcription factor NFkB. I analyzed the PLN promoter and found two regions that contained putative NFkB binding sites (Fig. 2-3A, N1 and N2). To determine if knockdown of NFkB expression by RNAi results in a decrease in Pln expression, I assayed NFkB (grey bars) and Pln (white bars) mRNA levels in cells treated with NFkB RNAi or with scrambled negative control RNAi (black bars) (Fig. 2-3C). NFkB knockdown was successfully decreased 50-60% in all three cell lines. In cell treated with NFkB RNAi, Pln levels were decreased approximately 70% in LNCaP and DU145 and 30% in LN4.

These results indicate that NFkB stimulates Pln expression in prostate cancer cells. To determine if NFkB binds directly to the Pln promoter I performed ChIP assays in each of the three cell lines (Fig. 2-3D). Primers from the PPM1D promoter were used as a positive control (PC) for direct NFkB binding (160). PCR analysis of primers flanking either the N1 or N2 regions of PLN promoter demonstrated that NFkB binds directly to both sites in the most metastatic cell line LN4 but does not bind to either site in LNCaP or DU145. These results indicate that the effect of NFkB on Pln transcription is direct in LN4 but indirect in the cell lines with lower metastatic potential and thus lower levels of Pln.

Perlecan Transcription Is Activated by p38 MAPK Signaling and ATF2

Oxidative stress caused by the accumulation of ROS has also been shown to activate p38 MAP kinase (161). Activation of p38 MAPK is also important for the malignant phenotype in prostate cancer cells, in part due to its ability to activate the transcription factor ATF2 by phosphorylation (146). To determine if ATF2 is a possible activator of Pln transcription I analyzed the promoter of PLN and found two regions that contained putative ATF2 binding sites (Fig. 2-4A, A1 and A2).

Figure 2-3: Inhibition of NADPH Oxidase (NOX) or NFkB results in decreased Pln mRNA. A.) Schematic of PLN promoter with regions of predicted NFkB binding sites (N1 and N2). B.) Real-time PCR analysis of Pln levels in cells treated with either DMSO (control, black bars), 20 uM, or 40 uM DPI (specific NOX inhibitor, white bars). Error bars indicate standard deviation. C.) Inhibition of NFkB by RNAi results in decreased levels of Pln mRNA. Real-time PCR analysis of NFkB and Pln normalized to levels of 18S. Black bars represent samples treated with scrambled RNAi treated samples, gray bars represent NFkB levels in NFkB RNAi treated cells, white bars represent Pln levels in NFkB RNAi treated cells. Error bars indicate standard deviation. Asterisk indicates $p < 0.05$. D.) NFkB binds directly to the PLN promoter at predicted binding sites in LN4 but not DU145 or LNCaP. Chromatin Immunoprecipitation analysis of LNCaP, DU145 and LN4 total chromatin, NFkB IP, no antibody (NoAB) and Mock samples. Samples were analyzed by PCR with primers flanking each predicted NFkB site. Positive control primers were used from the PPM1D promoter (160).

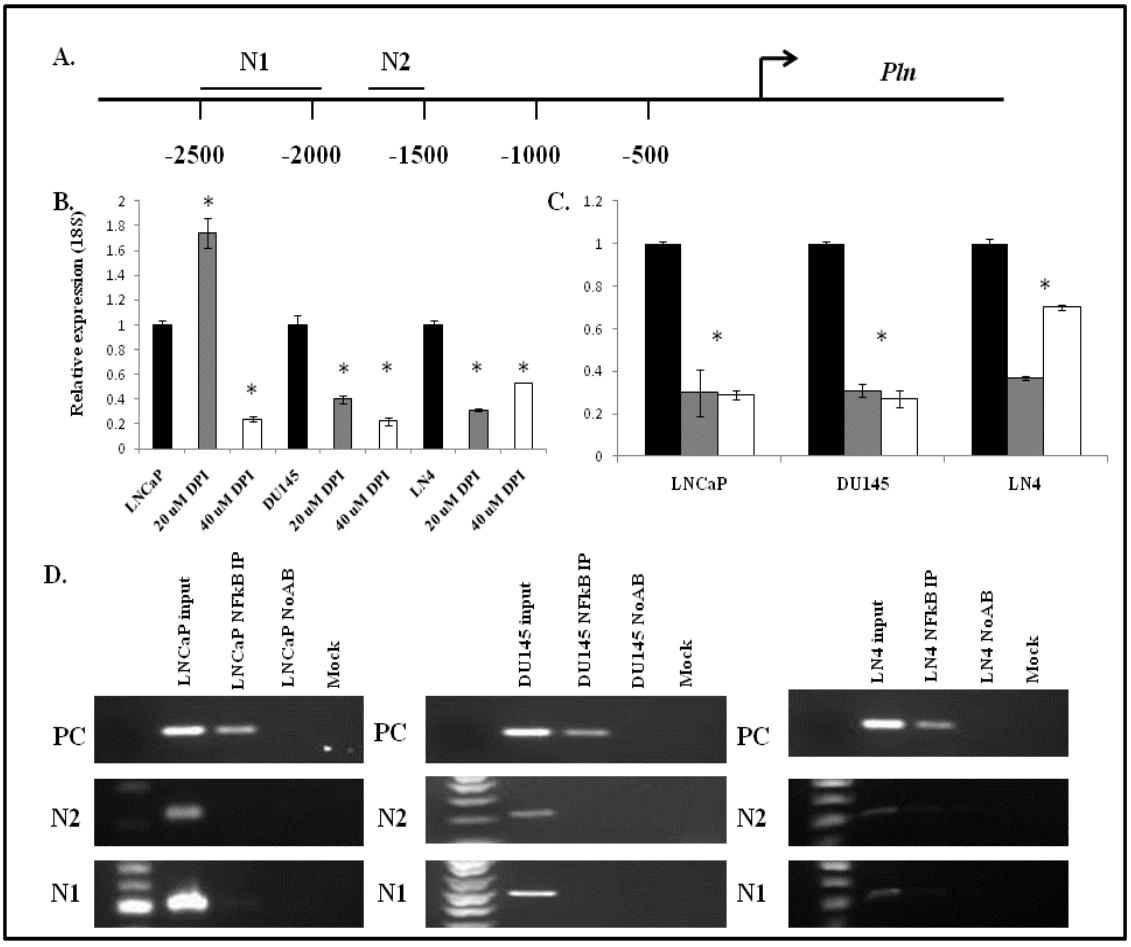
A.
N1
N2
Pln
-2500
-2000
-1500
-1000
-500
B.
Relative expression (18S)
LNCaP
20 uM DPI
40 uM DPI
DU145
20 uM DPI
40 uM DPI
LN4
20 uM DPI
40 uM DPI
C.
LNCaP
DU145
LN4
D.
LNCaP input
LNCaP NFkB IP
LNCaP NoAB
Mock
DU145 input
DU145 NFkB IP
DU145 NoAB
Mock
LN4 input
LN4 NFkB IP
LN4 NoAB
Mock
PC
N2
N1

I then asked if inhibition of p38 MAPK with the specific inhibitor SB202190 would result in a decrease in Pln mRNA. I used varying concentrations of the inhibitor in each cell and assayed for Pln transcription via qRT-PCR (Fig. 2-4B). I found that treatment with 20 μM SB202190 in LNCaP and DU145 resulted in a slight increase in Pln mRNA while producing a 70% decrease in LN4. Treatment with 40 μM and 80 μM inhibitor resulted in a dose-dependent decrease in Pln mRNA in all three cell lines. To determine if inhibition of p38 MAPK was resulting in decreased phosphorylation of the ATF2 transcription factor I treated each cell line with 40 μM SB202190 and performed quantitative western blots for phospho-ATF2. The inhibitor indeed led to a decrease in activated ATF2 in all cell lines (Fig. 2-4C). These results indicate that activity of p38 MAPK stimulates Pln transcription and activates the transcription factor ATF2 in prostate cancer cells. They also suggest that the most metastatic cell line LN4 is the most sensitive to p38 inhibition (Fig. 2-4D). To determine if ATF2 is acting to stimulate Pln expression I assayed both ATF2 (grey bars) and Pln (white bars) mRNA levels in cells treated with ATF2 RNAi or the negative control RNAi (black bars) (Fig. 2-4E). The results demonstrate that ATF2 levels were knocked down 80-90% by the RNAi. Pln levels were decreased approximately 75% in LNCaP and DU145 and 40% in LN4.

This suggests that ATF2 stimulates Pln transcription probably due to activation of ATF2 by p38 MAPK.

I then asked if the effect of ATF2 was direct or indirect by performing ChiP assays on the PLN promoter (Fig. 2-4F). Primers flanking ATF2 binding sites in the Insulin promoter were used as a positive control (PC) (162). PCR analysis with primers flanking the putative ATF2 binding sites in the Pln promoter demonstrates that ATF2 does not bind to the PLN promoter in either the A1 or A2 sites in any of the cell lines. These results indicate that the effect of ATF2 on Pln transcription is probably indirect in this model of prostate cancer progression.

Discussion

Stress-Inducible Transcription Factors Stimulate Pln Expression

To address my goal of understanding the molecular mechanisms of Pln upregulation in prostate cancer progression, I have introduced the LNCaP-DU145-LN4 cell line model that shows a 50-fold increase in Pln expression that correlates with increasing metastatic potential. The growth factor signaling pathways known to facilitate the progression of prostate cancer were shown to be modulated by Pln in this model.

Figure 2-4: Inhibition of p38 MAPK or ATF2 results in decrease in Pln mRNA. A.) Schematic of PLN promoter with regions of predicted ATF2 binding sites (A1 and A2). B.) Real-time PCR analysis of Pln levels in cells treated with either DMSO (control, black bars), 20 uM (dark gray bars), 40 uM (light gray bars) or 80 uM SB202190 (specific p38 MAPK inhibitor, white bars). Error bars indicate standard deviation. C.) Quantitative western blot showing decreased phospho-ATF2 levels in cells treated with 80 μM SB202190. phospho-ATF2 levels were normalized to actin in each sample. D.)Dose response graph showing percent inhibition of Pln transcription in each cell line with each concentration of SB202190. LNCaP samples (green line, diamonds), DU145 samples (red line, squares), LN4 samples (blue line, triangles). E.) Inhibition of ATF2 by RNAi results in decreased levels of Pln mRNA. Real-time PCR analysis of ATF2 and Pln normalized to levels of 18S. Black bars represent samples treated with scrambled RNAi treated samples, gray bars represent ATF2 levels in ATF2 RNAi treated cells, white bars represent Pln levels in ATF2 RNAi treated cells. Error bars indicate standard deviation. Asterisk indicates $p < 0.05$. F.) ATF2 does not bind directly to the PLN promoter at predicted binding sites in any of the cell lines. Chromatin Immunoprecipitation analysis of LNCaP, DU145 and LN4 total chromatin, ATF2 IP, no antibody (NoAB) and Mock samples. Samples were analyzed by PCR with primers flanking each predicted ATF2 site. Positive control primers were used from the human insulin promoter (162).

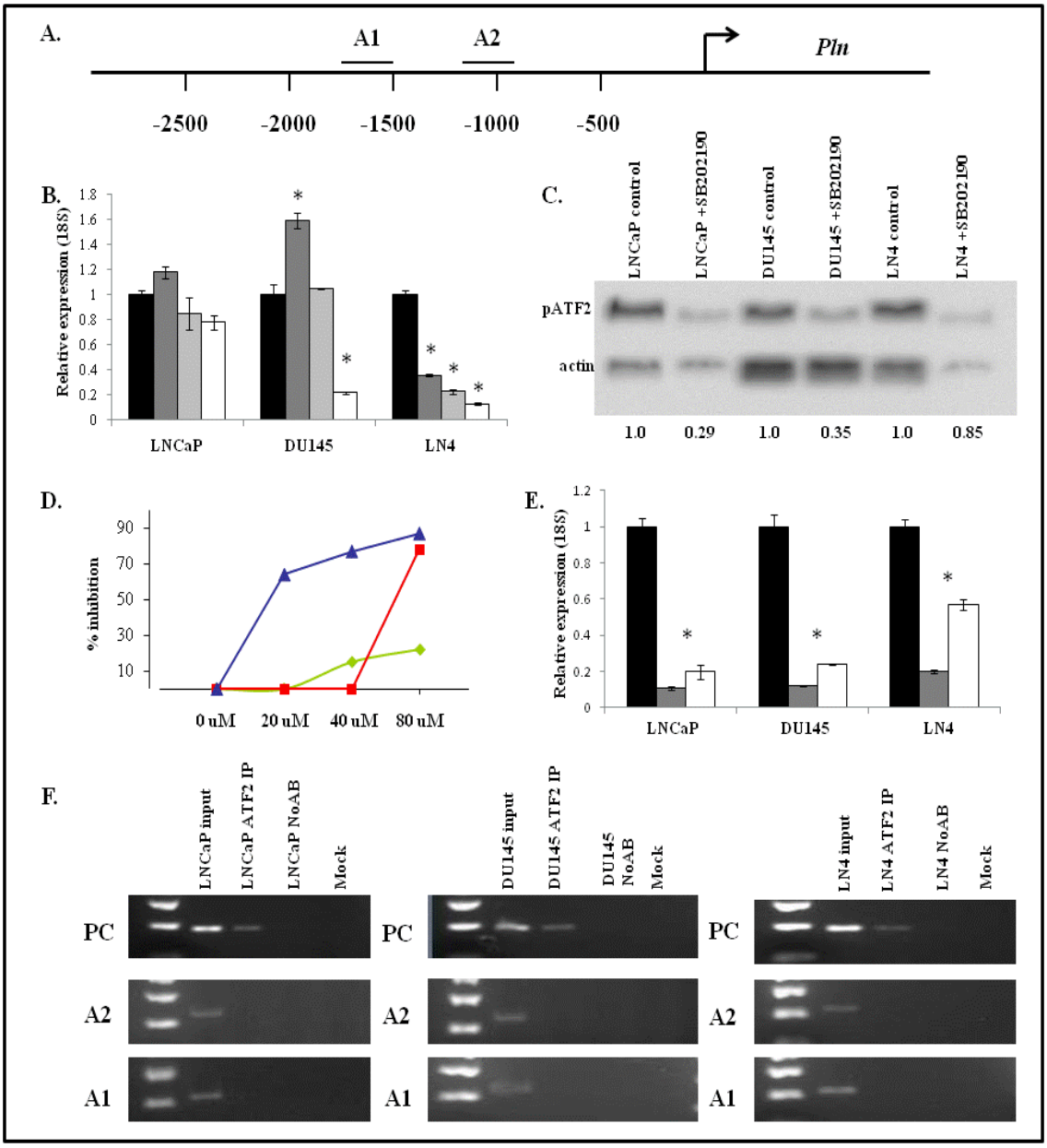
A.
A1
A2
Pln
-2500
-2000
-1500
-1000
-500
B.
Relative expression (18S)
LNCaP
DU145
LN4
C.
LNCaP control
LNCaP +SB202190
DU145 control
DU145 +SB202190
LN4 control
LN4 +SB202190
pATF2
actin
1.0
0.29
1.0
0.35
1.0
0.85
D.
% inhibition
0 uM
20 uM
40 uM
80 uM
E.
Relative expression (18S)
LNCaP
DU145
LN4
F.
LNCaP input
LNCaP ATF2 IP
LNCaP NoAB
Mock
DU145 input
DU145 ATF2 IP
DU145 NoAB
Mock
LN4 input
LN4 ATF2 IP
LN4 NoAB
Mock
PC
A2
A1

With this model I was able to address my hypothesis that cellular stress pathways and their activated transcription factors stimulate Pln expression in prostate cancer progression.

Previous studies have demonstrated that Pln expression is regulated by two of the growth factor signaling pathways that it modulates. TGFβ1 has been shown to induce Pln expression via the SMAD signal transducers ((163), (164), (165)). VEGF165 growth factor signaling through VEGFR2 has also been shown to stimulate Pln transcription in brain endothelial cells (166). Pln expression is also regulated by the inflammatory response via interleukins (167). Two studies evaluating the effect of hypoxia on Pln expression came to two different conclusions. Studies in rat cardiac endothelial cells demonstrate a significant decrease in Pln mRNA as a result of hypoxia (168). However, a study in T84 intestinal epithelial cells shows a large increase in Pln transcription via hypoxia (169). My studies focused on the primary transcription factor used in the tumor hypoxic response HIF1α. I show that, in general, HIF1α acts to stimulate Pln expression in this model of prostate cancer progression (Fig. 2-5). One exception to this was in LNCaP where overexpression of stabilized HIF1α resulted in an approximate 50% decrease in Pln levels. Since an estimated 1-2% of the human genome contains binding sites for HIF1α (111) producing a large pool of possible target genes, I propose that the concentration of HIF1α within these weakly tumorigenic LNCaP cells determines the overall effect on Pln expression. A sharp decrease in HIF1α via RNAi would result in the loss of a direct transcriptional activator of Pln while overexpression of the transcription factor could induce the expression of possible transcriptional

repressors of the Pln gene that would override any direct stimulatory effect. The approximate two-fold increases in Pln expression with overexpression of HIF1α coupled with the significant decrease via HIF1α RNAi in the more tumorigenic and metastatic DU145 and LN4 lines suggests that HIF1α is necessary for maximum Pln expression but may not be sufficient.

The accumulation of ROS in cancer cells has many deleterious effects. One of these may be the increase in growth factor signaling pathways caused by an increase in Pln levels. I have shown that both NFkB and ATF2 are necessary for the maximum transcription of Pln. Inhibition of the intracellular signaling pathways that activate these two ROS-inducible transcription factors is most effective at decreasing Pln levels in the more metastatic cell lines (Fig. 2-3B and 2-4B &D). These inhibitors were designed to decrease cellular levels of ROS (DPI) and the protein kinase p38 respectively. The increased sensitivity of Pln expression in more metastatic lines could simply be due to the fact that more Pln is being transcribed in these cells or it could be that other stress-inducible factors, in addition to NFkB and ATF2 that affect Pln expression are being affected in turn by these inhibitors.

To determine if these transcription factors stimulate Pln expression directly or indirectly I evaluated interaction between transcription factor and the PLN promoter via ChIP. I found that HIF1α binds to and occupies only the proximal H2 site in the LNCaP and DU145 lines while it occupies both H1 and H2 sites in the most metastatic LN4 line. I propose that increased levels of hypoxia that correlate with metastatic potential lead to increased levels of HIF1α protein. This enables HIF1α to facilitate the approximate 50-fold increase in Pln seen in the LN4 line. This line of thinking can also be used in regards to NFkB that occupies both the N1 and N2 sites of the PLN promoter in LN4 cells but seems to act indirectly in the LNCaP and DU145 cell lines. I could not detect a physical interaction between ATF2 and the PLN promoter in any of the cell lines that we tested. ATF2 must activate the expression of a different transcriptional activator that acts on the PLN promoter (Fig 2-5).

In summary, I demonstrate that the stress-inducible transcription factors HIF1α, NFkB, and ATF2 are involved in stimulating Pln expression in this model of prostate cancer progression using both direct and indirect mechanisms. These results provide insight into the complex molecular pathways that drive Pln expression in a subset of prostate cancer patients.

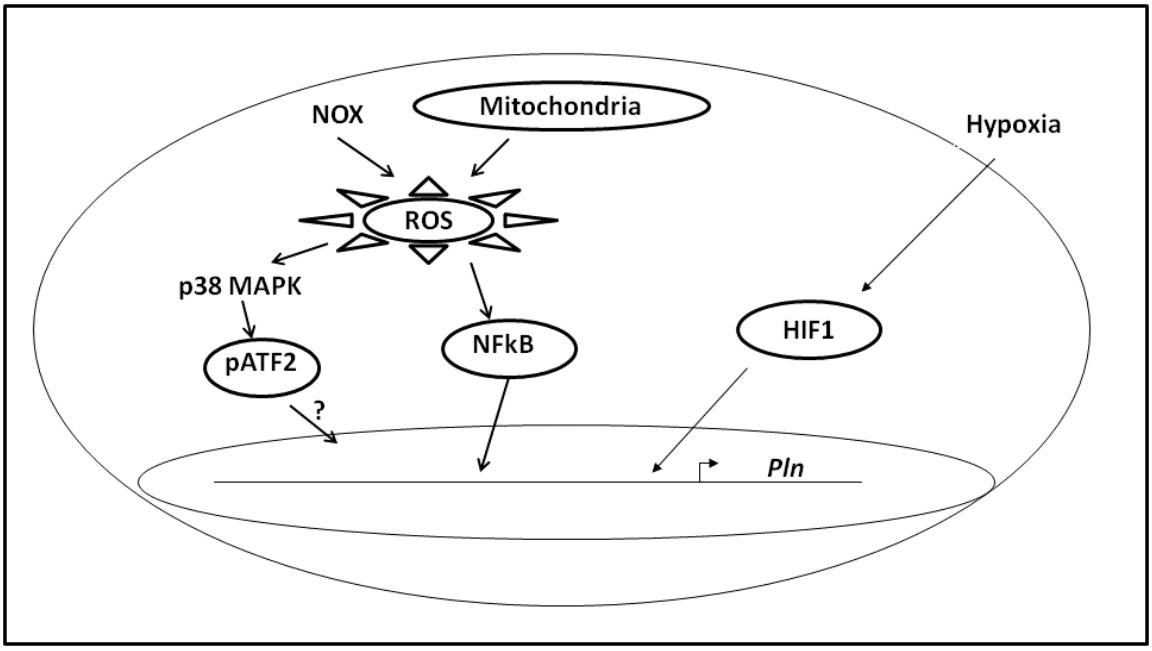

Figure 2-5: Model for regulation of Pln transcription by stress-activated transcription factors.

CHAPTER III

HEPARAN SULFATE 2-O-SULFOTRANSFERASE REGULATES PROLIFERATION AND INVASION OF PROSTATE CANCER CELLS

Heparan sulfate proteoglycans (HSPGs) are ubiquitous cell surface molecules that consist of a protein core with attached heparan sulfate (HS) glycosaminoglycan chains. HSPGs are extremely important in both development and cancer progression due to their regulation of cellular processes such as angiogenesis, tumor growth, proliferation, tumor invasion and metastasis. HSPGs control various processes by modulating a variety of growth factor signaling pathways such as SHH, FGF, VEGF, and TGFβ. All of these signaling pathways are abnormally activated in many cancers, including prostate cancer.

Prostate cancer is the second leading cause of cancer death in American men behind only lung cancer in its severity (1). HSPGs such as syndecan-1 and Pln are involved in the regulation of tumor growth and proliferation of prostate cancer cells ((170), (171),(93), (94)). Our group, along with collaborators, demonstrated the association of high levels of Pln protein with 54% of advanced prostate cancer tumors and its role in tumor cell proliferation by regulating SHH signaling (93). Interestingly, in the LNCaP-C42B cell line series, a well-known model of prostate cancer progression, SHH signaling increases with increasing metastatic potential but Perlecan protein levels do not. Instead, in this cell line series Perlecan isolated from more highly metastatic cell lines binds more SHH than an equal amount of Perlecan from more benign cell lines. This data suggested an alternative mechanism whereby during prostate cancer

progression cells produce a different, more efficient isoform of Perlecan protein to increase SHH signaling rather than simply expressing more of the same isoform as before. Given the bipartite structure of HSPGs and the known contribution of their sugar chains to the regulation of growth factor signaling, differential structure of the sugar chains is an obvious possibility in the generation of different Perlecan isoforms. Therefore we chose to investigate the role of HS chain structure on prostate cancer progression.

The HS chains attached to HSPGs can form specific complexes with growth factors as well as directly participate in growth factor-receptor complex formation. HS is an unbranched polymer of alternating residues of glucuronic acid (GlcA) and N-acetylglucosamine (GlcNAc). These HS chains undergo modification by series of heparan sulfate modification enzymes (HSMEs). The first modification is generally N-deacetylation and N-sulfation of GlcNAc residues by the NDST enzyme of which four tissue-specific isoforms exist. This modification is generally followed by the epimerization of GlcA residues at the C5 position by C5-GlcA epimerase (GLCE) yielding iduronic acid (IdoA). Further modification by O-sulfation can occur at various positions of the disaccharide by O-sulfotransferases (OSTs). Sulfation at either the C6 or C3 position of GlcNAc occurs by action of the enzymes 6OST or 3OST respectively. Multiple different isoforms exist for each of these OSTs. Sulfation at the C2 position of GlcA or IdoA residues occurs by the action of the enzyme 2OST.

The ability of HS to bind growth factors such as FGF, VEGF and hepatocyte growth factor has been shown to largely depend on the amount of HS sulfation ((172),

(173), (174), (175)). The general rule is that the higher degree of sulfation on the HS chain the greater the binding to growth factors. Of the different sulfotransferases that contribute to a higher degree of sulfation we have chosen to study the effect of 2OST on the proliferation and migration of prostate cancer cells in a cell line model of prostate cancer progression. The fact that only one isoform of the 2OST enzyme has been found to date makes it a convenient initial candidate to analyze its role in regulating HSPG function in prostate cancer.

Materials and Methods

Cell Lines and Culture Conditions

The LNCaP series (LNCaP, C4, C4-2, C4-2B) were obtained from Dr. L. Chung and grown at 37^{o}C and 5% CO_2 in T-medium supplemented with 5% fetal bovine serum (Invitrogen).

siRNA Transfection and Proliferation Assay

Purified and desalted siRNAs were purchased from either Sigma or Ambion as proprietary non-validated pool of two 2OST siRNAs (Sigma #'s: SASI_Hs01_00214049 and SASI_Hs01_00214052) and a scrambled siRNA control (Ambion). siRNA was carried out with Oligofectamine (Invitrogen) as described by the manufacturer. The effects of transfections were measured 24 hours after addition of reagents. BrdU (Sigma-Aldrich) was added to the cells at a final concentration of 20 μM and allowed to incubate for two hours. Immunocytochemistry on cell lines with scrambled or 2OST RNAi was carried out with anti-BrdU (Becton Dickinson) and HRP-conjugated secondary antibodies (Boehringer Mannheim) using standard techniques. Proliferation

was quantified by counting the number of BrdU-positive cells in a field of 100 done in triplicate.

Real-Time PCR

Total RNA isolated from cell lines using RNeasy MiniKit (Qiagen). Purified RNA was digested with DNase I (Invitrogen) and reverse transcribed using SuperScript III reverse transcriptase (Invitrogen). Oligo dT and random hexamer primers were used for the RT reaction. Samples were analyzed using Taqman Gene Expression Assays according to manufacturer's protocols (Applied Biosystems) on a BioRad iCycler machine. Each sample was run in triplicate at three different concentrations. Fold increase/decrease comparisons were calculated using the delta-delta CT method. Data for each sample is presented as the mean fold change compared to control and error is presented as standard deviation.

Migration Assay

Cell migration assays were performed using Matrigel Invasion Chambers from BD Biocoat (#354480) and control inserts (#354578) according to manufacturer's protocol. Number of C4-2B cells migrated through Matrigel was counted in control cells (scrambled siRNA treated) and experimental cells (2OST siRNA treated) in four separate fields in three independent experiments. The same experiment was performed in control inserts. The average number of invading cells through Matrigel (n = 12) was normalized to the average number of cells on control inserts (n = 12) to determine percent invasion. Error bars indicate standard deviation.

Phalloidin Staining and E-cadherin- phalloidin Double Labeling

C4-2B cells were treated with scrambled RNAi or 2OST RNAi as described above and cultured on glass coverslips coated in poly-L-lysine (BD Biocoat #354085). Cells were washed with PBS, fixed in 3% formaldehyde, permeabilized with PBST, treated with 1:1000 dilution of FITC-phalloidin (Dr. B. Perkins), and mounted in VectaShield mounting medium with DAPI (Vector Laboratories). Cells were imaged with fluorescence microscopy. Individual cells were first chosen by their nuclei under the DAPI channel, then the number of actin foci per cell were counted for each treatment (n=15 per treatment). The double labeling experiment was performed in much the same way as the phalloidin staining of C4-2B cells treated with either control or 2OST RNAi with a few modifications. Following permeabilization with PBST fixed cells were blocked with 0.1% FBS in PBS. α-E-cadherin antibody was added to a final concentration of 0.5 μg/mL for 30 minutes then cells were washed with PBS three times. A 1:1000 dilution of α-mouse Alexa 488 secondary antibody was added for 30 minutes then followed with three more rounds of washing. Cells were then treated with a 1:40 dilution of Alexa 546 phalloidin for 20 minutes then washed again. Cells were air dried and mounted on microscope slides in Vectashield mounting medium with DAPI.

Western Blotting

Total protein was isolated from C4-2B cells treated with scrambled or 2OST RNAi. 60 mg of total protein was run on a 15% SDS-PAGE gel, blotted on nitrocellulose, and probed for β-actin (Sigma-Aldrich) as a loading control. Primary antibodies used were either rabbit α-HS2ST1 (Santa Cruz #sc-130779) or mouse α-E-

cadherin (Invitrogen #18-0223). Secondary antibodies were either α-rabbit or α-mouse HRP. Imaging and densitometry analysis performed on a BioRad ChemiDoc XRS machine with Quantity One software. Densitometry values represent the mean of two independent experiments.

Results

Knockdown of 2OST Expression Results in Decreased Prostate Cancer Cell Proliferation

The LNCaP, C4, C4-2, and C4-2B cell line model of prostate cancer progression was originally identified in the laboratory of Dr. Leland Chung ((150), (151)). This series of lines was established via serial transplantation of cancer cells into nude mice. The LNCaP cell line was originally derived from a supraclavicular lymph node metastasis of a primary prostatic carcinoma (148). LNCaP cells mimic many of the characteristics of early stage prostate cancer in that they are weakly tumorigenic when inoculated into nude mice, their growth is androgen-sensitive, and they secrete low levels of PSA (148). The C4 subline shows higher levels of PSA expression than LNCaP, produces approximately 10 times more colonies in soft agar, and are still androgen-sensitive in their growth.

The next subline in the series, C4-2, is highly tumorigenic on its own, displays androgen-insensitive growth, and metastasizes to both the lymph node and bone. The final subline of the series, C4-2B, mimics the most advanced stage of prostate cancer. It is androgen-insensitive, secretes the highest levels of PSA and has the highest rate of metastasis and invasion.

To determine if the 2OST enzyme plays a role in the biological processes of this cell line series we first evaluated proliferation in each cell line either transfected with a scrambled control RNAi (black bars) or an RNAi directed against 2OST (white bars) (Figure 3-1A). We found that proliferation decreased in each of the four cell lines as a result of the 2OST RNAi. The proliferation of the most severe cell lines seemed to be the most sensitive to knockdown of 2OST expression. To verify a decrease in the amount of 2OST protein as a result of the RNAi treatment, I performed western blot analysis of C4-2B cells treated with either the control RNAi or 2OST RNAi. I was able to reproducibly detect an approximate decrease of 50% in levels of 2OST protein (Figure 3-1B). In summary, the 2OST enzyme is necessary for optimal proliferation of prostate cancer cells in the LNCaP to C4-2B cell line series.

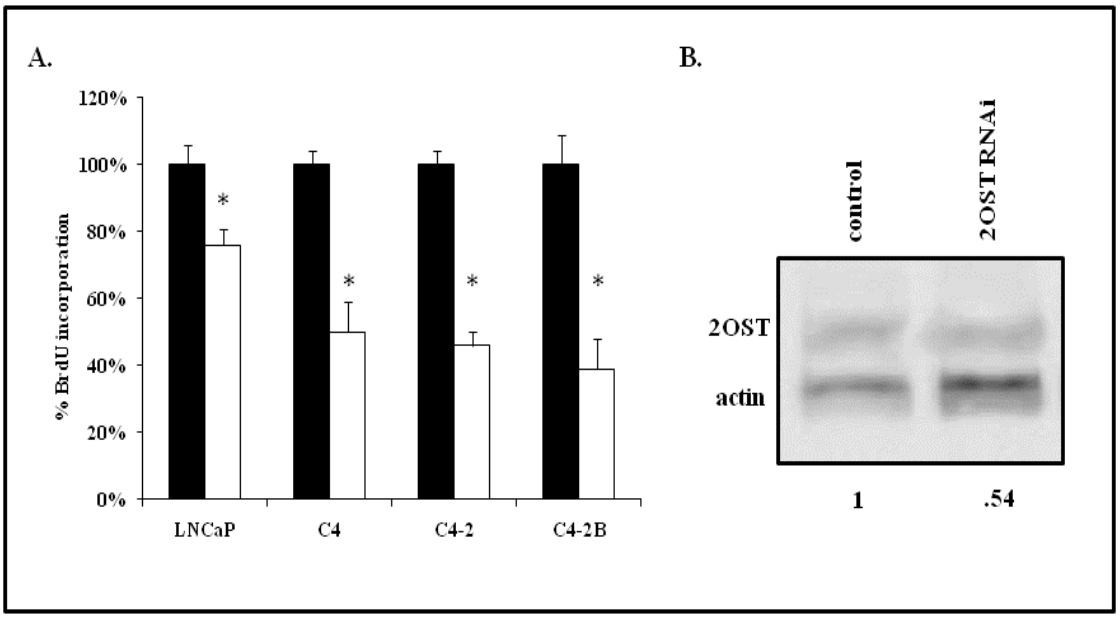

Figure 3-1: **Inhibition by 2OST siRNA decreases prostate cancer cell proliferation.** A. BrdU incorporation in LNCaP, C4, C4-2, and C4-2B cell lines. The cell lines are listed in order of increasing metastatic potential from left to right on the graph. All samples were normalized to controls (scrambled siRNA treated). Black bars represent control samples transfected with scrambled siRNA. White bars represent samples transfected with 2OST siRNA. Error bars represent n = 3 independent samples and standard deviation. Asterisk indicates $p < 0.05$. B. Western blot for verification of 2OST RNAi. Levels of 2OST in each sample were normalized to actin by densitometry. Values are representative of two independent experiments.

2OST Expression Correlates with Metastatic Potential and Knockdown of 2OST Expression Results in Decreased Prostate Cancer Cell Migration

Along with proliferation, cell invasion is one of the principal processes that are required for cancer progression and metastasis. To determine if 2OST plays a role in the invasive and metastatic potential of cell lines in the LNCaP-C42B series I first evaluated basal expression of the 2OST gene in each of the cell lines. When I carried out quantitative real-time PCR analysis of 2OST mRNA levels in the weakly tumorigenic LNCaP line as a normalization standard I observed a step-wise increase in 2OST expression as the cell lines increase in their metastatic potential (Figure 3-2A). Levels of 2OST increased four-fold in the C4-2B cell line as compared to LNCaP. This result demonstrates a direct correlation between metastatic potential and 2OST expression. This correlation led me to hypothesize that a decrease in 2OST expression would lead to a decrease in the invasive potential of these cells.

To determine if inhibition of 2OST by RNAi affects ability of prostate cancer cell invasion I evaluated the invasive potential of the most metastatic cell line C4-2B in an in vitro Matrigel invasion assay.

I chose C4-2B for this experiment due to its proliferation being the most sensitive to 2OST RNAi and it having the highest levels of 2OST expression. Approximately 80% of C4-2B cells treated with control RNAi invaded through the Matrigel demonstrating its high invasive potential (Figure 3-2B & C). Inhibition of 2OST by RNAi in C4-2B cells resulted in a significant decrease in the mean number of cells that invaded through the Matrigel ($p < 0.01$). Percent invasion of 2OST RNAi treated cells dropped to approximately 50% (Figure 3-2B & C). Figure 2C shows a representative field of cells for C4-2B cells treated with either the scrambled control RNAi (left panes) or the 2OST RNAi (right panes). The mean number of cells that invaded through Matrigel (top panes) were counted and normalized to the mean number of cells that traveled through control inserts that contained no Matrigel (bottom panes) to determine percent invasion.

Increased Actin and E-cadherin Accumulation in C4-2B Cells Treated with 2OST siRNA

Cell adhesion in epithelial cells is provided in the form of adherens junctions. These cell to cell contacts consist of the proteins E-cadherin, β-catenin, α-catenin, and actin filaments (176).

Figure 3-2: **2OST expression correlates with metastatic potential.** A. 2OST mRNA levels in LNCaP series of prostate cancer progression. 2OST mRNA was assayed by qRT-PCR and normalized to 18S rRNA. All samples were run in triplicate and overall 2OST message levels compared by setting 2OST levels in LNCaP to 1. Samples are presented by increasing metastatic potential (LNCaP, C4, C4-2, C4-2B). Error bars indicate standard deviation. Asterisk indicates $p < 0.05$. B. Inhibition by 2OST siRNA decreases Matrigel invasion by C4-2B cells. The number of C4-2B cells that migrated through Matrigel was counted for control cells (scrambled siRNA treated) and experimental cells (2OST siRNA treated) in four separate fields in three independent experiments. The same experiment was performed with control inserts. The average number of invading cells ($n = 12$) was normalized to the average number of cells on control inserts ($n = 12$) to determine percent invasion. Average % invasion for control and 2OST siRNA cells were 81.8 ± 6.88 and 49.8 ± 4.08 respectively ($p < 0.01$, asterisk). C. Representative images of C4-2B cells used in Matrigel assay. Cells that migrated through the matrigel in either control or 2OST RNAi samples are shown in top two panels. Cells used in control inserts are shown on the bottom two panels.

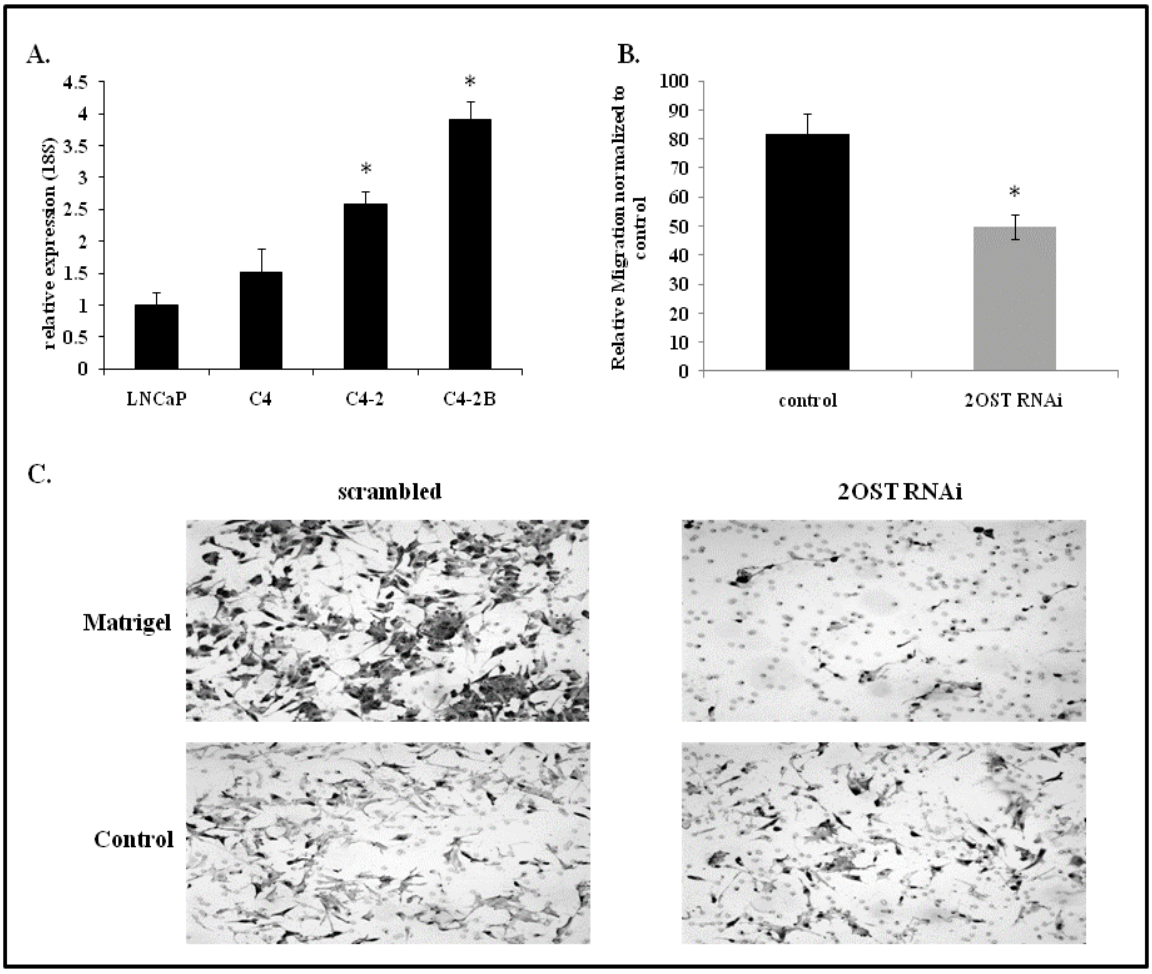
A.
relative expression (18S)
4.5
4
3.5
3
2.5
2
1.5
1
0.5
0
*
*
LNCaP
C4
C4-2
C4-2B
B.
Relative Migration normalized to control
100
90
80
70
60
50
40
30
20
10
0
*
control
2OST RNAi
C.
scrambled
2OST RNAi
Matrigel
Control

Adherens junctions are formed between epithelial cells, such as those in the prostate, when plasma-membrane spanning E-cadherin proteins recruit catenin molecules which in turn bind to actin filaments. The junctions are stabilized by the formation of E-cadherin clusters and then further stabilized by the accumulation of actin filaments at the contact region ((177), (178)). During the progression of metastatic disease, epithelial cells lose cell-cell contacts via adherens junctions and become fibroblast like in a process called the Epithelial-Mesenchymal Transformation (EMT). This loss of cell adhesion is a critical step in invasion and metastasis of cancer cells (177). Due to the decreased invasion of C4-2B cells that have been treated with 2OST RNAi, I hypothesized that 2OST acts to repress adherens junction formation. To test this hypothesis I evaluated the accumulation of actin via phalloidin staining in C4-2B cells treated either with control RNAi or 2OST RNAi (Figure 3-3A & B). I observed a significant increase in the mean number of actin foci per cell in C4-2B cells treated with 2OST RNAi as compared to control RNAi (Figure 3-3B). Figure 3A shows representative cells of each treatment. Notice the accumulation of phalloidin staining in the 2OST RNAi treated cell.

To determine if these actin foci might be corresponding to the formation of adherens junctions I evaluated actin-E-cadherin double labeling in C4-2B cells treated with either control RNAi or 2OST RNAi (Figure 3-3C). Control RNAi treated cells had very low levels of both actin and E-cadherin accumulation (top panes). 2OST RNAi treated cells once again had accumulation of actin as shown by phalloidin staining (bottom row, third panel from left). These 2OST RNAi treated cells also had significantly increased levels of E-cadherin accumulation at the membrane especially in the same regions that had increased actin accumulation (bottom panes, second and fourth panes from left). These results suggest that the inhibition of 2OST by RNAi is facilitating the formation of adherens junctions and thus a possible reversal of EMT and cancer progression.

The possibility exists that the loss of 2OST is allowing for an increase in E-cadherin expression that in turn allows for formation of these junctions. To test this possibility I performed western blot analysis of E-cadherin protein in C4-2B cells treated with either control RNAi or 2OST RNAi (Figure 3-3D). No significant increase in E-cadherin protein was observed in cells treated with 2OST RNAi. This result suggests that the localization of available E-cadherin in C4-2B cells changes from a more diffuse pattern to accumulation into foci when treated with 2OST RNAi.

Figure 3-3: Inhibition by 2OST RNAi increases actin foci in C4-2B cells. A. Fluorescence staining for F-actin (A and C) and nuclei (B and D) in C4-2B cells treated with 2OST siRNA (A and B) or scrambled siRNA (C and D). Notice the clustering of F-actin into foci in the 2OST siRNA treated cells. B. Quantitation of number of actin foci present per cell in C4-2B cells treated with scrambled siRNA (control, black bar) and 2OST siRNA (white bar). Mean number of foci per cell ± sem are 0.33 ± 0.03 and 1.14 ± 0.06 respectively (n = 15). Asterisk indicates $p < 0.05$. C. Inhibition by 2OST siRNA increases E-cadherin staining that colocalizes with actin foci in C4-2B cells. Fluorescence immunohistochemistry for DAPI stained nuclei (left column), E-cadherin (second column), F-actin (third column) and merged images (fourth column) in C4-2B cells treated with 2OST siRNA (bottom row) or scrambled siRNA (top row). Notice accumulation of E-cadherin between cells treated with 2OST siRNA. D. Inhibition by 2OST RNAi does not result in significant upregulation of E-cadherin protein. Western blot of E-cadherin in samples treated with scrambled RNAi or 2OST RNAi. Levels of E-cadherin were normalized to actin. Values represent two independent experiments.

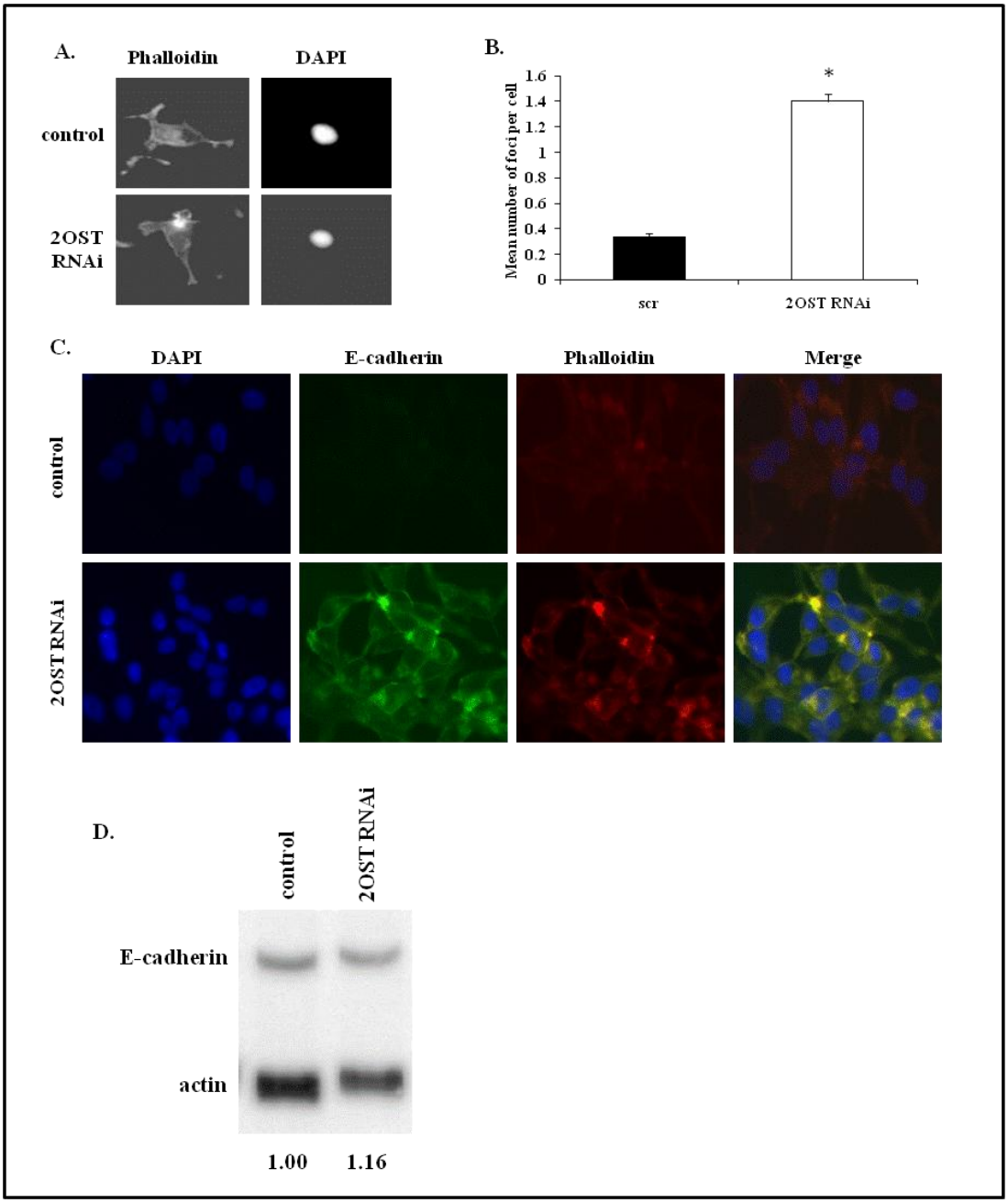
A.
Phalloidin
DAPI
control
2OST RNAi
B.
Mean number of foci per cell
1.6
1.4
1.2
1
0.8
0.6
0.4
0.2
0
*
scr
2OST RNAi
C.
DAPI
E-cadherin
Phalloidin
Merge
control
2OST RNAi
D.
control
2OST RNAi
E-cadherin
actin
1.00
1.16

Discussion

The 2OST Enzyme Is Involved in Prostate Cancer Cell Proliferation, Invasion, and Metastatic Potential

Studies analyzing the complete loss of HS in regards to organismal and molecular phenotypes show that HS is very important for biological processes in development and disease. In an attempt to look closer at HS fine structure, Merry et al described the molecular phenotypes of 2OST-null mice (98). They observed renal agenesis as well as eye and skeletal defects. Recently it was found that 2OST is essential for the FGF signaling required for chick limb bud outgrowth and development (100). I have chosen to analyze the effect of changes in HS fine structure via 2OST RNAi on prostate cancer cell proliferation and invasion. Previous studies in our group demonstrated that 2OST is required for maximal proliferation in the LNCaP cell line model of prostate cancer progression. The growth factors such as SHH and FGF that induce proliferation in these cells require a high degree of heparan sulfation to bind HS and ultimately activate signaling. I propose that the loss of 2OST activity decreases the degree of heparan sulfation thus decreasing growth factor signaling. However, studies in mice and *Drosophila* as well as my own unpublished work (results not shown) have shown that loss of 2OST results in compensatory increases in the activity of other HSMEs that attempt to maintain overall negative charge density on the HS chain ((98), (103)). From this I can propose that the results of 2OST knockdown on proliferation may be conservative if this kind of compensation is taking place.

I also demonstrate that increased expression of 2OST correlates with increasing metastatic potential in this cell line series. The need for upregulation of growth factor signaling to drive cancer cells from benign to metastatic would require an increase in the amount of heparan sulfation available in the extracellular matrix. I suggest that the expression of the 2OST enzyme is being upregulated to achieve this goal. A significant decrease in invasion of the highly metastatic C4-2B cells through Matrigel was also observed as a result of 2OST knockdown. I asked if this loss of 2OST was allowing the formation of adherens junctions that would increase cell adhesion and in turn decrease mobility. I found a significant increase in actin and E-cadherin accumulation at the periphery of these cells. One possible explanation for this is that C4-2B cells with normal levels of 2OST have increased Wnt signaling that would inhibit β-catenin from participating in formation of adherens junctions and toward the regulation of gene expression. However, we found no change in β-catenin localization in cells treated with 2OST RNAi (data not shown). Further studies are needed to determine the mechanism by which loss of 2OST results in increased adherens junctions.

In summary, I have demonstrated that the 2OST enzyme is important for two of the biological processes required for cancer progression. I believe that 2OST could be used as a therapeutic target in prostate cancer. In chapter 4 a study into the effect of growth factor signaling and the molecular mechanisms of 2OST upregulation will be discussed.

CHAPTER IV

HEPARAN SULFATE 2-O-SULFOTRANSFERASE REGULATES GROWTH FACTOR SIGNALING AND ITS EXPRESSION IS STIMULATED BY STRESS-ACTIVATED TRANSCRIPTION FACTORS IN PROSTATE CANCER CELLS

The heparan sulfate (HS) covalently attached to heparan sulfate proteoglycans (HSPGs) acts to modulate a number of growth factor pathways in development and disease. HS does this by controlling the interaction between the growth factor and its receptor in the extracellular matrix. The biosynthetic modifications of HS by heparan sulfate modification enzymes (HSMEs) are thought to play a key role in the ability of HS to bind these growth factors. Modulation of signaling pathways has been shown to affect biological processes in cancer progression such as angiogenesis, proliferation, invasion, and metastasis. I will be focusing on the SHH, FGF, VEGF, and TGFβ pathways. All of these signaling pathways are abnormally activated in many cancers, including prostate cancer.

Prostate cancer is the second leading cause of cancer death in American men behind only lung cancer in its severity (1). If this disease is caught in its early stages the patient usually has a very good prognosis. However, for advanced, androgen-insensitive prostate cancer the prognosis for patient survival is markedly decreased. Understanding the molecular mechanisms of disease progression is very important in diagnosing and treating advanced prostate cancer. Our group, along with collaborators, demonstrated the association of high levels of Pln protein, a HSPG, with 54% of advanced prostate cancer tumors and its role in tumor cell proliferation by regulation of SHH signaling

(93). This led to the hypothesis that a subset of prostate cancers reaches advanced stage by increasing growth factor signaling through increasing the amount of Pln coreceptor in the extracellular matrix. This increase in the secretion of Pln protein essentially causes an increase in the levels of extracellular HS available to modulate signaling. However, the other 46% of advanced prostate cancers maintained or showed a decrease in the amount of Pln expression compared to more benign tissue. Interestingly, in the LNCaP-C42B cell line series, a well-known model of prostate cancer progression, SHH signaling increases with increasing metastatic potential but Perlecan protein levels are maintained or decreased. Basically, this subset of advanced prostate cancers would not have the benefit of more Pln to provide increased extracellular HS to facilitate signaling. In light of this, I asked how the same amount of HSPG being secreted from advanced, metastatic tissue as from benign tissue could still produce an increase in growth factor signaling. Given the importance of the HS chains to a HSPG's ability to modulate growth factor signaling I chose to investigate HS chain structure in prostate cancer progression.

HS is an unbranched polymer of alternating residues of glucuronic acid (GlcA) and N-acetylglucosamine (GlcNAc). These HS chains undergo modification by series of HSMEs. The first modification is generally N-deacetylation and N-sulfation of GlcNAc residues by the NDST enzyme of which four tissue-specific isoforms exist. This modification is generally followed by the epimerization of GlcA residues at the C5 position by C5-GlcA epimerase (GLCE) yielding iduronic acid (IdoA). Further modification by O-sulfation can occur at various positions of the disaccharide by O-

sulfotransferases (OSTs). Sulfation at either the C6 or C3 position of GlcNAc occurs by action of the enzymes 6OST or 3OST respectively. Multiple different isoforms exist for each of these OSTs and sulfation at the C2 position of GlcA or IdoA residues is catalyzed by the 2OST enzyme.

The amount of sulfate modifications on a HS chain has been shown to increase its ability to bind growth factors such as FGF, VEGF, hepatocyte growth factor ((172), (173), (174), (175)). The general rule is that the higher the degree of sulfation on HS chains the greater the binding to growth factors. One possible way of increasing the amount of sulfation on HS chains is for the cell to increase the expression of the different OSTs. I have chosen to investigate the mechanisms controlling the expression of 2OST, in particular the role of stress, a common characteristic of growing tumors. Solid tumors, such as prostate cancer, make up approximately 90% of all cancers and result in significant mortality due to cell invasion and metastasis to distant vital organs such as the brain and lungs (106). The rapid proliferation associated with formation of a solid tumor induces stress in the tumor which can respond in various ways. Stressed cancer cells activate signaling pathways involved in survival by either repairing the damage caused by the stress or by activating cell migration to move away from the stress. However, if the amount of damage is high the cell will activate cell death pathways (105). Therefore, cellular stress is a mechanism of selection for cells within a tumor that will progress to more advanced disease.

Once a solid tumor forms, the decreased availability of oxygen, or hypoxia, becomes a source of cellular stress. The initial lack of vasculature within the mass of

cancerous cells and the relatively low diffusion limit of oxygen are two of the main reasons for hypoxia. In order for a tumor to grow larger than a diameter of approximately 2-5 mm it must be able to relieve the hypoxic stress by obtaining its own vasculature in the process of angiogenesis ((41-43)). However, tumor cells usually grow at rates that exceed their angiogenic response. Cells respond to this constant state of hypoxia by stabilizing the transcription factor hypoxia-inducible factor 1 α (HIF1α) which heterodimerizes with HIF1β and activates transcription of its target genes (112). The HIF1 heterodimer binds to specific sites called hypoxia response elements (HREs) within the promoter of a target gene. Genes involved in processes such as cell survival, proliferation, angiogenesis, cell adhesion, and metastasis are activated by HIF1α in response to hypoxia ((113-114, 155)). HIF1α is a logical candidate to control 2OST expression because it is overexpressed in prostate tumors (156) as well as in human prostate cancer cell lines (157).

The accumulation of ROS is another source of cellular stress shown to be associated with solid tumors (158). Increased metabolism and electron transport activity within the mitochondria due to rapid cellular proliferation and mutations in mitochondrial DNA are the major sources of ROS accumulation (132). ROS activates a number of stress-activated protein kinases. These kinases activate transcription factors that stimulate the expression of genes involved in cancer progression. One ROS-inducible protein kinase/transcription factor system that I have evaluated as a candidate to increase 2OST expression is the p38 MAPK/ATF2 system. Activation of p38/MAPK regulates gene expression by direct phosphorylation of a number of

transcription factors. Activation of ATF2 has been directly linked to p38 MAPK because inhibition of p38 results in decreased phosphorylation of ATF2 and a subsequent decrease in cell proliferation (142). Active phosphorylated ATF2 is overexpressed in prostate tumors compared to normal tissue (146) and may be involved in prostate cancer progression (143). Another ROS-inducible transcription factor is NFkB. NFkB is overexpressed in many cancers including prostate cancer (138). ROS-dependent activation of p38 MAPK, ATF2 and NFkB will be investigated in this study as a possible molecular mechanism for regulating transcription of 2OST.

In the present study I set out to determine if the 2OST enzyme is needed for optimal growth factor signaling in the highly metastatic prostate cancer cell line C4-2B. I show that inhibition of 2OST by RNAi resulted in decreased growth factor signaling and this could be due to, in the case of SHH, decreased HSPG-growth factor complex formation. I also set out to determine if the expression of 2OST in this cell line is activated by stress-activated transcription factors. I found that the proximal promoter of 2OST contains putative binding sites for HIF1α, ATF2, and NFkB. Inhibition of these transcription factors by RNAi resulted in a decrease in 2OST mRNA. Overexpression of a stabilized form of HIF1α led to an increase in 2OST expression. I also investigated the effects of inhibition of p38 MAPK signaling by the specific inhibitor SB202190 on 2OST mRNA levels. I also set out to address whether or not the effects of these transcription factors was direct or indirect by performing a ChIP assay which showed that HIF1α and ATF2 directly bind the 2OST promoter while NFkB appears to act in an indirect manner.

Materials and Methods

Cell Lines and Culture Conditions

C4-2B cells were obtained from ATCC and cultured in T-medium (Invitrogen) supplemented with 5% fetal bovine serum. Cells were maintained at 37^{o}C and 5% CO_2.

Reagents and Antibodies

SB202190 (Cat. # S7067) was purchased from Sigma Aldrich. Primary antibodies purchased from Santa Cruz Biotechnology (SCBT) are as follows: mouse anti-β-catenin (sc-7963, 1:500), mouse anti-phospho-ERK (sc-81492, 1:1000), rabbit anti-phospho-SMAD2/3 (sc-11769, 1:1000), mouse anti-phospho-ATF2 (sc-52941, 1:500), and rabbit anti-SHH (sc-9024, 1:500). Mouse anti-Pln antibody was purchased from US Biological (#H1890, 1:1000) and mouse anti-HIF1α antibody was purchased from Novus (NB100, 1:500). Purified mouse anti-β-actin antibody (A5316, 1:1000) was purchased from Sigma Aldrich. Anti-mouse HRP and anti-rabbit HRP secondary antibodies (1:10,000) were purchased from Jackson Labs. Antibodies for chromatin immunoprecipitation were used at a final concentration of 0.3 mg/mL and as follows: mouse anti-HIF1α (Novus Biologicals #NB100), rabbit anti-ATF2 (SCBT sc-6233), and rabbit anti-NFkB p65 (SCBT sc-109).

Transient Transfections

Transient transfections of siRNA were performed using Lipofectamine 2000 reagent (Invitrogen #11668027) for RNAi directed towards HIF1α, NFkB, or ATF2 (Ambion) according to manufacturer's protocol. 2OST RNAi (Sigma #'s: SASI_Hs01_00214049 and SASI_Hs01_00214052) was performed using

Oligofectamine transfection reagent (Invitrogen # 12252011) according to manufacturer's protocol. Briefly cells were cultured in 6-well plates at allowed to attach for 24 hours. siRNA was applied and cells were harvested for either protein or RNA after 24 hours. Scrambled siRNA was used as the negative control. Transient transfection of stabilized HIF1α (stHIF1α) (a kind gift from Dr. Eric Huang) as well as p2OST-lacZ reporter plasmid were also performed using Lipofectamine 2000 reagent according to manufacturer's protocol.

RNA Isolation and Real-Time PCR

Cells were grown to 80-90% confluence, scraped, centrifuged and washed with PBS. RNA isolation was performed with Qiagen RNEasy Mini-kit (#74104) according to manufacturer's protocol. 2 μg of RNA was used in each DNAse I reaction using DNAse I Amplification Grade from Invitrogen (#18068). Reverse transcription was performed with oligo dT and random hexamer primers using SuperScript III reverse transcriptase from Invitrogen (#18080044). Real-time PCR was performed using Taqman Gene Expression Assays with Taqman Universal PCR Master Mix from Applied Biosystems (#4324018). Each sample was run in triplicate at three different concentrations and normalized to levels of 18S rRNA. Reactions were performed using a BioRad C1000 Thermal Cycler machine. Error bars indicate standard deviation.

Western Blotting and Co-Immunoprecipitations

Isolation of total protein was done using the Mammalian Cell Lysis Kit from Sigma Aldrich (#MCL-1KT) according to manufacturer's protocol. Phosphatase inhibitors were used for each sample (Sigma Aldrich #P0044). Samples were prepared

and run on 15% SDS-PAGE and transferred onto nitrocellulose. Western blots were developed with Pierce ECL Western Blotting Substrate (#32106). Images and densitometry were obtained on a BioRad ChemiDoc XRS machine using Quantity One software. Densitometry values represent the mean of two independent experiments. Pln-SHH co-immunoprecipitations were performed as previously described (93). Briefly, conditioned medium from C4-2B cells treated with either control RNAi or 2OST RNAi was collected when cells reached 80-90% confluence in 100 x 15 culture dishes. Equivalent amounts of conditioned medium were immunoprecipitated with anti-Pln antibody and the bound complexes were run on SDS-PAGE. Bound SHH was observed by immunoblotting.

p2OST reporter plasmid and β-galactosidase assays

Two different constructs from the 2OST promoter were amplified by PCR and cloned into the pBLUE-TOPO TA vector (Invitrogen #K4831-01). "Full-length" p2OST consists of 2500 bases upstream and 435 bases downstream of the transcription start site while "4C" p2OST consists of 1500 bases upstream and 435 bases downstream of the transcription start site. Primers used to amplify the "full-length" promoter were: 5'-tcaaacggtgaaccaagacgctgt-3' and 5'-gaaacccgctgctcggg-3'. Primers used to amplify the "4C" promoter were: 5'-actccggtgtagtcccttaaca-3' and 5'-gaaacccgctgctcggg-3'. β-galactosidase assays to evaluate the amount of transcription from each of the p2OST constructs were performed using the β-gal Assay Kit (Invitrogen #K1455-01) according to manufacturer's protocol. Briefly, varying concentrations of each cell lysate were incubated with ONPG as a substrate and 1X Cleavage Buffer for 30 minutes and the

reactions were halted with Stop Buffer. Absorbance at 420 nm was used to quantify activity in a Bio Mate 3 spectrophotometer.

Chromatin Immunoprecipitation

C4-2B cells were cross-linked by adding formaldehyde directly to cell culture medium to a final concentration of 1%. Cross-linking was allowed to proceed for 10 min at room temperature then stopped with addition of glycine to a final concentration of 0.125 M. Cells were washed twice with ice-cold PBS and swollen with PBS for 10 minutes at 37^{o}C. Cells were scraped, washed once with PBS then pelleted by centrifugation. Pellets were resuspended in Cell Lysis Buffer (5 mM PIPES pH 8.0, 85 mM KCl, 0.5% Triton X-100, protease inhibitor cocktail) for 10 minutes on ice. Cellular extract was pelleted by centrifugation then nuclei were resuspended in Nuclei Lysis Buffer (50 mM Tris-Cl pH 8.0, 10 mM EDTA, 1% SDS, protease inhibitor cocktail) for 10 minutes on ice. Total chromatin was then sonicated for twelve 20 second pulses at setting 2. After centrifugation at 12,000 g chromatin was pre-cleared with Protein A/G Plus Beads then divided into aliquots. Antibody was added to each aliquot for a final concentration of 0.3 mg/mL and incubated on a rotating platform overnight at 4^{o}C. Antibody-protein complexes were immunoprecipitated with Protein A/G Plus Beads. Samples were washed extensively and eluted in Elution Buffer (50 mM $NaHCO_3$, 1% SDS). Bound DNA fragments were isolated and analyzed by PCR. Primers used to amplify the region of the 2OST promoter from -1157 to -707 (H1) were: 5’-ttaaaagcacaaatcgcactca-3’ and 5’-gaaaagggtggggaggact-3’. Primers used to amplify the region from -581 to -231 (H2 and A2) were: 5’-ggcaccagacacccactc-3’ and 5’-

aagaaggcggggctaaaac-3'. Primers used to amplify the region from -1499 to -1219 (A1) were: 5'-actccggtgtagtcccttaaca-3' and 5'-tttttaaatgatgttcgttgtcttc-3'. Primers used to amplify the region from +224 to +435 (N1) were: 5'-gactggagaggcgagaagg-3' and 5'-gaaacccgctgctcggg-3'. Primers used to amplify the region from -176 to +53 (N2) were: 5'-caaccgtaaaccgaaccaag-3' and 5'-tccctctcttccttccttcc-3'.

Promoter Analysis

Prediction of transcription factor binding sites in the human 2OST promoter was done with the ALGGEN-PROMO prediction program.

Results

Inhibition by 2OST RNAi Results in Decreased Growth Factor Signaling and Complex Formation between Perlecan and SHH in Prostate Cancer Cells

The LNCaP, C4, C4-2, and C4-2B prostate cancer cells were originally developed in the laboratory of Dr. Leland Chung ((150-151)). I have found that levels of 2OST mRNA increase over four-fold as the metastatic potential of these cell lines increases (Fig. 3-2A). I have chosen to investigate the effect of inhibition of 2OST by RNAi on essential growth factor signaling pathways in the highly metastatic cell line C4-2B.

To determine whether 2OST modulates growth factor signaling in C4-2B cells, I evaluated commonly used assays to determine levels of FGF, TGFβ, Wnt and Sonic Hedgehog SHH signaling in cells transfected with 2OST RNAi. To first verify that transfection of C4-2B with 2OST RNAi was successful I evaluated 2OST mRNA levels via quantitative real-time PCR (qRT-PCR) in cells treated with either control RNAi

(black bar) or 2OST RNAi (white bar) (Fig. 4-1A). 2OST mRNA levels were successfully knocked down 86% in cells treated with 2OST RNAi as compared to the control RNAi sample used as a normalization control and set to 1.

To determine the effect of 2OST RNAi on FGF signaling, I performed quantitative western blots analyzing levels of phospo-ERK. Densitometry shows that phospho-ERK levels were decreased 50% in C4-2B as a result of 2OST inhibition by RNAi when using actin levels as normalization controls (Fig. 4-1B). I then assayed the effect of 2OST knockdown on TGFβ signaling by performing quantitative western blots for phospho-SMAD2 while using total SMAD2 as a normalization control. Levels of phospho-SMAD were decreased approximately 35% in C4-2B transfected with 2OST RNAi (Fig 4-1C). I assayed levels of β-catenin as readout of the effect of 2OST RNAi on Wnt signaling. Levels of β-catenin were decreased approximately 15% in C4-2B transfected with 2OST RNAi compared to controls (Fig. 4-1D).

Finally, to determine the effect of 2OST RNAi on SHH signaling, I performed qRT-PCR on RNA isolated from C4-2B cells treated with either control RNAi (black bars) or 2OST RNAi (white bars) and evaluated levels of the response genes *PTCH* and

GLI1 (Fig. 4-1E). I show that *PTCH* levels decrease approximately 40% and *GLI1* levels decrease approximately 70% as a result of 2OST knockdown. Our group has previously shown that SHH binds more readily to Pln secreted from the highly metastatic C4-2B as compared to Pln secreted from the weakly tumorigenic LNCaP cell line (93). To determine if the 2OST enzyme is required for optimal Pln-SHH complex formation in C4-2B, I performed co-immunoprecipitation analysis in which Pln protein was pulled down from conditioned medium of C4-2B cells treated with either control RNAi or 2OST RNAi. Western blotting to determine the levels of SHH bound to equivalent levels of Pln in each treatment reveals a significant decrease in Pln-SHH complex formation in samples treated with 2OST RNAi as compared to control RNAi (Fig. 4-1F). Overall, my results suggest that the 2OST enzyme is needed for optimal growth factor signaling in the highly metastatic prostate cancer cell line C4-2B.

HIF1α Stimulates Expression of 2OST by Directly Binding Promoter in C4-2B

The cellular stress hypoxia has been shown to correlate with increased tumor invasiveness and metastatic potential (117).

Figure 4-1: 2OST modulates growth factor signaling in cell line model of prostate cancer progression. A.) Inhibition by 2OST RNAi in C4-2B verified by Real-time PCR. Black bar represents cells treated with scrambled negative control RNAi and gray bar represents cells treated with 2OST RNAi. 2OST RNAi samples were normalized to control at 1. Error bars indicate standard deviation. B.) Decreased FGF signaling in cells treated with 2OST RNAi. Western blotting for phospho-ERK and β-actin performed as described in Materials & Methods. Levels of p-ERK are normalized to β-actin. Densitometry figures are shown below each sample and are representative of two independent experiments. C.) Decreased TGFβ signaling in cells treated with 2OST RNAi. Levels of p-SMAD 2 normalized to total SMAD2. D.) Decreased Wnt signaling in cells treated with 2OST RNAi. Levels of β-catenin normalized to β-actin. E.) Decreased SHH signaling in cells treated with 2OST RNAi. Real-time PCR analysis of SHH pathway response genes PTCH and GLI1 was performed. Error bars indicate standard deviation. Asterisk indicates $p < 0.05$. F.) Decreased complex formation between SHH and Pln. Pln was immunoprecipitated from conditioned media from either control RNAi or 2OST RNAi cells. Left pane shows western blot for SHH bound to equal amounts of Pln. Right panel shows equal amounts of SHH in input samples from co-immunoprecipitation.

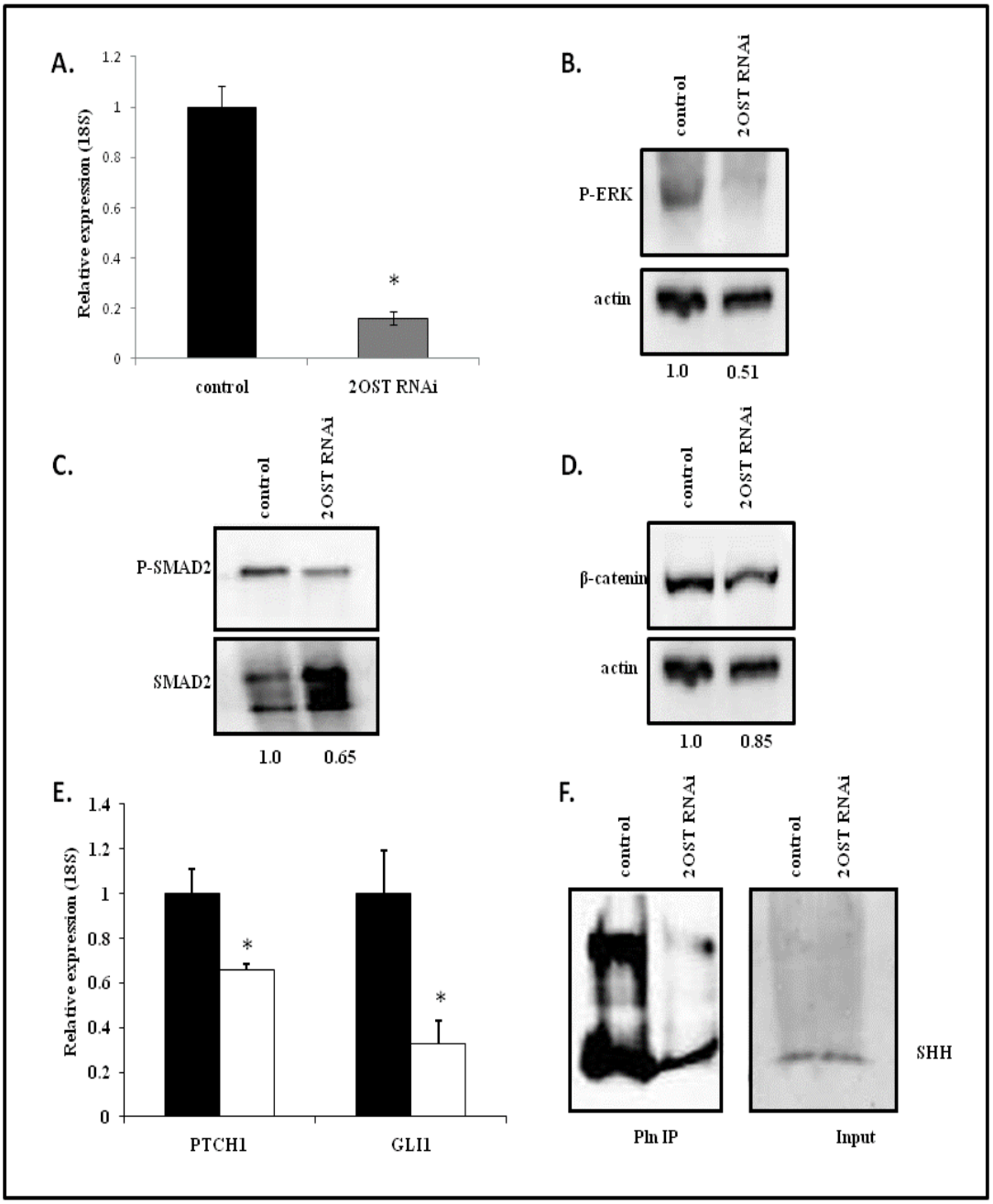
A.
Relative expression (18S)
1.2
1
0.8
0.6
0.4
0.2
0
*
control
2OST RNAi
B.
control
2OST RNAi
P-ERK
actin
1.0
0.51
C.
control
2OST RNAi
P-SMAD2
SMAD2
1.0
0.65
D.
control
2OST RNAi
β-catenin
actin
1.0
0.85
E.
Relative expression (18S)
1.4
1.2
1
0.8
0.6
0.4
0.2
0
*
*
PTCH1
GLI1
F.
control
2OST RNAi
control
2OST RNAi
SHH
Pln IP
Input

Tumor cells respond to hypoxia by stabilizing the HIF1α transcription factor via the inhibition of hydroxylases that lead to HIF1α degradation. HIF1α activates transcription by binding to HREs in promoters of target genes. To investigate whether HIF1α activates 2OST expression, I analyzed the sequence of the proximal 2OST promoter and found putative HREs approximately 1000 bases (H1) and 500 bases (H2) upstream of the transcription start site (Fig. 4-2A). I then asked if overexpression of HIF1α would be able to activate transcription of the *2OST* gene. To answer this question I evaluated levels of 2OST mRNA via qRT-PCR in C4-2B cells transfected with either an empty control vector (black bar) or a vector expressing a stabilized form of HIF1α (gray bar). It was found that 2OST levels increased approximately two-fold in cells overexpressing the stabilized HIF1α (Fig. 4-2B). To verify accumulation of HIF1α due the overexpression vector I performed western blot analysis and found significantly increased levels of HIF1α as a result of the stabilized HIF1α transgene (Fig. 4-2C). To determine if RNAi-mediated knockdown of HIF1α expression affected levels of 2OST mRNA, I analyzed levels of both HIF1α and 2OST mRNA in samples transfected with HIF1α RNAi (white bars) compared to control RNAi samples (black bars).

HIF1α levels were decreased 90% while 2OST mRNA was decreased 45% as a result of the HIF1α RNAi (Fig 4-2D). These results suggest that the HIF1α transcription factor activates expression of the 2OST gene in C4-2B prostate cancer cells.

I then asked if the effect of HIF1α on *2OST* transcription was direct or indirect. To answer this I performed chromatin immunoprecipition (ChIP) assays to evaluate physical interactions between transcription factor and promoter at the putative HREs. HIF1α has previously been shown to directly bind the VEGF promoter (43). Primers for the VEGF promoter flanking HREs were used as a positive control (PC) and PCR analysis of chromatin pulled down with HIF1α IP demonstrated that HIF1α does indeed bind this promoter in C4-2B. PCR analysis using primers flanking the H1 and H2 regions of the 2OST promoter showed that HIF1α binds directly to the proximal H2 site but no physical interaction was detected at the H1 site (Fig. 4-2E). Overall these results suggest that HIF1α activates 2OST transcription by directly binding its promoter.

p38 MAPK Signaling and ATF2 Stimulate Transcription of 2OST in C4-2B

Accumulation of ROS and the resulting oxidative stress has been shown to activate p38 MAP kinase (161).

Figure 4-2: HIF1α activates 2OST expression in model of prostate cancer progression. A.) Schematic of 2OST promoter with regions of HREs (H1 and H2). B.) C4-2B cells were transfected with vector expressing stHIF1α. Real-time PCR for 2OST levels normalized to 18S levels in each sample. Black bars represent control vector alone transfected samples and gray bars represent stHIF1α transfected samples. Error bars indicate standard deviation. C.) Western blot for HIF1α shows increased accumulation of stabilized transcription factor in cells transfected with stHIF1α vector. D.) Inhibition of HIF1α by RNAi results in decreased levels of 2OST mRNA. Real-time PCR analysis of HIF1α and 2OST normalized to levels of 18S. Black bars represent samples treated with scrambled RNAi treated samples, white bars represent levels of either HIF1α or 2OST in HIF1α RNAi treated cells. Error bars indicate standard deviation. Asterisk indicates $p < 0.05$. E.) HIF1α binds directly to the 2OST promoter at predicted HREs. Chromatin Immunoprecipitation analysis of C4-2B total chromatin, HIF1α IP, no antibody (NoAB) and Mock samples. Samples were analyzed by PCR with primers flanking each HRE site. Positive control primers were used from the VEGF promoter (43).

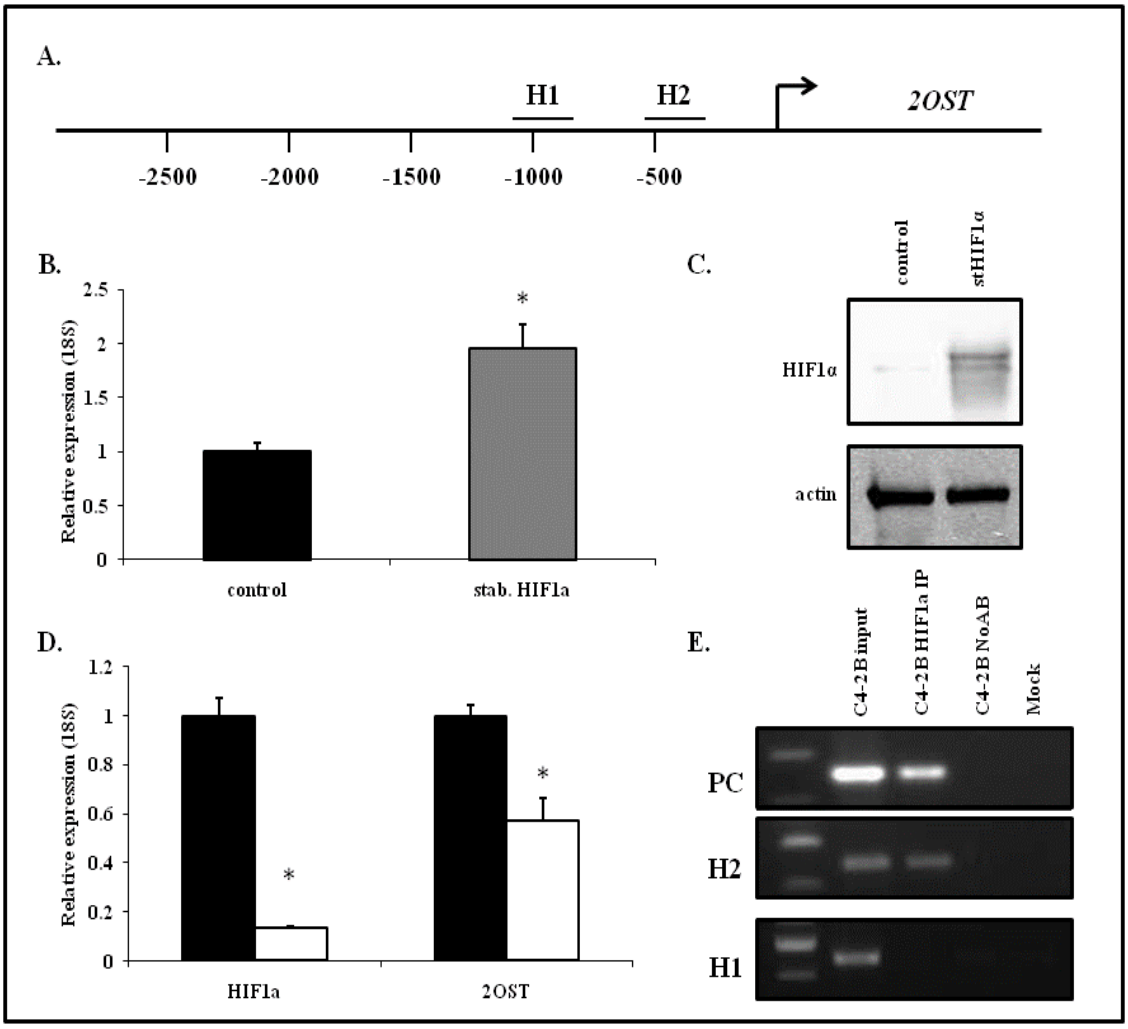
A.
H1
H2
2OST
-2500
-2000
-1500
-1000
-500
B.
Relative expression (18S)
2.5
2
1.5
1
0.5
0
*
control
stab. HIF1a
C.
control
stHIF1α
HIF1α
actin
D.
Relative expression (18S)
1.2
1
0.8
0.6
0.4
0.2
0
*
*
HIF1a
2OST
E.
C4-2B input
C4-2B HIF1a IP
C4-2B NoAB
Mock
PC
H2
H1

Activation of p38 MAPK is also important for the malignant phenotype in prostate cancer cells, and this due in part activation of the transcription factor ATF2 by phosphorylation (146). I asked if ATF2 could be a possible transcriptional activator of 2OST expression. Analysis of the sequence of the 2OST promoter showed two possible regions of ATF2 binding sites that I have labeled A1 and A2 (Fig. 4-3A). To determine if p38 MAPK signaling was involved in 2OST expression I evaluated levels of 2OST mRNA by qRT-PCR in cells treated with either DMSO control (black bar) or increasing concentrations of the specific p38 inhibitor SB202190. I found that treatment with 40 μM SB202190 (gray bar) resulted in a 55% decrease in 2OST levels while treatment with 80 μM inhibitor (white bar) resulted in a 90% decrease (Fig. 4-3B). This dose-dependent effect of p38 MAPK inhibitor suggests that signaling from the ROS-inducible protein kinase is important for optimal 2OST expression. I wanted to verify this effect by making two different β-galactosidase reporter constructs to assay for 2OST promoter activity. The "full-length" promoter represents the region from 2500 bases upstream of the transcription start to 435 bases downstream and the "4C" promoter represents the region from 1500 bases upstream to 435 bases downstream. I evaluated 2OST promoter activity in C4-2B cells transfected with one of the reporter constructs treated with either DMSO control (black bars) or 80 μM SB202190 (gray bars) (Fig. 4-3C). I found that treatment with the p38 inhibitor resulted in a significant decrease in promoter activity with both constructs. . In addition, upon comparison of results from the "full-length" reporter and the "4C" reporter it became evident that deletion of the 1000 bases most 5'

in our promoter construct leads to an increase in 2OST reporter expression, suggesting the existence of a previously unsuspected inhibitory sequence between -1500 and -2500. I then asked if inhibition of p38 MAPK leads to a decrease in active ATF2 transcription factor in C4-2B. To answer this, western blot analysis was performed evaluating levels of phospho-ATF2 in cells treated with DMSO control or 80 μM SB202190. I observed a significant decrease in active phosphorylated ATF2 levels as a result of p38 inhibition (Fig. 4-3D). To determine if ATF2 is acting to stimulate 2OST expression I assayed both ATF2 and 2OST mRNA levels in cells treated with ATF2 RNAi (gray bars) or the negative control RNAi (black bars) (Fig. 4-3E). The results demonstrate that while ATF2 levels were knocked down 90% 2OST levels were decreased approximately 75% by the RNAi treatment. These results suggest that p38 MAPK activates ATF2 which in turn stimulates 2OST expression in the C4-2B cell line.

I then asked if the effect of ATF2 was direct or indirect by performing ChiP assays on the 2OST promoter. Primers flanking ATF2 binding sites in the Insulin promoter were used as a positive control (PC) (162). PCR analysis with primers flanking the putative ATF2 binding sites in the 2OST promoter demonstrates a physical interaction between ATF2 and the promoter at the A2 site (Fig. 4-3F). This result suggests that the effect of ATF2 on 2OST expression is direct by binding of the proximal A2 site.

Figure 4-3: Inhibition of p38 MAPK or ATF2 results in decrease in 2OST mRNA. A.) Schematic of 2OST promoter with regions of predicted ATF2 binding sites (A1 and A2). B.) Real-time PCR analysis of 2OST levels in cells treated with either DMSO (control, black bars), 40 μM (gray bars), or 80 uM SB202190 (specific p38 MAPK inhibitor, white bars). Error bars indicate standard deviation. C.) 2OST promoter β-galactosidase reporter assay in cells treated with either DMSO control (black bars) or 80 μM SB202190 (gray bars). Full length 2OST promoter represents region 2500 bases upstream to 500 bases downstream of transcription start site. 4C represents region 1500 bases upstream to 500 bases downstream from start site. Error bars indicate standard deviation. D.) Western blot showing decreased levels of phospho-ATF2 in cells treated with 80 μM SB202190. E.) Inhibition of ATF2 by RNAi results in decreased levels of 2OST mRNA. Real-time PCR analysis of ATF2 and 2OST normalized to levels of 18S. Black bars represent samples treated with scrambled RNAi, gray bars represent either ATF2 or 2OST levels in ATF2 RNAi treated cells. Error bars indicate standard deviation. Asterisk indicates $p < 0.05$. F.) ATF2 does not bind directly to the 2OST promoter at predicted binding sites in any of the cell lines. Chromatin Immunoprecipitation analysis of C4-2B total chromatin, ATF2 IP, no antibody (NoAB) and Mock samples. Samples were analyzed by PCR with primers flanking each predicted ATF2 site. Positive control primers were used from the human insulin promoter (162).

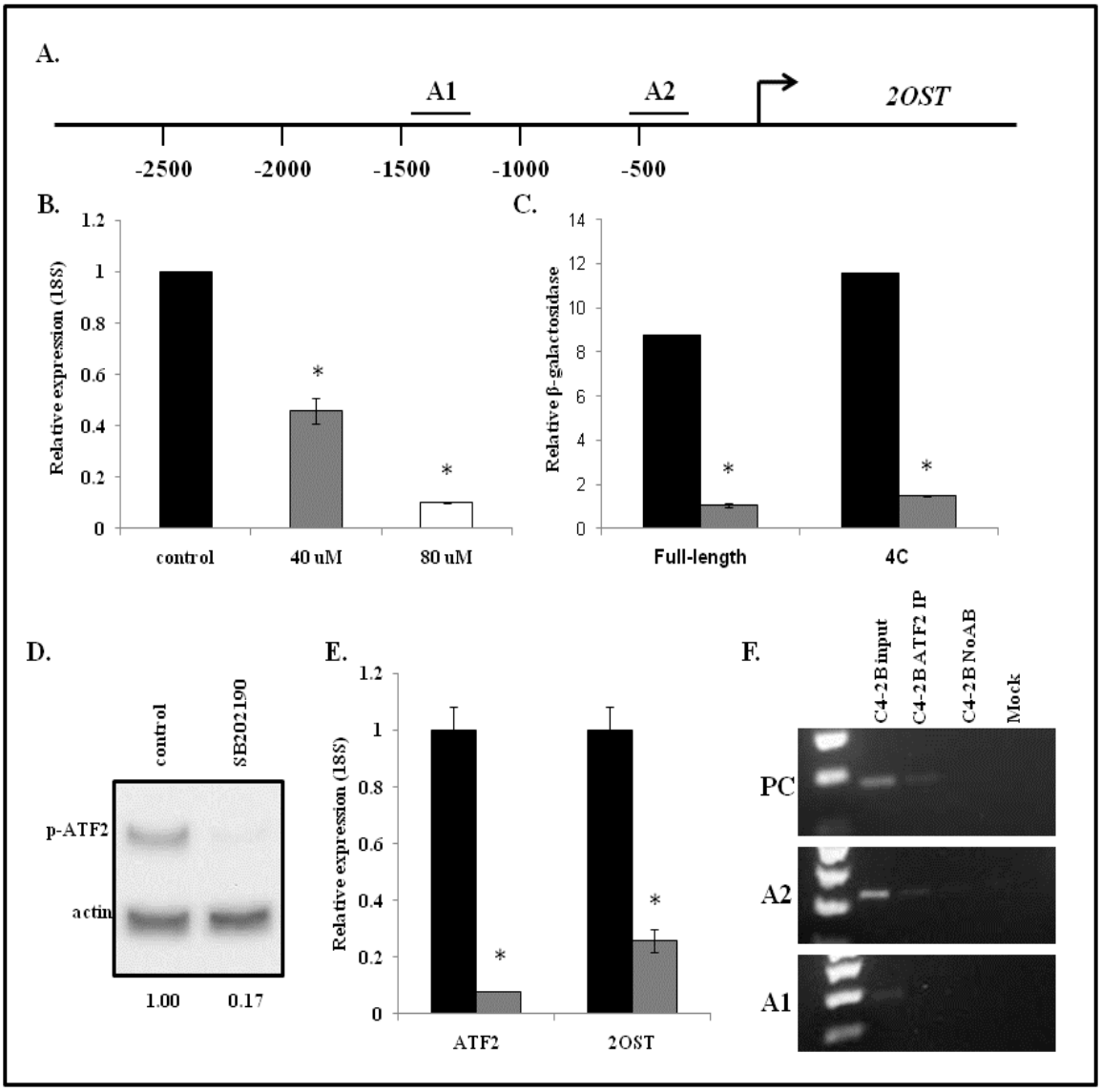
A.
A1
A2
2OST
-2500
-2000
-1500
-1000
-500
B.
Relative expression (18S)
control
40 uM
80 uM
C.
Relative β-galactosidase
Full-length
4C
D.
control
SB202190
p-ATF2
actin
1.00
0.17
E.
Relative expression (18S)
ATF2
2OST
F.
C4-2B input
C4-2B ATF2 IP
C4-2B NoAB
Mock
PC
A2
A1

NFkB Indirectly Activates 2OST Expression in C4-2B

The ROS-inducible transcription factor NFkB is another candidate transcription factor that may induce 2OST expression. NFkB activates genes involved in cell survival, cell growth, proliferation, angiogenesis, and metastasis. I analyzed the 2OST promoter and found two regions that contained putative NFkB binding sites (Fig. 4-4A, N1 and N2). To determine if knockdown of NFkB expression by RNAi results in a decrease in 2OST expression, I assayed NFkB and 2OST mRNA levels in cells treated with NFkB RNAi (gray bars) or with scrambled negative control RNAi (black bars) (Fig. 4-4B). NFkB levels were successfully knocked down approximately 80% by the RNAi treatment and 2OST levels also decreased approximately 80%. These results indicate that NFkB induces 2OST expression in C4-2B prostate cancer cells.

To determine if NFkB binds directly to the 2OST promoter I once again performed ChIP to assay for physical interaction with the promoter (Fig. 4-4C). Primers from the PPM1D promoter were used as a positive control (PC) for direct NFkB binding (160). PCR analysis of primers flanking either the N1 or N2 regions of 2OST promoter demonstrated that NFkB does not bind directly to either putative binding site in the promoter. These results indicate that the effect of NFkB on 2OST transcription is probably indirect in C4-2B.

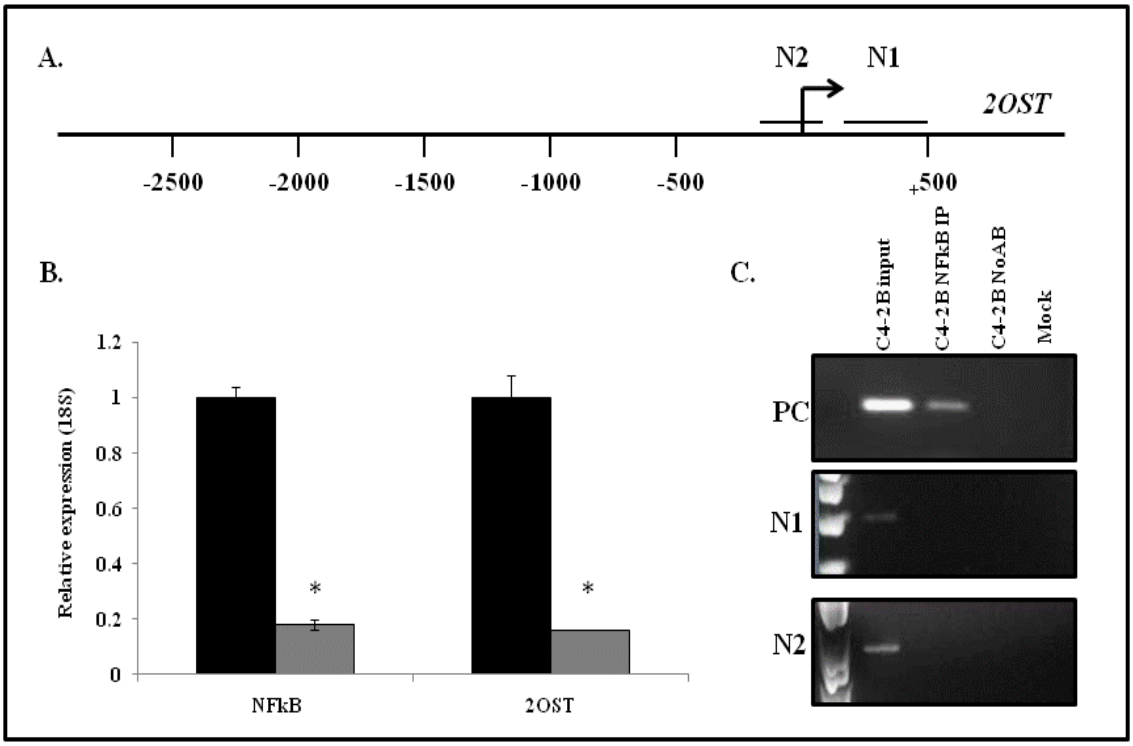

Figure 4-4: Inhibition of NFkB by RNAi results in decreased 2OST mRNA. A.) Schematic of 2OST promoter with regions of predicted NFkB binding sites (N1 and N2). B.) Inhibition of NFkB by RNAi results in decreased levels of 2OST mRNA. Real-time PCR analysis of NFkB and 2OST normalized to levels of 18S. Black bars represent samples treated with scrambled RNAi treated samples and gray bars represent either NFkB or 2OST levels in NFkB RNAi treated cells. Error bars indicate standard deviation. Asterisk indicates $p < 0.05$. D.) NFkB does not bind directly to the 2OST promoter at predicted binding sites in C4-2B. Chromatin Immunoprecipitation analysis of C4-2B total chromatin, NFkB IP, no antibody (NoAB) and Mock samples. Samples were analyzed by PCR with primers flanking each predicted NFkB site. Positive control primers were used from the PPM1D promoter (160).

Discussion

2OST Modulates Growth Factor Signaling in C4-2B and Its Expression is Stimulated by Stress-activated Transcription Factors

In this chapter I have presented my work towards understanding how 2OST affects growth factor signaling in highly metastatic prostate cancer cells and how the expression of 2OST is upregulated as the disease progresses. I have shown that inhibition of 2OST results in a decrease in the levels of FGF, TGFβ, Wnt, and SHH signaling (Figs. 4-1B-F). The hypothesis was that a decrease in 2OST levels would cause a decrease in the degree of heparan sulfation on the HS chains of HSPGs. This decreased sulfation would limit the ability of the HSPG to bind these growth factors. I show that the ability of Pln to bind the SHH growth factor is significantly reduced in cells with decreased 2OST.

As discussed in Chapter 3, the compensatory upregulation in the activity of other sulfotransferases such as 6OST or NDST1 to maintain overall negative charge density on the HS chain may be masking some of the effect of 2OST knockdown on growth factor signaling. Due to this compensation, understanding the sole effect of 2OST may not be possible without understanding the regulatory mechanisms of the compensation. However, I believe that this data coupled with the data in Chapter 3 regarding decreased proliferation and invasion makes 2OST an attractive target for cancer therapy.

The LNCaP, C4, C4-2, C4-2B cell line series was previously shown by our group to model progression to metastatic disease without the advantage of increasing levels of Pln in the extracellular matrix. I show that 2OST is instead upregulated to help provide the

increase in extracellular HS that is needed. My hypothesis was that the cellular stress known to correlate with advanced metastatic disease activates expression of 2OST. I show that the stress-inducible transcription factors HIF1α, ATF2 and NFkB all stimulate 2OST expression since expression of 2OST drops when any of these transcription factors are inhibited by RNAi. However, overexpression of stable HIF1α by a transgene only increased 2OST expression two-fold compared to the four-fold increase observed across the cell line model (Fig. 4-2B&C). I propose that HIF1α is necessary for maximum 2OST expression but may not be sufficient.

I also show that the ROS-inducible protein kinase, p38 MAPK, stimulates 2OST expression (Fig 4-5). This is probably due to p38 MAPK activating ATF2 by phosphorylating it. I analyzed the effect of this kinase via the specific p38 inhibitor SB202190. Phosphorylation is a major event in many biological processes including those that drive cancer progression. Many kinase inhibitors are in clinical trials to test their efficacy in therapy (179). I propose that the effect of p38 MAPK signaling on 2OST expression makes this kinase an ideal drug target.

The physical interactions between transcription factors and the 2OST promoter were also analyzed via ChIP. I found that HIF1α binds the promoter at the proximal H2 site but not the H1 (Fig. 4-2E).

This suggests that HIF1α acts to stimulate 2OST expression in a direct manner (Fig. 4-5). I obviously cannot rule out an additional indirect effect of 2OST since I did not rule out every other possible HIF1α target and its effect on 2OST. I also analyzed the ROS-inducible transcription factors NFkB and ATF2 in regards to physical interaction with the promoter. I found that ATF2 directly binds at the proximal A2 site while the effect of NFkB seems indirect with no physical interaction observed. (Fig. 4-5).

Overall, I have introduced a plausible alternative mechanism for prostate cancer cells to achieve metastasis without increase expression of Pln. Another possibility would be to increase the expression of other HSPGs such as Glypican and Syndecan. To date no correlation between Glypican and prostate cancer progression has been published. Two recent studies suggest that Syndecan-1 correlates with increasing metastatic potential in prostate cancer patients ((170, 180)). Analysis of expression of GlcA C5-epimerase, the only other HSME with only one known isoform, as well as the other HSMEs is also needed in prostate cancer to fully understand the mechanisms by which increased extracellular HS is achieved.

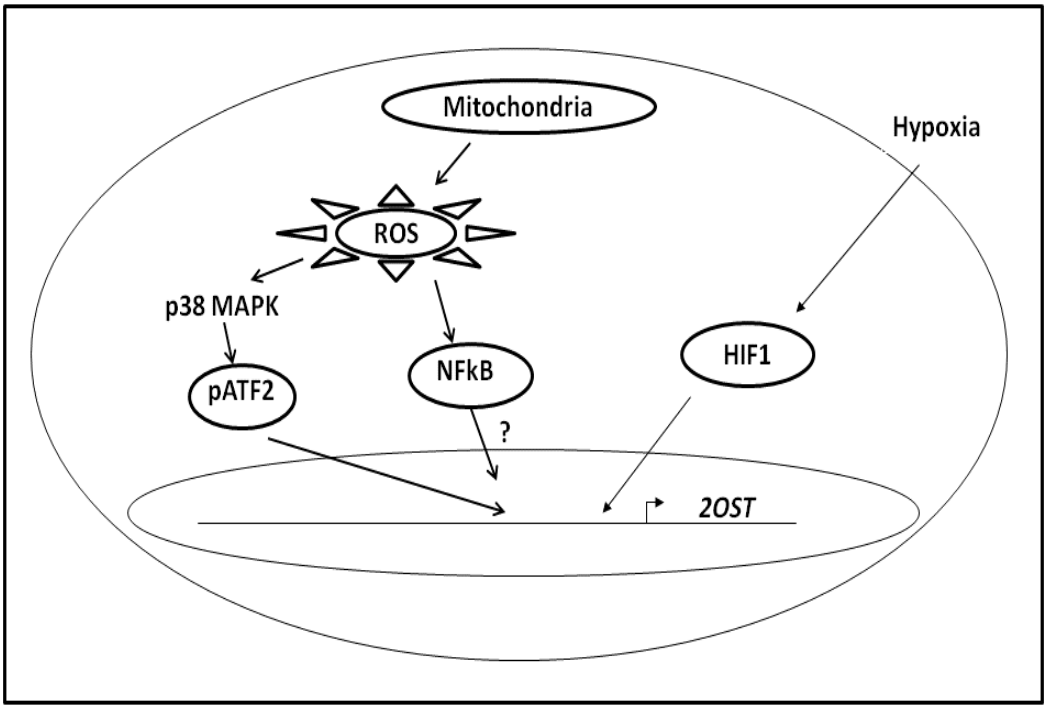

Figure 4-5: Model for upregulation of 2OST transcription by stress-activated transcription factors.

CHAPTER V

SUMMARY

The purpose of this study was to evaluate two different models in which increased extracellular HS may drive prostate cancer progression. First I wanted to determine whether upregulation of an HS modification enzyme could contribute to metastatic behaviors as upregulation of the HSPG protein core Pln has already been shown to do. Secondly, I wanted to investigate whether increased expression of the Pln protein core and the 2OST enzyme is due to a common general mechanism, specifically stress responses that increase in prostate cancer cell lines with increasing metastatic potential.

From previous work in our lab and those of our collaborators, we identified two subsets of prostate tumors. It was observed that 54% of tumors in this study had increased levels of Pln that correlated with increasing Gleason Grade while the remaining 46% either maintained or had decreased levels of Pln but still progressed to advanced disease. I set out to determine possible molecular mechanisms for both of these subsets.

To address how Pln is upregulated in prostate cancer progression, I introduced the LNCaP-DU145-LN4 cell line model that was representative of those tumors with increased Pln. This model had a 50-fold increase in Pln expression when comparing the highly metastatic LN4 line to the weakly tumorigenic LNCaP line. To further establish this cell line model, I demonstrate that Pln is required for maximum signaling of the

SHH, FGF, and TGFβ pathways, all known to be essential in cancer progression, in this model.

I then asked if stress-activated transcription factors were possible candidates for driving the increase in Pln expression. I found that inhibition of HIF1α, NFkB, or ATF2 by RNAi resulted in a significant decrease in Pln mRNA levels. I propose that HIF1α is necessary but not sufficient for maximal Pln expression and it acts through direct contact with the Pln promoter. HIF1α occupation of the promoter increases in highly metastatic cell lines. I also propose that the ROS-inducible NFkB and ATF2 transcription factors are necessary for maximal Pln expression. Results suggest that NFkB acts through a direct mechanism in LN4 by occupying both putative binding sites of the promoter and acts indirectly in LNCaP and DU145 with no detectable occupation of the promoter. It is possible that the expression of a coactivator needed by NFkB to bind the Pln promoter increases in the LN4 line. This would allow for NFkB to directly participate in causing maximal Pln expression. I propose that ATF2 acts to stimulate Pln expression exclusively in an indirect manner since I did not detect binding at putative ATF2 binding sites in any of the cell lines.

Small-molecule inhibition of either the extra-mitochondrial ROS generator NOX or the ROS-inducible protein kinase p38 MAPK resulted in decreased levels of Pln expression. This inhibition of Pln expression was dose dependent for both inhibitors. Pln expression in more metastatic lines seemed to be more sensitive to this inhibition. I then asked how 46% of prostate cancers were able to reach advanced stage without this upregulation of Pln. I focused on possible candidates that would provide increased

heparan sulfation in the extracellular matrix to make HSPGs better able to bind growth factors and facilitate disease progression. Results suggest that the 2OST enzyme, a heparan sulfate sulfotransferase, is required for maximal growth factor signaling by SHH, FGF, TGFβ, and Wnt as well as proliferation and invasion of prostate cancer cells.

To determine a possible mechanism of the decreased invasion observed upon knock-down of 2OST expression, I analyzed two different hallmarks of adherens junction formation, accumulation of actin and E-cadherin into foci on the cell surface. Cells treated with 2OST RNAi had significant increase in these two hallmarks. I propose that the activity of 2OST in prostate cancer progression is to inhibit cell adhesion through adherens junctions thus allowing cells to invade and possibly metastasize by Epithelial-Mesenchymal Transformation. Results also show that the expression of 2OST increases four-fold as prostate cancer cells in the LNCaP, C4, C4-2, C4-2B series become more metastatic.

To determine if 2OST is regulated by cellular stress much like Pln, I once again analyzed the effect of HIF1α, NFkB, and ATF2. I found that these transcription factors are necessary for maximal 2OST expression as well in the highly metastatic C4-2B cell line. Once again, results indicate that HIF1α is necessary but not sufficient for 2OST expression and it acts by directly binding the 2OST promoter. ATF2 also stimulates 2OST expression by a direct mechanism with detectable binding at the proximal putative binding site. Results suggest that NFkB stimulates 2OST expression in an indirect manner in the highly metastatic C4-2B. The results for both NFkB and ATF2 binding at

the 2OST promoter are different than the direct and indirect mechanisms, respectively, that were seen for Pln expression in the highly metastatic LN4 line.

The overall model that guided the research of this dissertation is shown in Figure 5-1. The model proposes that stress, such as hypoxia or the accumulation of ROS that are inherent in solid tumors, activates an intracellular stress response such as the activation of p38 MAPK. This response leads to the activation of a number of transcription factors that ultimately stimulate the expression of either HSPGs such as Pln or HSMEs such as 2OST. Upregulation of either or both classes of genes leads to an increase in the amount of extracellular HS. This increase of HS or heparan sulfation leads to more growth factor (GF) being able to interact with its receptor thus more GF signaling. The increase in signaling, a hallmark of cancer progression, leads to increased expression of target genes of the pathway.

In comparing the two cell line models tested in this dissertation, we found that the LNCaP, DU145, LN4 series had increased Pln expression but maintained levels of 2OST and the LNCaP, C4, C4-2, C4-2B had increased levels of 2OST but no increase in Pln. I have shown that the respective increases in Pln or 2OST are stimulated by stress-activated transcription factors. The next question would be to ask if the factors to activate both genes are available and active in both cell line series, why are both genes not turned on in both series. I propose that these transcription factors need specific binding partners to activate a specific gene. The binding partners (other transcription factors) needed by HIF1α, NFkB, and ATF2 to activate Pln expression in the LNCaP, C4, C4-2, C4-2B series are not available but are present at high enough concentration in

the LNCaP, DU145, LN4 series. The same though would apply to 2OST upregulation in these lines. Another possibility to explain the difference in regulation of the Pln and 2OST promoters in different cell models is the chromatin structure of the different promoters. For example, the Pln promoter may be inaccessible to transcriptional activators in the LNCaP-C4-2B cell model whereas the 2OST promoter is more accessible.

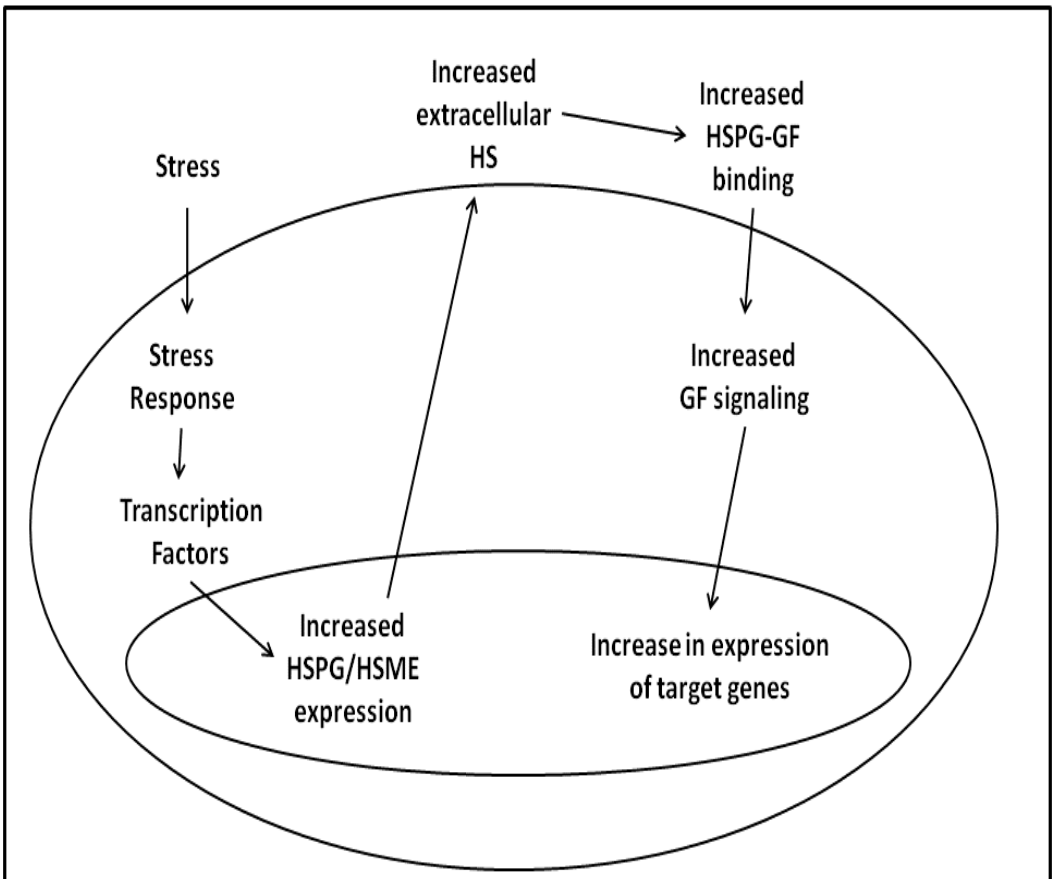

Figure 5-1: Overall model for stress regulation of extracellular HS

I propose that this model of hypoxia and ROS accumulation resulting in increased extracellular HS could be applied to the progression of many types of cancers other than prostate cancer. The stress conditions analyzed in this model are inherent to the formation of solid tumors. It is estimated that 90% of cancers diagnosed are solid tumors. We know that HSPGs such as Pln are ubiquitously found in the basement membrane where they modulate growth factor signaling events. This information suggests that my model could possibly be applied to the progression of most solid tumors. Cancers of the blood such as leukemias and lymphomas would not be included due to the lack of hypoxia in the blood.

In this dissertation I have described the effect of stress on Pln and 2OST. The future directions for this project are numerous. In regards to the amount of stress needed to produce a response, quantitation of the level of hypoxic stress (via pO_2) or the accumulation of ROS needed to activate expression of HSPGs or HSMEs could be done. Analysis of the effect of stress-activated pathways on other HSPGs such as Syndecan-1, that has recently been seen to correlate with advanced disease, should also be performed. I chose to analyze changes in 2OST expression partly due to the simplicity of analysis of an HSME with only one known isoform. GlcA C5-Epimerase (GLCE), whose activity is thought to be needed prior to 2OST function, also has only one known isoform. Other sulfotransferases such as NDST, 6OST, and 3OST could be analyzed in regards to the effect of stress on their expression. Each of these enzymes has multiple known isoforms. The isoforms known to not be expressed in the prostate could be excluded from the analysis. Real-time PCR analysis of the 6OST1, 6OST2, NDST1, NDST2, and

GLCE genes in the LNCaP, C4, C4-2, C4-2B series shows that expression is increased as cells become more metastatic for all of these genes except for 6OST2 (data not shown). Le et al performed a beautiful study in 2002 where they analyzed the effect of hypoxia on the expression of HSPGs and HSMEs in regards to FGF signaling in HUVEC endothelial cells (181). They found that hypoxia resulted in a reduction of Syndecan -1, 2, and 4 as well as Glypican-1. They saw no increase in Pln expression as a result of hypoxia. This group also reported increases in 2OST, NDST1 and 2, as well as increased 6OST1 with hypoxic treatment. This type of analysis needs to be done in models of cancer progression to obtain a full view of how increased extracellular HS is achieved. To determine if increased expression of 2OST or any HSME via stress actually causes an increase in the degree of heparan sulfation on HSPGs, one could use emerging mass-spectroscopy techniques in the field of glycobiology. This kind of study would be critical for determining the validity of the model shown.

Tumor cells respond to stress stimuli in many ways to promote progression to metastasis. I propose that the primary response is to increase available extracellular HS because of the requirement for growth factor signaling in cancer progression. These signaling pathways are enhanced by increases in extracellular HS. To address this hypothesis one could induce stress in early stage prostate cancer cells while treating the cells with a reversible inhibitor of proteoglycan sulfation such as sodium chlorate and analyze the ability of these cells to progress to metastasis. These samples would be compared to stressed cells without sodium chlorate treatment and to unstressed cells. If my hypothesis is correct the behavior of the stressed cells with sodium chlorate

treatment would be more similar to the unstressed cells than the stressed cells without sodium chlorate treatment.

I have shown that 2OST is required for prostate cancer cell proliferation and invasion. The activity of this enzyme is to transfer sulfate groups to HS chains on HSPGs. 2OST could act on glypicans, syndecans, or Pln to modulate these cell behaviors in prostate cancer. However, no association between glypicans and prostate cancer has been shown to date. I propose that 2OST acts primarily by modifying the HS chains of Pln to promote prostate cancer progression. To address this hypothesis, one could overexpress 2OST in prostate cancer cells while knocking down the expression of various HSPGs via RNAi. These cells would be compared to cells overexpressing 2OST. If my hypothesis is correct, the largest decrease in cell proliferation, invasion, and metastasis would be in those cells overexpressing 2OST while knocking down expression of Pln via RNAi.

Both Pln and 2OST have been shown to be involved in development and Pln has been shown to be involved in various diseases such as prostate cancer, Schwartz-Jampel syndrome, and Silverman-Handmaker type dyssegmental dysplasia. It is essential to understand how these genes are regulated. My work has shown that the expression of both genes is stimulated by the cellular stress response. I have also demonstrated a novel role of the 2OST enzyme in prostate cancer cell proliferation and invasion. Further studies are needed to acquire an exhaustive analysis of the regulation of these important genes. I propose that my studies have laid the groundwork for identifying new therapeutic targets for treating prostate cancer and most cancers that form solid tumors.

REFERENCES

1. Society AC. Prostate Cancer key statistics. [website] 2010 [updated 06/30/2010]; Available from: http://www.cancer.org/Cancer/ProstateCancer/DetailedGuide/prostate-cancer-key-statistics.

2. Bello-DeOcampo D, Tindall DJ. TGF-betal/Smad signaling in prostate cancer. Curr Drug Targets 2003;4:197-207.

3. Sogani PC, Fair WR. Treatment of advanced prostatic cancer. Urol Clin North Am 1987;14:353-71.

4. Gao H, Ouyang X, Banach-Petrosky WA, Gerald WL, Shen MM, Abate-Shen C. Combinatorial activities of Akt and B-Raf/Erk signaling in a mouse model of androgen-independent prostate cancer. Proc Natl Acad Sci U S A 2006;103:14477-82.

5. Verhagen AP, Ramaekers FC, Aalders TW, Schaafsma HE, Debruyne FM, Schalken JA. Colocalization of basal and luminal cell-type cytokeratins in human prostate cancer. Cancer Res 1992;52:6182-7.

6. De Marzo AM, Meeker AK, Epstein JI, Coffey DS. Prostate stem cell compartments: expression of the cell cycle inhibitor p27Kip1 in normal, hyperplastic, and neoplastic cells. Am J Pathol 1998;153:911-9.

7. Konishi N, Hiasa Y, Hayashi I, Matsuda H, Tsuzuki T, Ming T, Kitahori Y, Shiraishi T, Yatani R, Shimazaki J. p53 mutations occur in clinical, but not latent, human prostate carcinoma. Jpn J Cancer Res 1995;86:57-63.

8. Aaronson SA. Growth factors and cancer. Science 1991;254:1146-53.

9. Mellado B, Codony J, Ribal MJ, Visa L, Gascon P. Molecular biology of androgen-independent prostate cancer: the role of the androgen receptor pathway. Clin Transl Oncol 2009;11:5-10.

10. Nusslein-Volhard C, Wieschaus E. Mutations affecting segment number and polarity in Drosophila. Nature 1980;287:795-801.

11. Pepinsky RB, Rayhorn P, Day ES, Dergay A, Williams KP, Galdes A, Taylor FR, Boriack-Sjodin PA, Garber EA. Mapping sonic hedgehog-receptor interactions by steric interference. J Biol Chem 2000;275:10995-1001.

12. Kelleher FC, Fennelly D, Rafferty M. Common critical pathways in embryogenesis and cancer. Acta Oncol 2006;45:375-88.

13. Pasca di Magliano M, Hebrok M. Hedgehog signalling in cancer formation and maintenance. Nat Rev Cancer 2003;3:903-11.

14. Vezina CM, Lin TM, Peterson RE. AHR signaling in prostate growth, morphogenesis, and disease. Biochem Pharmacol 2009;77:566-76.

15. Datta S, Datta MW. Sonic Hedgehog signaling in advanced prostate cancer. Cell Mol Life Sci 2006;63:435-48.

16. Lamm ML, Catbagan WS, Laciak RJ, Barnett DH, Hebner CM, Gaffield W, Walterhouse D, Iannaccone P, Bushman W. Sonic hedgehog activates mesenchymal Gli1 expression during prostate ductal bud formation. Dev Biol 2002;249:349-66.

17. Berman DM, Desai N, Wang X, Karhadkar SS, Reynon M, Abate-Shen C, Beachy PA, Shen MM. Roles for Hedgehog signaling in androgen production and prostate ductal morphogenesis. Dev Biol 2004;267:387-98.

18. Pu Y, Huang L, Prins GS. Sonic hedgehog-patched Gli signaling in the developing rat prostate gland: lobe-specific suppression by neonatal estrogens reduces ductal growth and branching. Dev Biol 2004;273:257-75.

19. Wang BE, Shou J, Ross S, Koeppen H, De Sauvage FJ, Gao WQ. Inhibition of epithelial ductal branching in the prostate by sonic hedgehog is indirectly mediated by stromal cells. J Biol Chem 2003;278:18506-13.

20. Sanchez P, Hernandez AM, Stecca B, Kahler AJ, DeGueme AM, Barrett A, Beyna M, Datta MW, Datta S, Ruiz i Altaba A. Inhibition of prostate cancer proliferation by interference with SONIC HEDGEHOG-GLI1 signaling. Proc Natl Acad Sci U S A 2004;101:12561-6.

21. Gibbs M, Stanford JL, McIndoe RA, Jarvik GP, Kolb S, Goode EL, Chakrabarti L, Schuster EF, Buckley VA, Miller EL, Brandzel S, Li S, Hood L, Ostrander EA. Evidence for a rare prostate cancer-susceptibility locus at chromosome 1p36. Am J Hum Genet 1999;64:776-87.

22. Xu J, Gillanders EM, Isaacs SD, Chang BL, Wiley KE, Zheng SL, Jones M, Gildea D, Riedesel E, Albertus J, Freas-Lutz D, Markey C, Meyers DA, Walsh PC, Trent JM, Isaacs WB. Genome-wide scan for prostate cancer susceptibility genes in the Johns Hopkins hereditary prostate cancer families. Prostate 2003;57:320-5.

23. Karhadkar SS, Bova GS, Abdallah N, Dhara S, Gardner D, Maitra A, Isaacs JT, Berman DM, Beachy PA. Hedgehog signalling in prostate regeneration, neoplasia and metastasis. Nature 2004;431:707-12.

24. Sheng T, Li C, Zhang X, Chi S, He N, Chen K, McCormick F, Gatalica Z, Xie J. Activation of the hedgehog pathway in advanced prostate cancer. Mol Cancer 2004;3:29.

25. Johnson DE, Williams LT. Structural and functional diversity in the FGF receptor multigene family. Adv Cancer Res 1993;60:1-41.

26. Kimelman D, Kirschner M. Synergistic induction of mesoderm by FGF and TGF-beta and the identification of an mRNA coding for FGF in the early Xenopus embryo. Cell 1987;51:869-77.

27. De Moerlooze L, Spencer-Dene B, Revest JM, Hajihosseini M, Rosewell I, Dickson C. An important role for the IIIb isoform of fibroblast growth factor receptor 2 (FGFR2) in mesenchymal-epithelial signalling during mouse organogenesis. Development 2000;127:483-92.

28. Aigner A, Butscheid M, Kunkel P, Krause E, Lamszus K, Wellstein A, Czubayko F. An FGF-binding protein (FGF-BP) exerts its biological function by parallel paracrine stimulation of tumor cell and endothelial cell proliferation through FGF-2 release. Int J Cancer 2001;92:510-7.

29. Reynolds AR, Kyprianou N. Growth factor signalling in prostatic growth: significance in tumour development and therapeutic targeting. Br J Pharmacol 2006;147 Suppl 2:S144-52.

30. Harmer NJ, Ilag LL, Mulloy B, Pellegrini L, Robinson CV, Blundell TL. Towards a resolution of the stoichiometry of the fibroblast growth factor (FGF)-FGF receptor-heparin complex. J Mol Biol 2004;339:821-34.

31. Turner N, Grose R. Fibroblast growth factor signalling: from development to cancer. Nat Rev Cancer 2010;10:116-29.

32. Kwabi-Addo B, Ozen M, Ittmann M. The role of fibroblast growth factors and their receptors in prostate cancer. Endocr Relat Cancer 2004;11:709-24.

33. Cronauer MV, Hittmair A, Eder IE, Hobisch A, Culig Z, Ramoner R, Zhang J, Bartsch G, Reissigl A, Radmayr C, Thurnher M, Klocker H. Basic fibroblast growth factor levels in cancer cells and in sera of patients suffering from proliferative disorders of the prostate. Prostate 1997;31:223-33.

34. Dorkin TJ, Robinson MC, Marsh C, Bjartell A, Neal DE, Leung HY. FGF8 over-expression in prostate cancer is associated with decreased patient survival and persists in androgen independent disease. Oncogene 1999;18:2755-61.

35. Giri D, Ropiquet F, Ittmann M. Alterations in expression of basic fibroblast growth factor (FGF) 2 and its receptor FGFR-1 in human prostate cancer. Clin Cancer Res 1999;5:1063-71.

36. Song Z, Powell WC, Kasahara N, van Bokhoven A, Miller GJ, Roy-Burman P. The effect of fibroblast growth factor 8, isoform b, on the biology of prostate carcinoma cells and their interaction with stromal cells. Cancer Res 2000;60:6730-6.

37. Fox JC, Shanley JR. Antisense inhibition of basic fibroblast growth factor induces apoptosis in vascular smooth muscle cells. J Biol Chem 1996;271:12578-84.

38. Ortega S, Ittmann M, Tsang SH, Ehrlich M, Basilico C. Neuronal defects and delayed wound healing in mice lacking fibroblast growth factor 2. Proc Natl Acad Sci U S A 1998;95:5672-7.

39. Folkman J, Shing Y. Angiogenesis. J Biol Chem 1992;267:10931-4.

40. Greene GF, Kitadai Y, Pettaway CA, von Eschenbach AC, Bucana CD, Fidler IJ. Correlation of metastasis-related gene expression with metastatic potential in human prostate carcinoma cells implanted in nude mice using an in situ messenger RNA hybridization technique. Am J Pathol 1997;150:1571-82.

41. Kim KJ, Li B, Winer J, Armanini M, Gillett N, Phillips HS, Ferrara N. Inhibition of vascular endothelial growth factor-induced angiogenesis suppresses tumour growth in vivo. Nature 1993;362:841-4.

42. Lara PN, Jr., Twardowski P, Quinn DI. Angiogenesis-targeted therapies in prostate cancer. Clin Prostate Cancer 2004;3:165-73.

43. Gray MJ, Zhang J, Ellis LM, Semenza GL, Evans DB, Watowich SS, Gallick GE. HIF-1alpha, STAT3, CBP/p300 and Ref-1/APE are components of a transcriptional complex that regulates Src-dependent hypoxia-induced expression of VEGF in pancreatic and prostate carcinomas. Oncogene 2005;24:3110-20.

44. Ferrara N, Gerber HP, LeCouter J. The biology of VEGF and its receptors. Nat Med 2003;9:669-76.

45. Ferrer FA, Miller LJ, Lindquist R, Kowalczyk P, Laudone VP, Albertsen PC, Kreutzer DL. Expression of vascular endothelial growth factor receptors in human prostate cancer. Urology 1999;54:567-72.

46. Jackson MW, Bentel JM, Tilley WD. Vascular endothelial growth factor (VEGF) expression in prostate cancer and benign prostatic hyperplasia. J Urol 1997;157:2323-8.

47. Mazzucchelli R, Montironi R, Santinelli A, Lucarini G, Pugnaloni A, Biagini G. Vascular endothelial growth factor expression and capillary architecture in high-grade PIN and prostate cancer in untreated and androgen-ablated patients. Prostate 2000;45:72-9.

48. Ferrer FA, Miller LJ, Andrawis RI, Kurtzman SH, Albertsen PC, Laudone VP, Kreutzer DL. Angiogenesis and prostate cancer: in vivo and in vitro expression of angiogenesis factors by prostate cancer cells. Urology 1998;51:161-7.

49. Wikstrom P, Bergh A, Damber JE. Transforming growth factor-beta1 and prostate cancer. Scand J Urol Nephrol 2000;34:85-94.

50. Webber MM, Bello D, Kleinman HK, Wartinger DD, Williams DE, Rhim JS. Prostate specific antigen and androgen receptor induction and characterization of an immortalized adult human prostatic epithelial cell line. Carcinogenesis 1996;17:1641-6.

51. Wikstrom P, Damber J, Bergh A. Role of transforming growth factor-beta1 in prostate cancer. Microsc Res Tech 2001;52:411-9.

52. Lee C. Role of androgen in prostate growth and regression: stromal-epithelial interaction. Prostate Suppl 1996;6:52-6.

53. Massague J. TGF-beta signal transduction. Annu Rev Biochem 1998;67:753-91.

54. Guo Y, Kyprianou N. Restoration of transforming growth factor beta signaling pathway in human prostate cancer cells suppresses tumorigenicity via induction of caspase-1-mediated apoptosis. Cancer Res 1999;59:1366-71.

55. Wikstrom P, Stattin P, Franck-Lissbrant I, Damber JE, Bergh A. Transforming growth factor beta1 is associated with angiogenesis, metastasis, and poor clinical outcome in prostate cancer. Prostate 1998;37:19-29.

56. Perry KT, Anthony CT, Steiner MS. Immunohistochemical localization of TGF beta 1, TGF beta 2, and TGF beta 3 in normal and malignant human prostate. Prostate 1997;33:133-40.

57. Wilson MJ, Sellers RG, Wiehr C, Melamud O, Pei D, Peehl DM. Expression of matrix metalloproteinase-2 and -9 and their inhibitors, tissue inhibitor of metalloproteinase-1 and -2, in primary cultures of human prostatic stromal and epithelial cells. J Cell Physiol 2002;191:208-16.

58. Festuccia C, Bologna M, Gravina GL, Guerra F, Angelucci A, Villanova I, Millimaggi D, Teti A. Osteoblast conditioned media contain TGF-beta1 and modulate the migration of prostate tumor cells and their interactions with extracellular matrix components. Int J Cancer 1999;81:395-403.

59. Bruckheimer EM, Kyprianou N. Bcl-2 antagonizes the combined apoptotic effect of transforming growth factor-beta and dihydrotestosterone in prostate cancer cells. Prostate 2002;53:133-42.

60. Kang HY, Lin HK, Hu YC, Yeh S, Huang KE, Chang C. From transforming growth factor-beta signaling to androgen action: identification of Smad3 as an androgen receptor coregulator in prostate cancer cells. Proc Natl Acad Sci U S A 2001;98:3018-23.

61. Yardy GW, Brewster SF. Wnt signalling and prostate cancer. Prostate Cancer Prostatic Dis 2005;8:119-26.

62. Robinson DR, Zylstra CR, Williams BO. Wnt signaling and prostate cancer. Curr Drug Targets 2008;9:571-80.

63. Eaton S. Release and trafficking of lipid-linked morphogens. Curr Opin Genet Dev 2006;16:17-22.

64. Zeng X, Tamai K, Doble B, Li S, Huang H, Habas R, Okamura H, Woodgett J, He X. A dual-kinase mechanism for Wnt co-receptor phosphorylation and activation. Nature 2005;438:873-7.

65. Dajani R, Fraser E, Roe SM, Yeo M, Good VM, Thompson V, Dale TC, Pearl LH. Structural basis for recruitment of glycogen synthase kinase 3beta to the axin-APC scaffold complex. EMBO J 2003;22:494-501.

66. Willert K, Jones KA. Wnt signaling: is the party in the nucleus? Genes Dev 2006;20:1394-404.

67. Tycko B, Li CM, Buttyan R. The Wnt/beta-catenin pathway in Wilms tumors and prostate cancers. Curr Mol Med 2007;7:479-89.

68. Roose J, Clevers H. TCF transcription factors: molecular switches in carcinogenesis. Biochim Biophys Acta 1999;1424:M23-37.

69. Clevers H. Wnt/beta-catenin signaling in development and disease. Cell 2006;127:469-80.

70. Veeman MT, Axelrod JD, Moon RT. A second canon. Functions and mechanisms of beta-catenin-independent Wnt signaling. Dev Cell 2003;5:367-77.

71. Chen G, Shukeir N, Potti A, Sircar K, Aprikian A, Goltzman D, Rabbani SA. Up-regulation of Wnt-1 and beta-catenin production in patients with advanced metastatic prostate carcinoma: potential pathogenetic and prognostic implications. Cancer 2004;101:1345-56.

72. Zhu H, Mazor M, Kawano Y, Walker MM, Leung HY, Armstrong K, Waxman J, Kypta RM. Analysis of Wnt gene expression in prostate cancer: mutual inhibition by WNT11 and the androgen receptor. Cancer Res 2004;64:7918-26.

73. Katoh M. Differential regulation of WNT2 and WNT2B expression in human cancer. Int J Mol Med 2001;8:657-60.

74. Wissmann C, Wild PJ, Kaiser S, Roepcke S, Stoehr R, Woenckhaus M, Kristiansen G, Hsieh JC, Hofstaedter F, Hartmann A, Knuechel R, Rosenthal A, Pilarsky C. WIF1, a component of the Wnt pathway, is down-regulated in prostate, breast, lung, and bladder cancer. J Pathol 2003;201:204-12.

75. de la Taille A, Rubin MA, Chen MW, Vacherot F, de Medina SG, Burchardt M, Buttyan R, Chopin D. Beta-catenin-related anomalies in apoptosis-resistant and hormone-refractory prostate cancer cells. Clin Cancer Res 2003;9:1801-7.

76. Bubendorf L, Schopfer A, Wagner U, Sauter G, Moch H, Willi N, Gasser TC, Mihatsch MJ. Metastatic patterns of prostate cancer: an autopsy study of 1,589 patients. Hum Pathol 2000;31:578-83.

77. Nader HB, Buonassisi V, Colburn P, Dietrich CP. Heparin stimulates the synthesis and modifies the sulfation pattern of heparan sulfate proteoglycan from endothelial cells. J Cell Physiol 1989;140:305-10.

78. Tumova S, Woods A, Couchman JR. Heparan sulfate proteoglycans on the cell surface: versatile coordinators of cellular functions. Int J Biochem Cell Biol 2000;32:269-88.

79. Belting M. Heparan sulfate proteoglycan as a plasma membrane carrier. Trends Biochem Sci 2003;28:145-51.

80. Hassell JR, Robey PG, Barrach HJ, Wilczek J, Rennard SI, Martin GR. Isolation of a heparan sulfate-containing proteoglycan from basement membrane. Proc Natl Acad Sci U S A 1980;77:4494-8.

81. Whitelock JM, Melrose J, Iozzo RV. Diverse cell signaling events modulated by perlecan. Biochemistry 2008;47:11174-83.

82. Kirn-Safran C, Farach-Carson MC, Carson DD. Multifunctionality of extracellular and cell surface heparan sulfate proteoglycans. Cell Mol Life Sci 2009;66:3421-34.

83. Datta S, Pierce M, Datta MW. Perlecan signaling: helping hedgehog stimulate prostate cancer growth. Int J Biochem Cell Biol 2006;38:1855-61.

84. Arikawa-Hirasawa E, Watanabe H, Takami H, Hassell JR, Yamada Y. Perlecan is essential for cartilage and cephalic development. Nat Genet 1999;23:354-8.

85. Costell M, Gustafsson E, Aszodi A, Morgelin M, Bloch W, Hunziker E, Addicks K, Timpl R, Fassler R. Perlecan maintains the integrity of cartilage and some basement membranes. J Cell Biol 1999;147:1109-22.

86. Merz DC, Alves G, Kawano T, Zheng H, Culotti JG. UNC-52/perlecan affects gonadal leader cell migrations in C. elegans hermaphrodites through alterations in growth factor signaling. Dev Biol 2003;256:173-86.

87. Park Y, Rangel C, Reynolds MM, Caldwell MC, Johns M, Nayak M, Welsh CJ, McDermott S, Datta S. Drosophila perlecan modulates FGF and hedgehog signals to activate neural stem cell division. Dev Biol 2003;253:247-57.

88. Lindner JR, Hillman PR, Barrett AL, Jackson MC, Perry TL, Park Y, Datta S. The Drosophila Perlecan gene trol regulates multiple signaling pathways in different developmental contexts. BMC Dev Biol 2007;7:121.

89. Giros A, Morante J, Gil-Sanz C, Fairen A, Costell M. Perlecan controls neurogenesis in the developing telencephalon. BMC Dev Biol 2007;7:29.

90. Cohen IR, Murdoch AD, Naso MF, Marchetti D, Berd D, Iozzo RV. Abnormal expression of perlecan proteoglycan in metastatic melanomas. Cancer Res 1994;54:5771-4.

91. Sharma B, Handler M, Eichstetter I, Whitelock JM, Nugent MA, Iozzo RV. Antisense targeting of perlecan blocks tumor growth and angiogenesis in vivo. J Clin Invest 1998;102:1599-608.

92. Zhou Z, Wang J, Cao R, Morita H, Soininen R, Chan KM, Liu B, Cao Y, Tryggvason K. Impaired angiogenesis, delayed wound healing and retarded tumor growth in perlecan heparan sulfate-deficient mice. Cancer Res 2004;64:4699-702

93. Datta MW, Hernandez AM, Schlicht MJ, Kahler AJ, DeGueme AM, Dhir R, Shah RB, Farach-Carson C, Barrett A, Datta S. Perlecan, a candidate gene for the CAPB locus, regulates prostate cancer cell growth via the Sonic Hedgehog pathway. Mol Cancer 2006;5:9.

94. Savore C, Zhang C, Muir C, Liu R, Wyrwa J, Shu J, Zhau HE, Chung LW, Carson DD, Farach-Carson MC. Perlecan knockdown in metastatic prostate cancer cells reduces heparin-binding growth factor responses in vitro and tumor growth in vivo. Clin Exp Metastasis 2005;22:377-90.

95. Esko JD, Selleck SB. Order out of chaos: assembly of ligand binding sites in heparan sulfate. Annu Rev Biochem 2002;71:435-71.

96. Blackhall FH, Merry CL, Lyon M, Jayson GC, Folkman J, Javaherian K, Gallagher JT. Binding of endostatin to endothelial heparan sulphate shows a differential requirement for specific sulphates. Biochem J 2003;375:131-9.

97. Kobayashi M, Habuchi H, Yoneda M, Habuchi O, Kimata K. Molecular cloning and expression of Chinese hamster ovary cell heparan-sulfate 2-sulfotransferase. J Biol Chem 1997;272:13980-5.

98. Merry CL, Bullock SL, Swan DC, Backen AC, Lyon M, Beddington RS, Wilson VA, Gallagher JT. The molecular phenotype of heparan sulfate in the Hs2st-/- mutant mouse. J Biol Chem 2001;276:35429-34.

99. Kinnunen T, Huang Z, Townsend J, Gatdula MM, Brown JR, Esko JD, Turnbull JE. Heparan 2-O-sulfotransferase, hst-2, is essential for normal cell migration in Caenorhabditis elegans. Proc Natl Acad Sci U S A 2005;102:1507-12.

100. Kobayashi T, Habuchi H, Tamura K, Ide H, Kimata K. Essential role of heparan sulfate 2-O-sulfotransferase in chick limb bud patterning and development. J Biol Chem 2007;282:19589-97.

101. Merrill C, Bayraktaroglu L, Kusano A, Ganetzky B. Truncated RanGAP encoded by the Segregation Distorter locus of Drosophila. Science 1999 Mar;283:1742-5.

102. Xu D, Song D, Pedersen LC, Liu J. Mutational study of heparan sulfate 2-O-sulfotransferase and chondroitin sulfate 2-O-sulfotransferase. J Biol Chem 2007;282:8356-67.

103. Kamimura K, Koyama T, Habuchi H, Ueda R, Masu M, Kimata K, Nakato H. Specific and flexible roles of heparan sulfate modifications in Drosophila FGF signaling. J Cell Biol 2006;174:773-8.

104. Cadwallader AB, Yost HJ. Combinatorial expression patterns of heparan sulfate sulfotransferases in zebrafish: III. 2-O-sulfotransferase and C5-epimerases. Dev Dyn 2007;236:581-6.

105. Ahmed Abdal Dayem H-YC, Jung-Hyun Kim and Ssang-Goo Cho Role of Oxidative Stress in Stem, Cancer, and Cancer Stem Cells. Cancers 2010;2:859-84.

106. Brown JM. Exploiting the hypoxic cancer cell: mechanisms and therapeutic strategies. Mol Med Today 2000;6:157-62.

107. Vaupel P, Mayer A, Hockel M. Tumor hypoxia and malignant progression. Methods Enzymol 2004;381:335-54.

108. Folkman J. Angiogenesis and apoptosis. Semin Cancer Biol 2003;13:159-67.

109. Horn L, Sandler A. Chemotherapy and antiangiogenic agents in non-small-cell lung cancer. Clin Lung Cancer 2007;8 Suppl 2:S68-73.

110. Semenza GL, Wang GL. A nuclear factor induced by hypoxia via de novo protein synthesis binds to the human erythropoietin gene enhancer at a site required for transcriptional activation. Mol Cell Biol 1992;12:5447-54.

111. Brahimi-Horn MC, Chiche J, Pouyssegur J. Hypoxia and cancer. J Mol Med 2007;85:1301-7.

112. Semenza GL. HIF-1, O2, and the 3 PHDs: How Animal Cells Signal Hypoxia to the Nucleus Cell 2001;107:1-3.

113. Schofield CJ, Ratcliffe PJ. Oxygen sensing by HIF hydroxylases. Nat Rev Mol Cell Biol 2004;5:343-54.

114. Manalo DJ, Rowan A, Lavoie T, Natarajan L, Kelly BD, Ye SQ, Garcia JG, Semenza GL. Transcriptional regulation of vascular endothelial cell responses to hypoxia by HIF-1. Blood 2005;105:659-69.

115. Semenza GL. Vasculogenesis, angiogenesis, and arteriogenesis: mechanisms of blood vessel formation and remodeling. J Cell Biochem 2007;102:840-7.

116. Movsas B, Chapman JD, Hanlon AL, Horwitz EM, Pinover WH, Greenberg RE, Stobbe C, Hanks GE. Hypoxia in human prostate carcinoma: an Eppendorf PO2 study. Am J Clin Oncol 2001;24:458-61.

117. Vaupel P, Kelleher DK, Hockel M. Oxygen status of malignant tumors: pathogenesis of hypoxia and significance for tumor therapy. Semin Oncol 2001;28:29-35.

118. Movsas B, Chapman JD, Hanlon AL, Horwitz EM, Greenberg RE, Stobbe C, Hanks GE, Pollack A. Hypoxic prostate/muscle pO2 ratio predicts for biochemical failure in patients with prostate cancer: preliminary findings. Urology 2002;60:634-9.

119. Sohal RS, Weindruch R. Oxidative stress, caloric restriction, and aging. Science 1996;273:59-63.

120. Valko M, Rhodes CJ, Moncol J, Izakovic M, Mazur M. Free radicals, metals and antioxidants in oxidative stress-induced cancer. Chem Biol Interact 2006;160:1-40.

121. Parke DV, Sapota A. Chemical toxicity and reactive oxygen species. Int J Occup Med Environ Health 1996;9:331-40.

122. Elchuri S, Oberley TD, Qi W, Eisenstein RS, Jackson Roberts L, Van Remmen H, Epstein CJ, Huang TT. CuZnSOD deficiency leads to persistent and widespread oxidative damage and hepatocarcinogenesis later in life. Oncogene 2005;24:367-80.

123. Li JJ, Oberley LW, St Clair DK, Ridnour LA, Oberley TD. Phenotypic changes induced in human breast cancer cells by overexpression of manganese-containing superoxide dismutase. Oncogene 1995;10:1989-2000.

124. Van Remmen H, Ikeno Y, Hamilton M, Pahlavani M, Wolf N, Thorpe SR, Alderson NL, Baynes JW, Epstein CJ, Huang TT, Nelson J, Strong R, Richardson A. Life-long reduction in MnSOD activity results in increased DNA damage and higher incidence of cancer but does not accelerate aging. Physiol Genomics 2003;16:29-37.

125. Chu FF, Esworthy RS, Doroshow JH. Role of Se-dependent glutathione peroxidases in gastrointestinal inflammation and cancer. Free Radic Biol Med 2004;36:1481-95.

126. Wiseman H, Halliwell B. Damage to DNA by reactive oxygen and nitrogen species: role in inflammatory disease and progression to cancer. Biochem J 1996;313:17-29.

127. Halliwell B. Oxidative stress and cancer: have we moved forward? Biochem J 2007;401:1-11.

128. Vaquero EC, Edderkaoui M, Pandol SJ, Gukovsky I, Gukovskaya AS. Reactive oxygen species produced by NAD(P)H oxidase inhibit apoptosis in pancreatic cancer cells. J Biol Chem 2004;279:34643-54.

129. Irani K, Xia Y, Zweier JL, Sollott SJ, Der CJ, Fearon ER, Sundaresan M, Finkel T, Goldschmidt-Clermont PJ. Mitogenic signaling mediated by oxidants in Ras-transformed fibroblasts. Science 1997;275:1649-52.

130. Savaraj N, Wei Y, Unate H, Liu PM, Wu CJ, Wangpaichitr M, Xia D, Xu HJ, Hu SX, Tien Kuo M. Redox regulation of matrix metalloproteinase gene family in small cell lung cancer cells. Free Radic Res 2005;39:373-81.

131. Oberley TD. Oxidative damage and cancer. Am J Pathol 2002;160:403-8.

132. Petros JA, Baumann AK, Ruiz-Pesini E, Amin MB, Sun CQ, Hall J, Lim S, Issa MM, Flanders WD, Hosseini SH, Marshall FF, Wallace DC. mtDNA mutations increase tumorigenicity in prostate cancer. Proc Natl Acad Sci U S A 2005;102:719-24.

133. Arbiser JL, Petros J, Klafter R, Govindajaran B, McLaughlin ER, Brown LF, Cohen C, Moses M, Kilroy S, Arnold RS, Lambeth JD. Reactive oxygen generated by Nox1 triggers the angiogenic switch. Proc Natl Acad Sci U S A 2002;99:715-20.

134. Sen R, Baltimore D. Inducibility of kappa immunoglobulin enhancer-binding protein Nf-kappa B by a posttranslational mechanism. Cell 1986;47:921-8.

135. Kabe Y, Ando K, Hirao S, Yoshida M, Handa H. Redox regulation of NF-kappaB activation: distinct redox regulation between the cytoplasm and the nucleus. Antioxid Redox Signal 2005;7:395-403.

136. Chapman NR, Perkins ND. Inhibition of the RelA(p65) NF-kappaB subunit by Egr-1. J Biol Chem 2000;275:4719-25.

137. Storz P, Toker A. Protein kinase D mediates a stress-induced NF-kappaB activation and survival pathway. EMBO J 2003;22:109-20.

138. Suh J, Rabson AB. NF-kappaB activation in human prostate cancer: important mediator or epiphenomenon? J Cell Biochem 2004;91:100-17.

139. Palayoor ST, Youmell MY, Calderwood SK, Coleman CN, Price BD. Constitutive activation of IkappaB kinase alpha and NF-kappaB in prostate cancer cells is inhibited by ibuprofen. Oncogene 1999;18:7389-94.

140. Gasparian AV, Yao YJ, Kowalczyk D, Lyakh LA, Karseladze A, Slaga TJ, Budunova IV. The role of IKK in constitutive activation of NF-kappaB transcription factor in prostate carcinoma cells. J Cell Sci 2002;115:141-51.

141. Huang S, Pettaway CA, Uehara H, Bucana CD, Fidler IJ. Blockade of NF-kappaB activity in human prostate cancer cells is associated with suppression of angiogenesis, invasion, and metastasis. Oncogene 2001;20:4188-97.

142. Recio JA, Merlino G. Hepatocyte growth factor/scatter factor activates proliferation in melanoma cells through p38 MAPK, ATF-2 and cyclin D1. Oncogene 2002;21:1000-8.

143. Vlahopoulos SA, Logotheti S, Mikas D, Giarika A, Gorgoulis V, Zoumpourlis V. The role of ATF-2 in oncogenesis. Bioessays 2008;30:314-27.

144. Reimold AM, Grusby MJ, Kosaras B, Fries JW, Mori R, Maniwa S, Clauss IM, Collins T, Sidman RL, Glimcher MJ, Glimcher LH. Chondrodysplasia and neurological abnormalities in ATF-2-deficient mice. Nature 1996;379:262-5.

145. Hai TW, Liu F, Coukos WJ, Green MR. Transcription factor ATF cDNA clones: an extensive family of leucine zipper proteins able to selectively form DNA-binding heterodimers. Genes Dev 1989;3:2083-90.

146. Ricote M, Garcia-Tunon I, Bethencourt F, Fraile B, Onsurbe P, Paniagua R, Royuela M. The p38 transduction pathway in prostatic neoplasia. J Pathol 2006;208:401-7.

147. Navone NM, Logothetis CJ, von Eschenbach AC, Troncoso P. Model systems of prostate cancer: uses and limitations. Cancer Metastasis Rev 1998;17:361-71.

148. Horoszewicz JS, Leong SS, Kawinski E, Karr JP, Rosenthal H, Chu TM, Mirand EA, Murphy GP. LNCaP model of human prostatic carcinoma. Cancer Res 1983;43:1809-18.

149. Veldscholte J, Berrevoets CA, Brinkmann AO, Grootegoed JA, Mulder E. Anti-androgens and the mutated androgen receptor of LNCaP cells: differential effects on binding affinity, heat-shock protein interaction, and transcription activation. Biochemistry 1992;31:2393-9.

150. Wu HC, Hsieh JT, Gleave ME, Brown NM, Pathak S, Chung LW. Derivation of androgen-independent human LNCaP prostatic cancer cell sublines: role of bone stromal cells. Int J Cancer 1994;57:406-12.

151. Thalmann GN, Anezinis PE, Chang SM, Zhau HE, Kim EE, Hopwood VL, Pathak S, von Eschenbach AC, Chung LW. Androgen-independent cancer progression and bone metastasis in the LNCaP model of human prostate cancer. Cancer Res 1994;54:2577-81.

152. Stone KR, Mickey DD, Wunderli H, Mickey GH, Paulson DF. Isolation of a human prostate carcinoma cell line (DU 145). Int J Cancer 1978;21:274-81.

153. Pettaway CA, Pathak S, Greene G, Ramirez E, Wilson MR, Killion JJ, Fidler IJ. Selection of highly metastatic variants of different human prostatic carcinomas using orthotopic implantation in nude mice. Clin Cancer Res 1996;2:1627-36.

154. Iozzo RV, Cohen IR, Grassel S, Murdoch AD. The biology of perlecan: the multifaceted heparan sulphate proteoglycan of basement membranes and pericellular matrices. Biochem J 1994;302:625-39.

155. Semenza GL. Hypoxia and cancer. Cancer Metastasis Rev 2007;26:223-4.

156. Zhong H, De Marzo AM, Laughner E, Lim M, Hilton DA, Zagzag D, Buechler P, Isaacs WB, Semenza GL, Simons JW. Overexpression of hypoxia-inducible factor 1alpha in common human cancers and their metastases. Cancer Res 1999;59:5830-5.

157. Zhong H, Agani F, Baccala AA, Laughner E, Rioseco-Camacho N, Isaacs WB, Simons JW, Semenza GL. Increased expression of hypoxia inducible factor-1alpha in rat and human prostate cancer. Cancer Res 1998;58:5280-4.

158. Dakubo GD, Parr RL, Costello LC, Franklin RB, Thayer RE. Altered metabolism and mitochondrial genome in prostate cancer. J Clin Pathol 2006;59:10-6.

159. Kumar B, Koul S, Khandrika L, Meacham RB, Koul HK. Oxidative stress is inherent in prostate cancer cells and is required for aggressive phenotype. Cancer Res 2008;68:1777-85.

160. Lowe JM, Cha H, Yang Q, Fornace AJ, Jr. Nuclear factor-kappaB (NF-kappaB) is a novel positive transcriptional regulator of the oncogenic Wip1 phosphatase. J Biol Chem 2010;285:5249-57.

161. Benhar M, Dalyot I, Engelberg D, Levitzki A. Enhanced ROS production in oncogenically transformed cells potentiates c-Jun N-terminal kinase and p38 mitogen-activated protein kinase activation and sensitization to genotoxic stress. Mol Cell Biol 2001;21:6913-26.

162. Hay CW, Ferguson LA, Docherty K. ATF-2 stimulates the human insulin promoter through the conserved CRE2 sequence. Biochim Biophys Acta 2007;1769:79-91.

163. Iozzo RV, Pillarisetti J, Sharma B, Murdoch AD, Danielson KG, Uitto J, Mauviel A. Structural and functional characterization of the human perlecan gene

promoter. Transcriptional activation by transforming growth factor-beta via a nuclear factor 1-binding element. J Biol Chem 1997;272:5219-28.

164. Dodge GR, Kovalszky I, Hassell JR, Iozzo RV. Transforming growth factor beta alters the expression of heparan sulfate proteoglycan in human colon carcinoma cells. J Biol Chem 1990;265:18023-9.

165. Morris JE, Gaza G, Potter SW. Specific stimulation of basal lamina heparan sulfate proteoglycan in mouse uterine epithelium by Matrigel and by transforming growth factor-beta 1. In Vitro Cell Dev Biol Anim 1994;30A:120-8.

166. Kaji T, Yamamoto C, Oh-i M, Fujiwara Y, Yamazaki Y, Morita T, Plaas AH, Wight TN. The vascular endothelial growth factor VEGF165 induces perlecan synthesis via VEGF receptor-2 in cultured human brain microvascular endothelial cells. Biochim Biophys Acta 2006;1760:1465-74.

167. Hashimoto-Uoshima M, Noguchi K, Suzuki M, Murata A, Yanagishita M, Ishikawa I. Effects of interleukin-4 on proteoglycan accumulation in human gingival fibroblasts. J Periodontal Res 2002;37:42-9.

168. Li YZ, Liu XH, Cai LR. Down-regulation of perlecan expression contributes to the inhibition of rat cardiac microvascular endothelial cell proliferation induced by hypoxia. Sheng Li Xue Bao 2007;59:221-6.

169. Furuta GT, Dzus AL, Taylor CT, Colgan SP. Parallel induction of epithelial surface-associated chemokine and proteoglycan by cellular hypoxia: implications for neutrophil activation. J Leukoc Biol 2000;68:251-9.

170. Brimo F, Vollmer RT, Friszt M, Corcos J, Bismar TA. Syndecan-1 expression in prostate cancer and its value as biomarker for disease progression. BJU Int 2010;106:418-23.

171. Shimada K, Nakamura M, De Velasco MA, Tanaka M, Ouji Y, Konishi N. Syndecan-1, a new target molecule involved in progression of androgen-independent prostate cancer. Cancer Sci 2009;100:1248-54.

172. Flaumenhaft R, Moscatelli D, Rifkin DB. Heparin and heparan sulfate increase the radius of diffusion and action of basic fibroblast growth factor. J Cell Biol 1990;111:1651-9.

173. Ornitz DM, Yayon A, Flanagan JG, Svahn CM, Levi E, Leder P. Heparin is required for cell-free binding of basic fibroblast growth factor to a soluble receptor and for mitogenesis in whole cells. Mol Cell Biol 1992;12:240-7.

174. Kreuger J, Spillmann D, Li JP, Lindahl U. Interactions between heparan sulfate and proteins: the concept of specificity. J Cell Biol 2006;174:323-7.

175. Ashikari-Hada S, Habuchi H, Kariya Y, Itoh N, Reddi AH, Kimata K. Characterization of growth factor-binding structures in heparin/heparan sulfate using an octasaccharide library. J Biol Chem 2004;279:12346-54.

176. Kemler R. From cadherins to catenins: cytoplasmic protein interactions and regulation of cell adhesion. Trends Genet 1993;9:317-21.

177. Gloushankova NA. Changes in regulation of cell-cell adhesion during tumor transformation. Biochemistry (Mosc) 2008;73:742-50.

178. Chu YS, Thomas WA, Eder O, Pincet F, Perez E, Thiery JP, Dufour S. Force measurements in E-cadherin-mediated cell doublets reveal rapid adhesion strengthened by actin cytoskeleton remodeling through Rac and Cdc42. J Cell Biol 2004;167:1183-94.

179. Cohen P. Protein kinases--the major drug targets of the twenty-first century? Nat Rev Drug Discov 2002;1:309-15.

180. Zellweger T, Ninck C, Mirlacher M, Annefeld M, Glass AG, Gasser TC, Mihatsch MJ, Gelmann EP, Bubendorf L. Tissue microarray analysis reveals prognostic significance of syndecan-1 expression in prostate cancer. Prostate 2003;55:20-9.

181. Li J, Shworak NW, Simons M. Increased responsiveness of hypoxic endothelial cells to FGF2 is mediated by HIF-1alpha-dependent regulation of enzymes involved in synthesis of heparan sulfate FGF2-binding sites. J Cell Sci 2002;115:1951-9.

VITA

Brent Wade Ferguson
Address: MS 2128 TAMU College Station, TX 77843
E-mail: brentwade@gmail.com

Education and Positions held:
Graduate Research Assistant, 2005 - 2010
Texas A&M University, College Station
B.S, Chemistry & Biology
West Texas A&M University
Canyon, TX, 2003

Publications:
1. **Ferguson, BW** and Datta, S. (2010). Hypoxia and ROS signaling stimulate transcription of *PERLECAN* in cell line model of prostate cancer progression. In preparation.

2. **Ferguson, BW** and Datta, S. (2010). Heparan-Sulfate 2-O-Sulfotransferase regulates Heparan-binding Growth Factor Signaling in C4-2B prostate cancer cells. In preparation.

3. **Ferguson, B**.*, Cadwalader, E.*, Schlicht, M., Datta, M., Datta, S. and Yost, J. (2010). 2OST regulates growth factor signaling and cell adhesion in development and disease. In preparation. *These two authors contributed equally to this article.

Oral and Poster Presentations:
1. Oral Presentation. **Brent Ferguson** (2007). Perlecan heparan-sulfate fine structure and SHH signaling in advanced prostate cancer. Department of Biochemistry/Biophysics Research Competition, Texas A&M University

2. Oral Presentation. **Brent Ferguson**[1], Michael Schlicht[2], Alexandra Migdal[2], Payal Shah[2], Milton Datta[2], Sumana Datta[1]: (2007) Perlecan heparan-sulfate fine structure and SHH signaling in advanced prostate cancer. American Society of Investigative Pathology, Washington, DC.

3. Poster Presentation. **Brent Ferguson** (2006). The Effect of Mutations in Heparan-Sulfate synthesis/modification enzymes on Hedgehog signaling and Neuroblast proliferation in *Drosophila melanogaster*. *Drosophila* Research Conference, Houston, TX.

Grants and Fellowships:
Pathways to the Doctorate Fellowship, 2004